

A biweekly mode in the equatorial Indian Ocean

Debasis Sengupta & Retish Senan

Center for Atmospheric and Oceanic Sciences

Indian Institute of Science, Bangalore

V. S. N. Murty & V. Fernando

National Institute of Oceanography, Goa

IOM, 1 Dec 2004

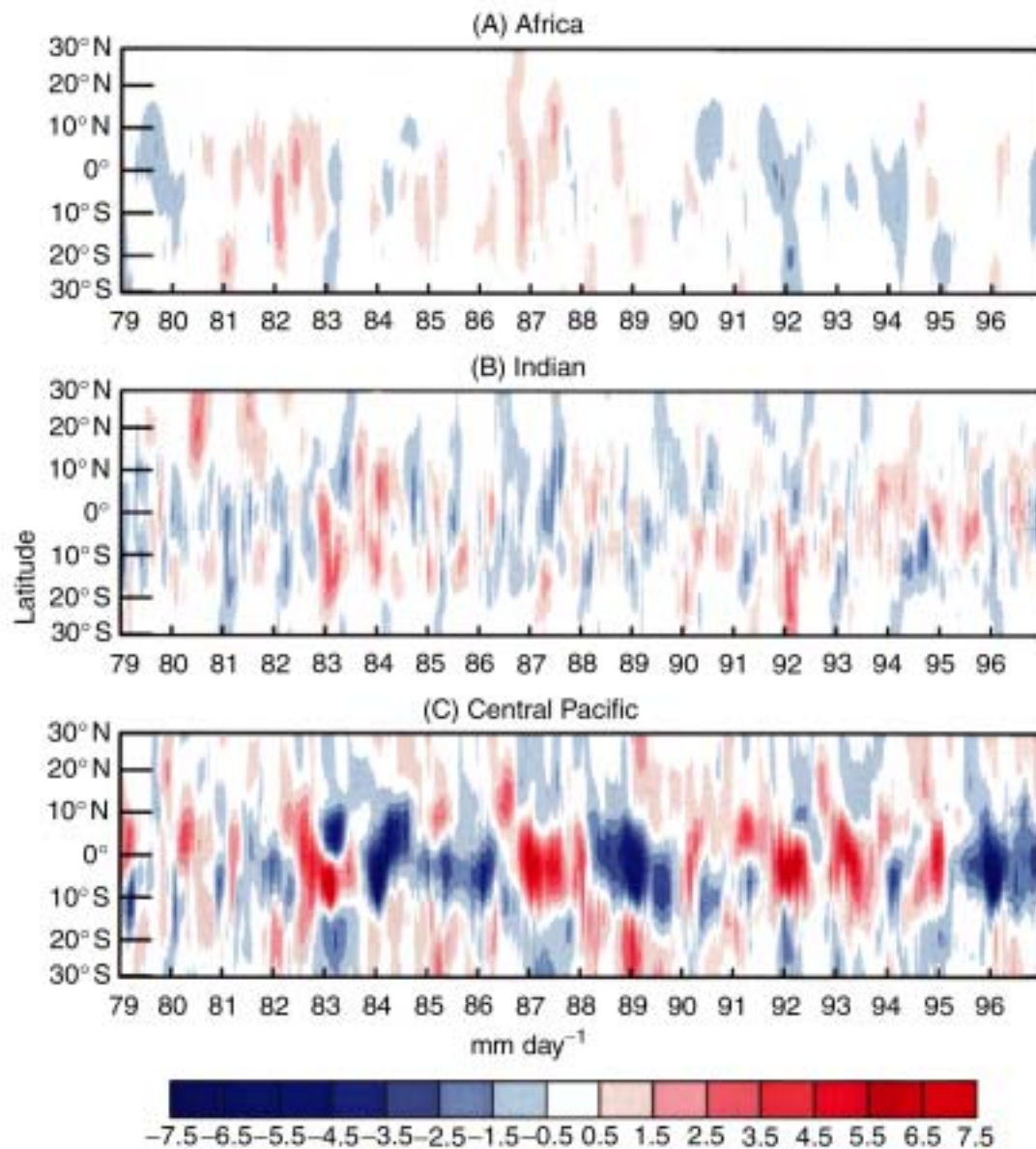
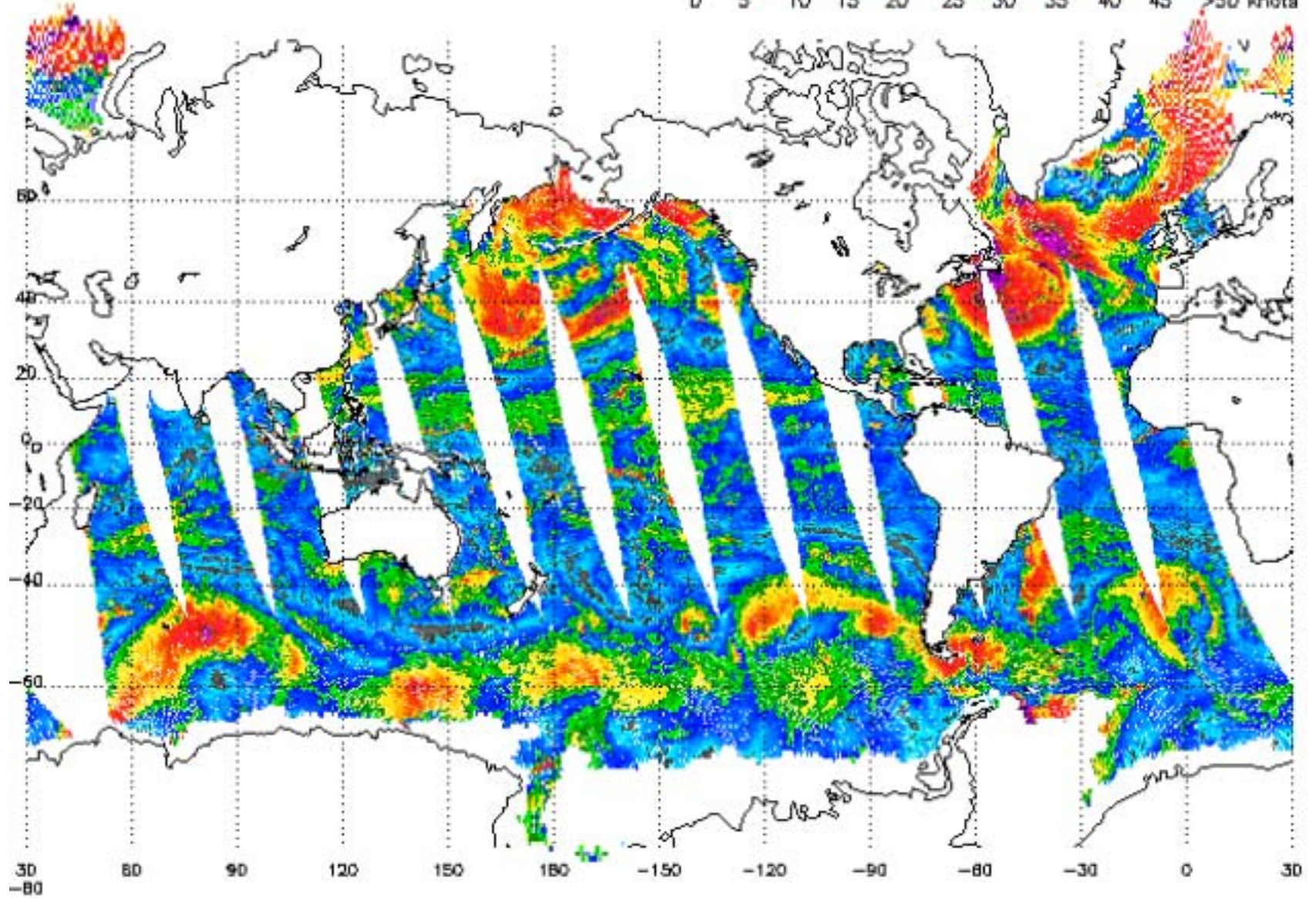


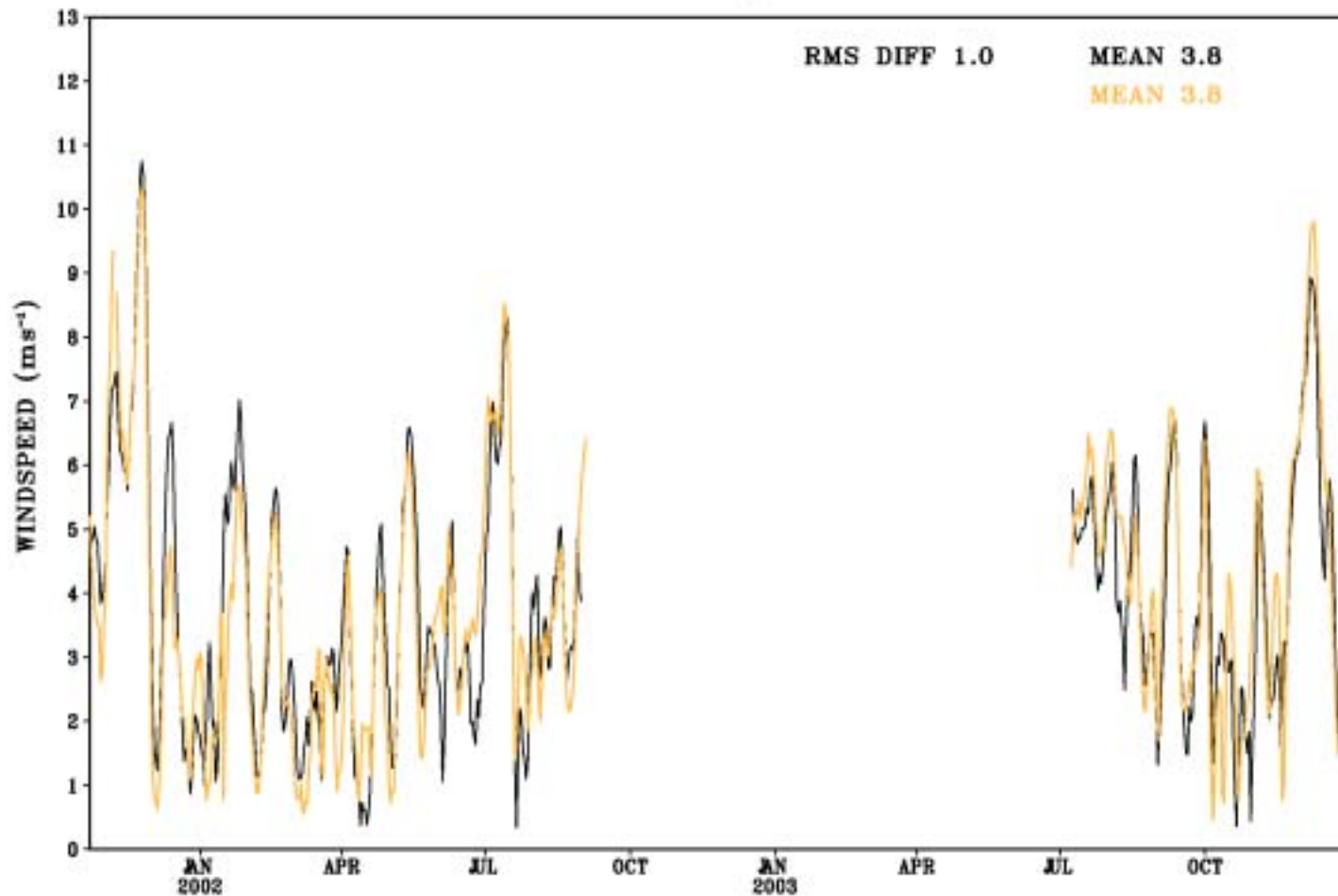
Figure 9 Time–latitude diagrams of the anomalies in rainfall associated with the ITCZ zonally averaged over three different longitude sectors: (A) Africa, 10–40° E; (B) Indian, 60–100° E; and (C) central Pacific, 160° E–160° W. Departures are computed from the mean annual cycles shown in **Figure 8**. (Source: National Oceanographic and Atmospheric Administration’s (NOAA) Climate Prediction Center (CPC) Merged Analysis of Precipitation (CMAP).)

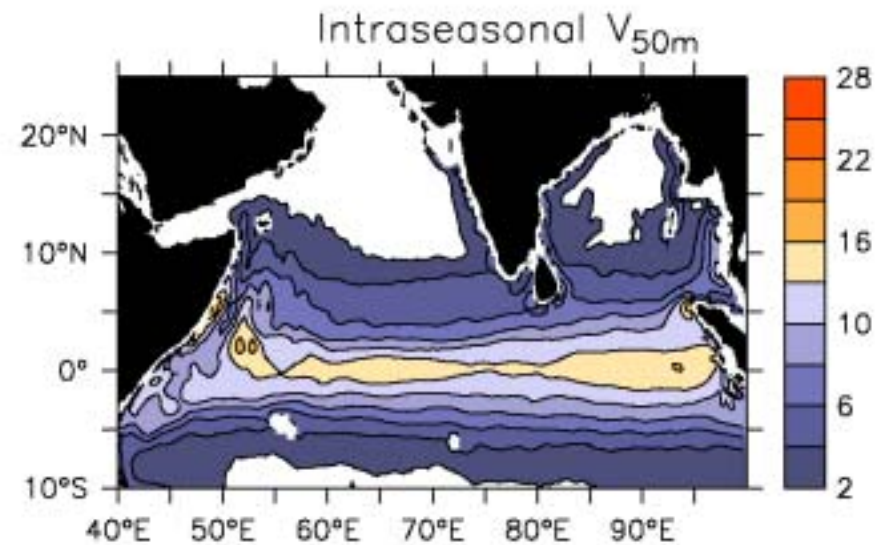
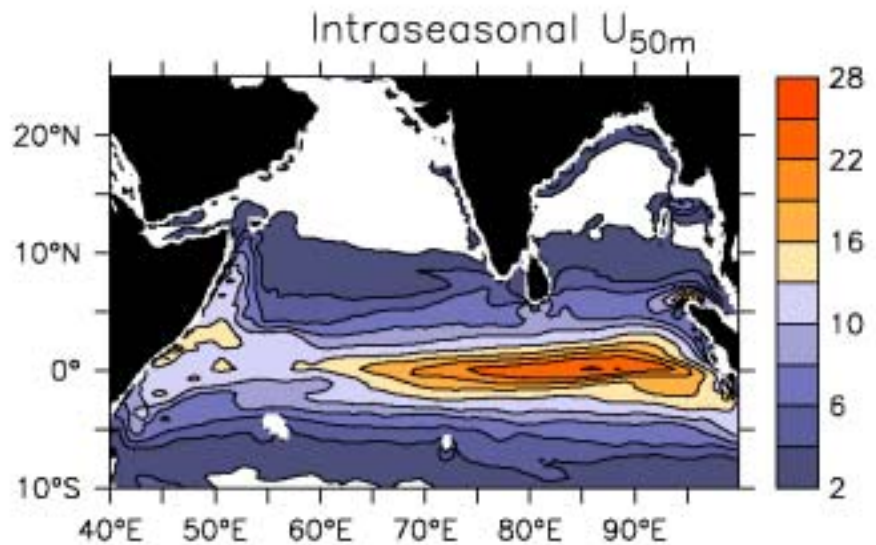
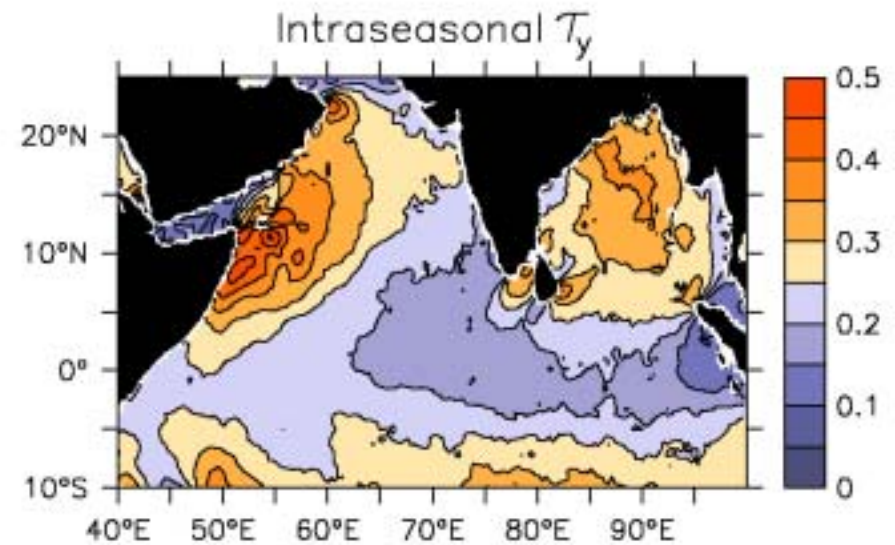
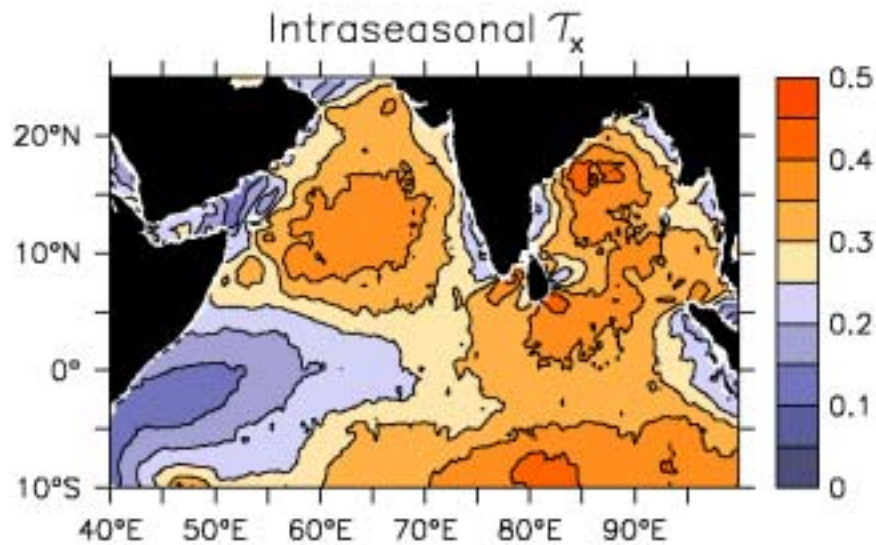
80 QUIKSCAT NRT Winds Jan 27 05:08 GMT 2004 ascending



7 DAY WINDSPEED (ms^{-1}) at 1.66°S, 90°E

TRITON QSCAT

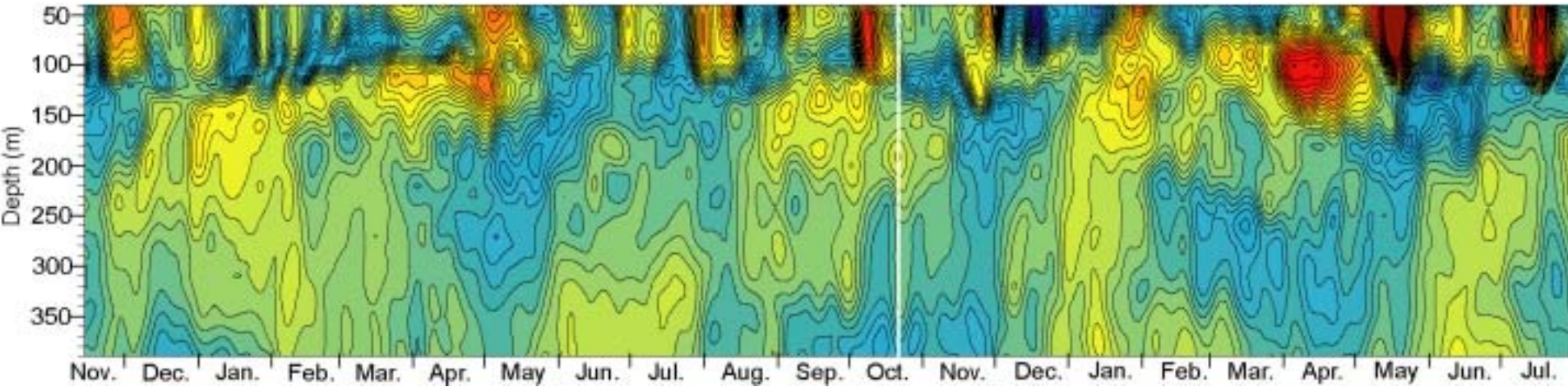




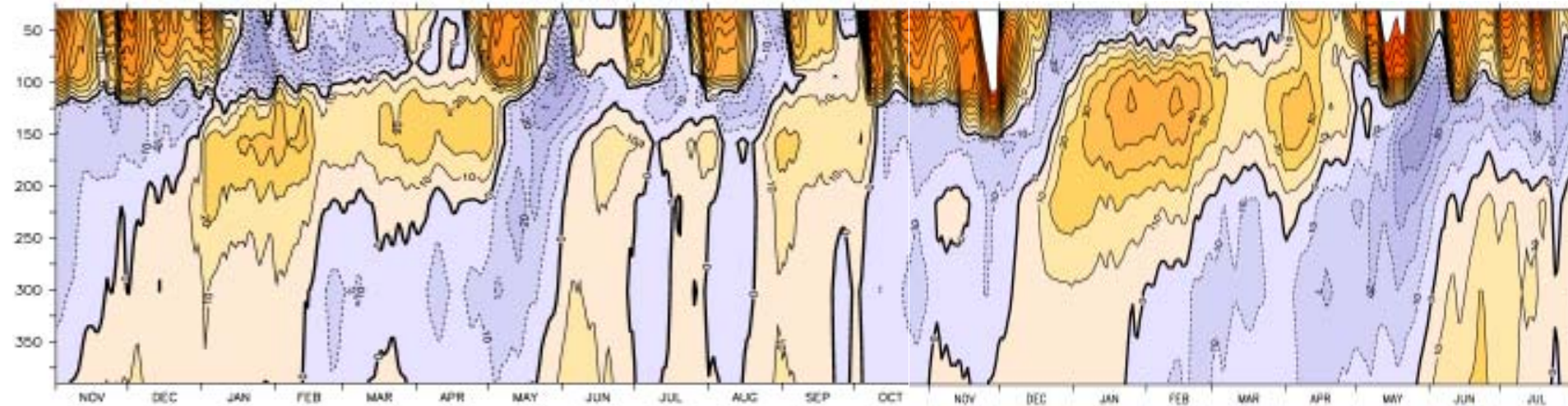
10-60 day current is strong in the equatorial waveguide; it is mostly wind forced

ZONAL VELOCITY 0° 90°E

OBS (MASUMOTO, 2004)



MODEL

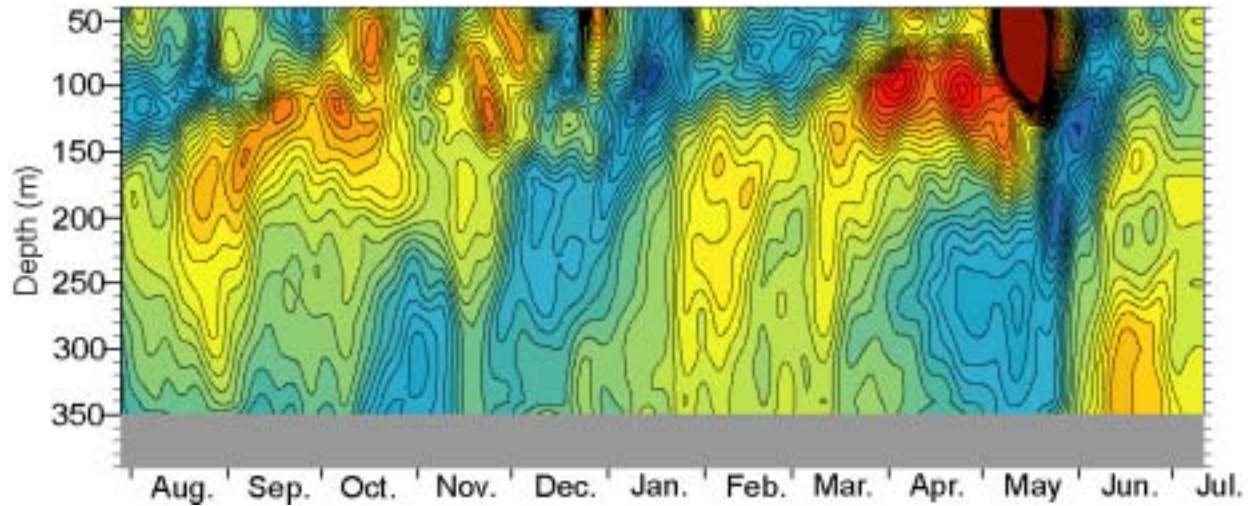


2001

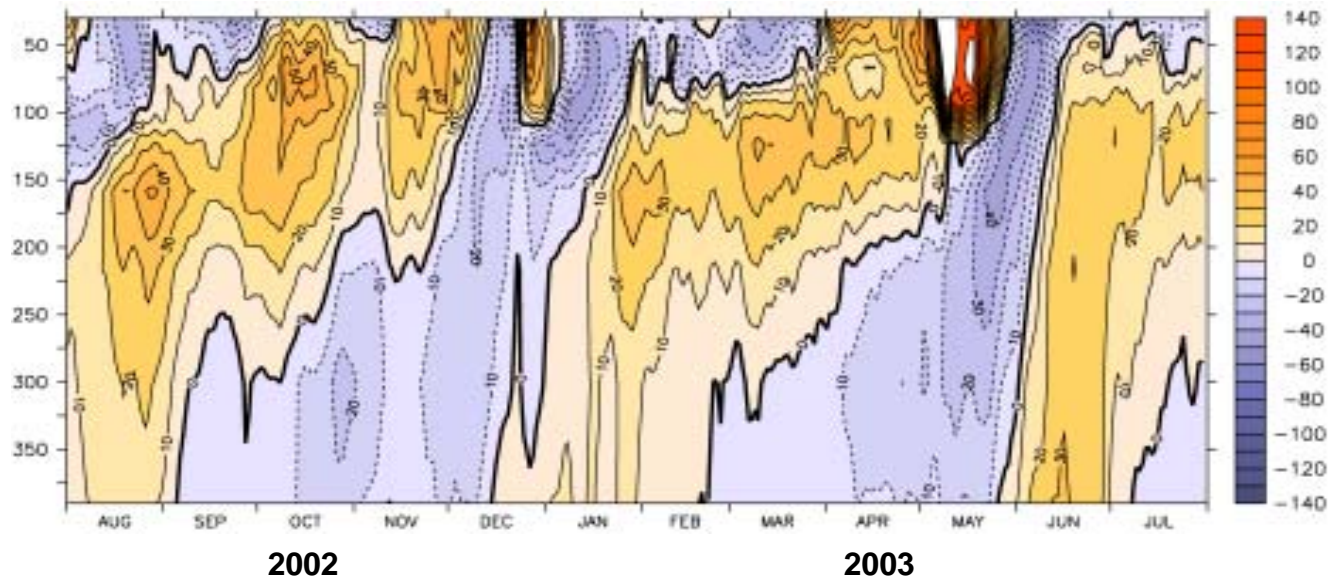
2002

ZONAL VELOCITY 0° 90°E

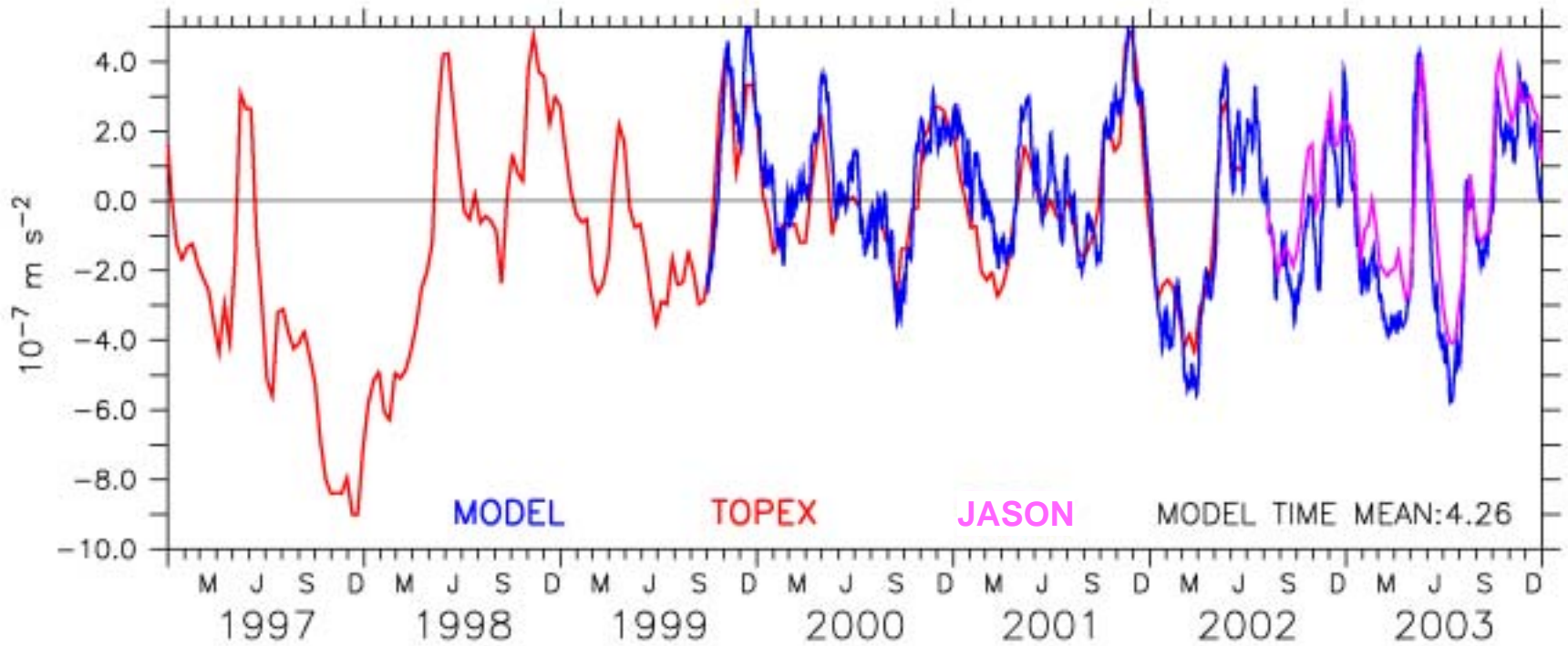
OBS

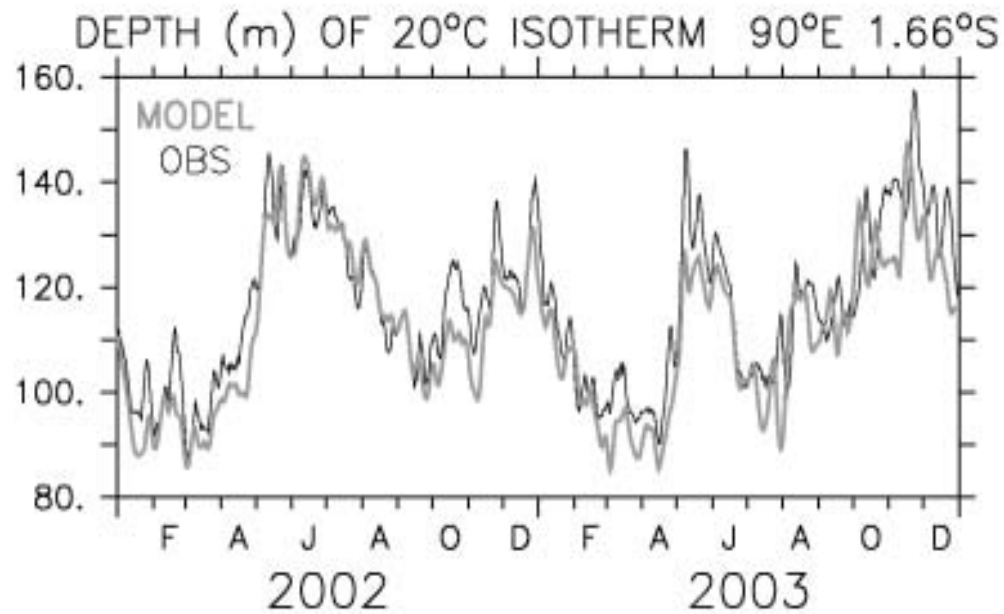
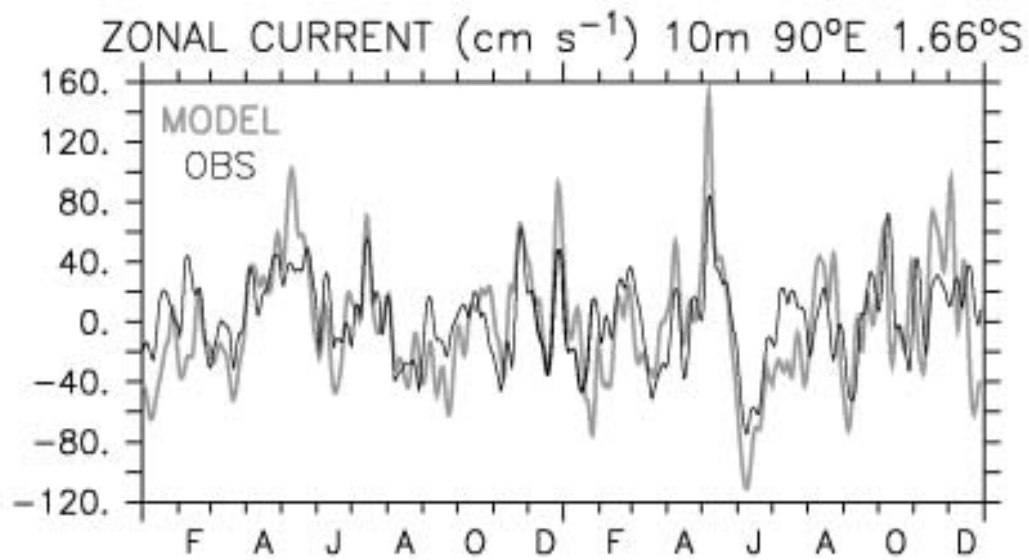


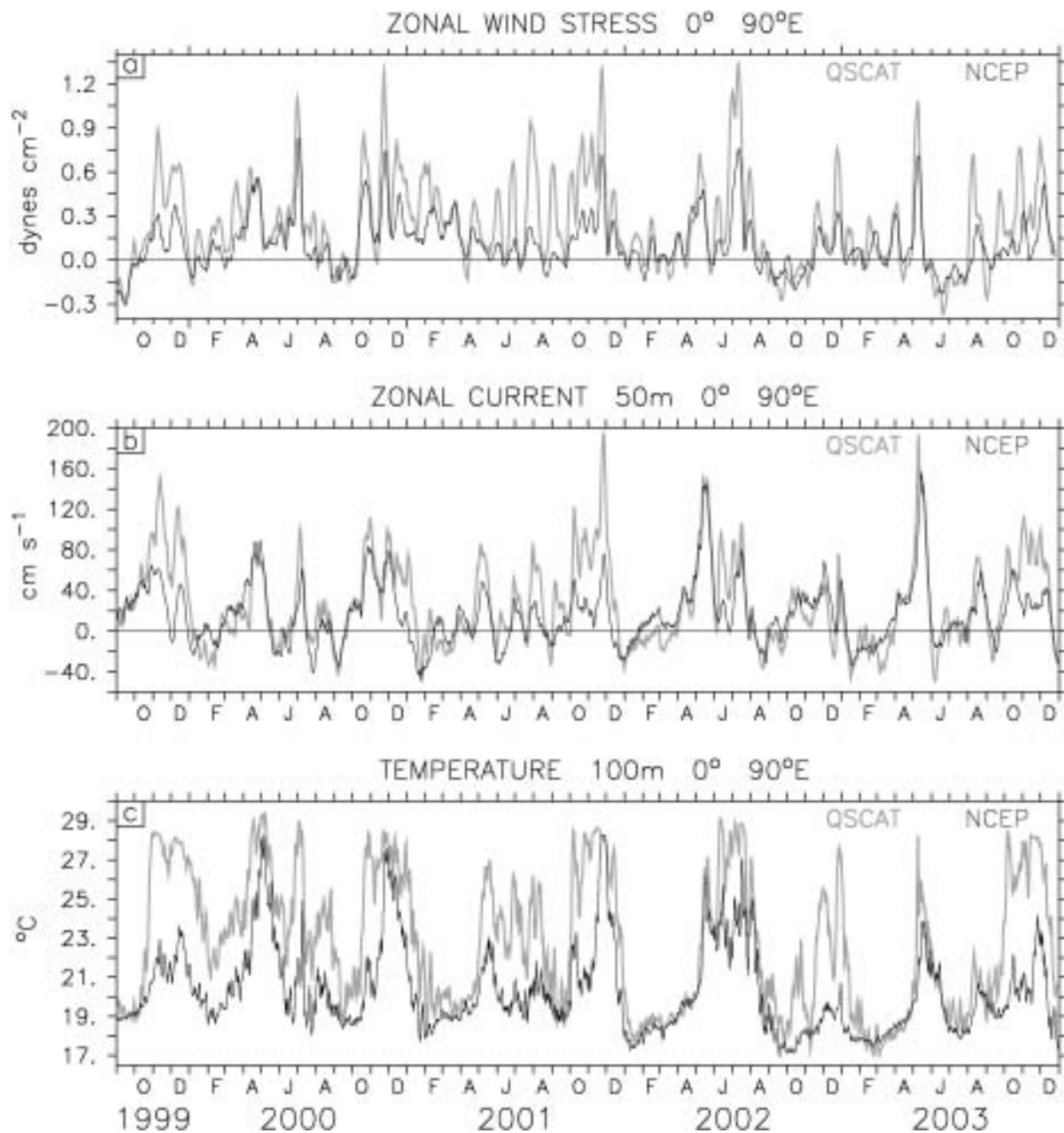
MODEL



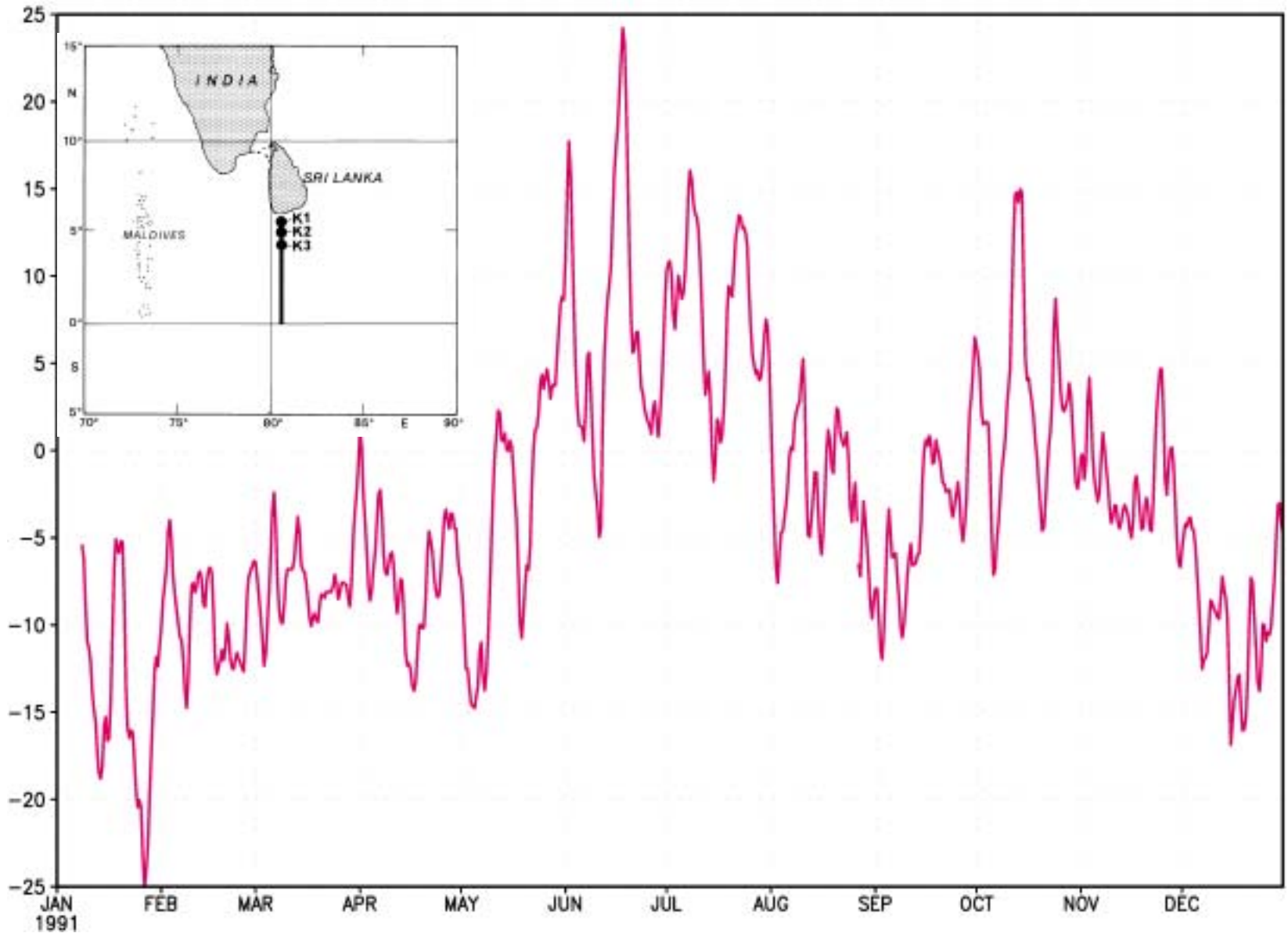
ZONAL PRESSURE GRADIENT 60-95°E 2°S-2°N

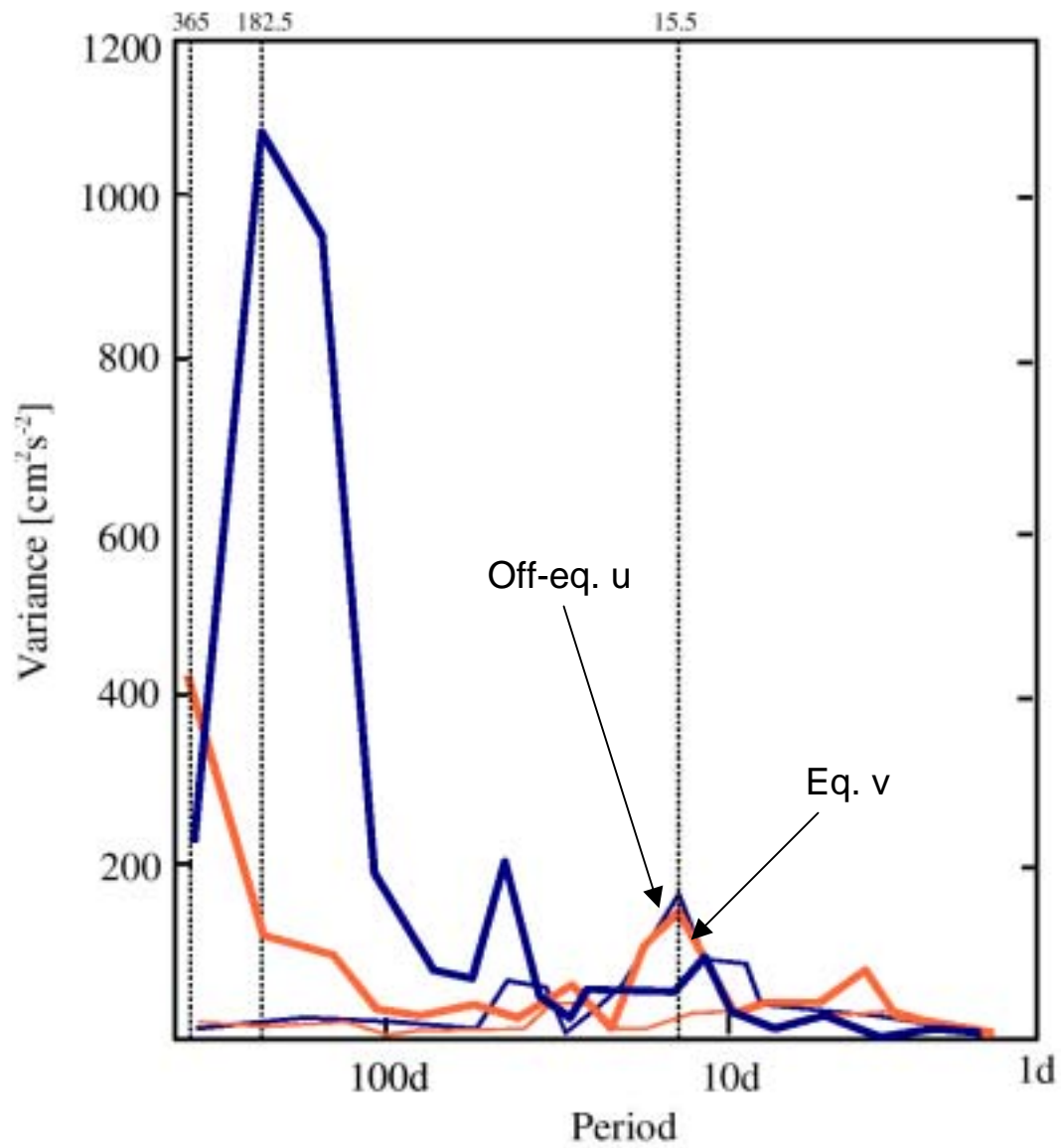




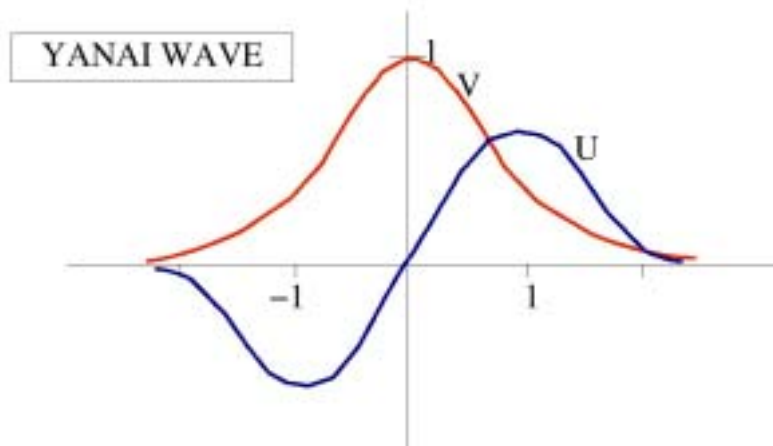
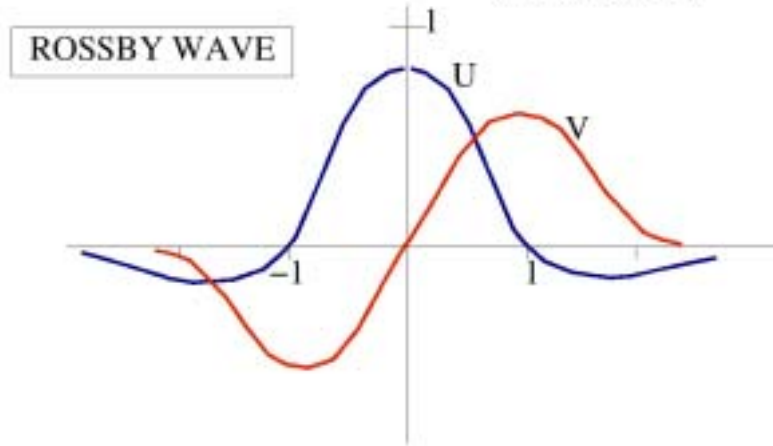
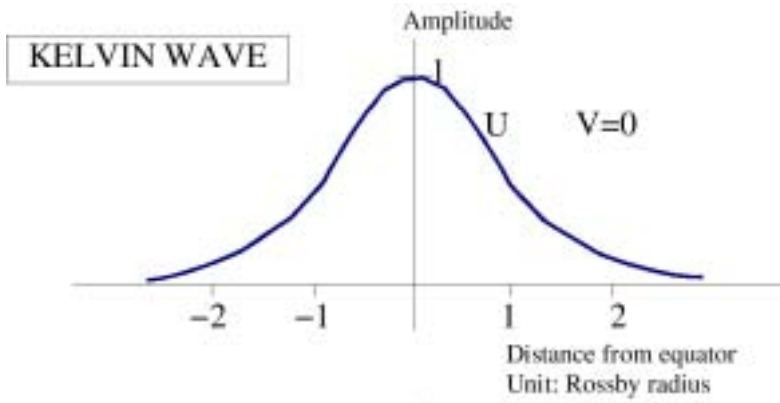


Upper Ocean Volume Transport (Sv) 80.5°E 3.5–5.6°N



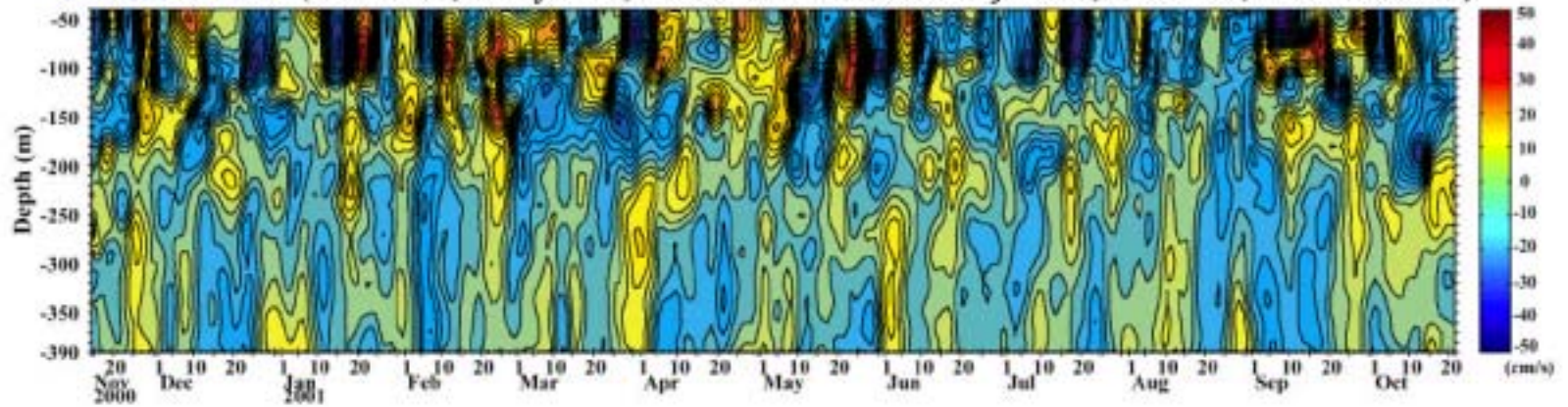


Reppin et al., 1996; Schott & McCreary, 2001

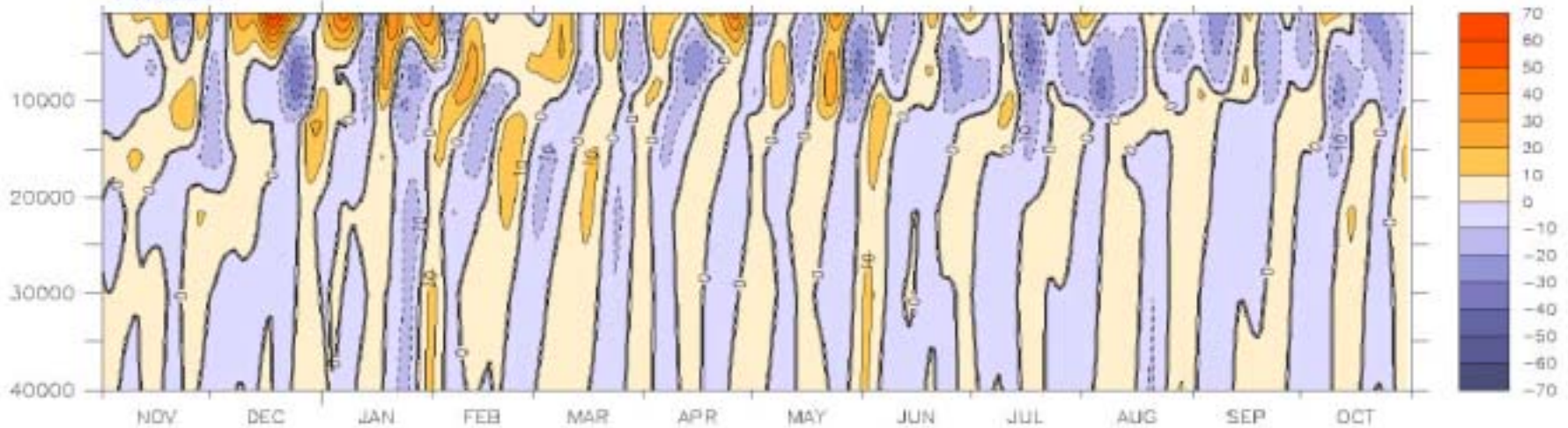


MERIDIONAL VELOCITY (cm s^{-1}) 90°E EQUATOR

OBSERVATION (Masumoto, Murty et al., Presented at IOGOSS Conference, Mauritius, November 2002)

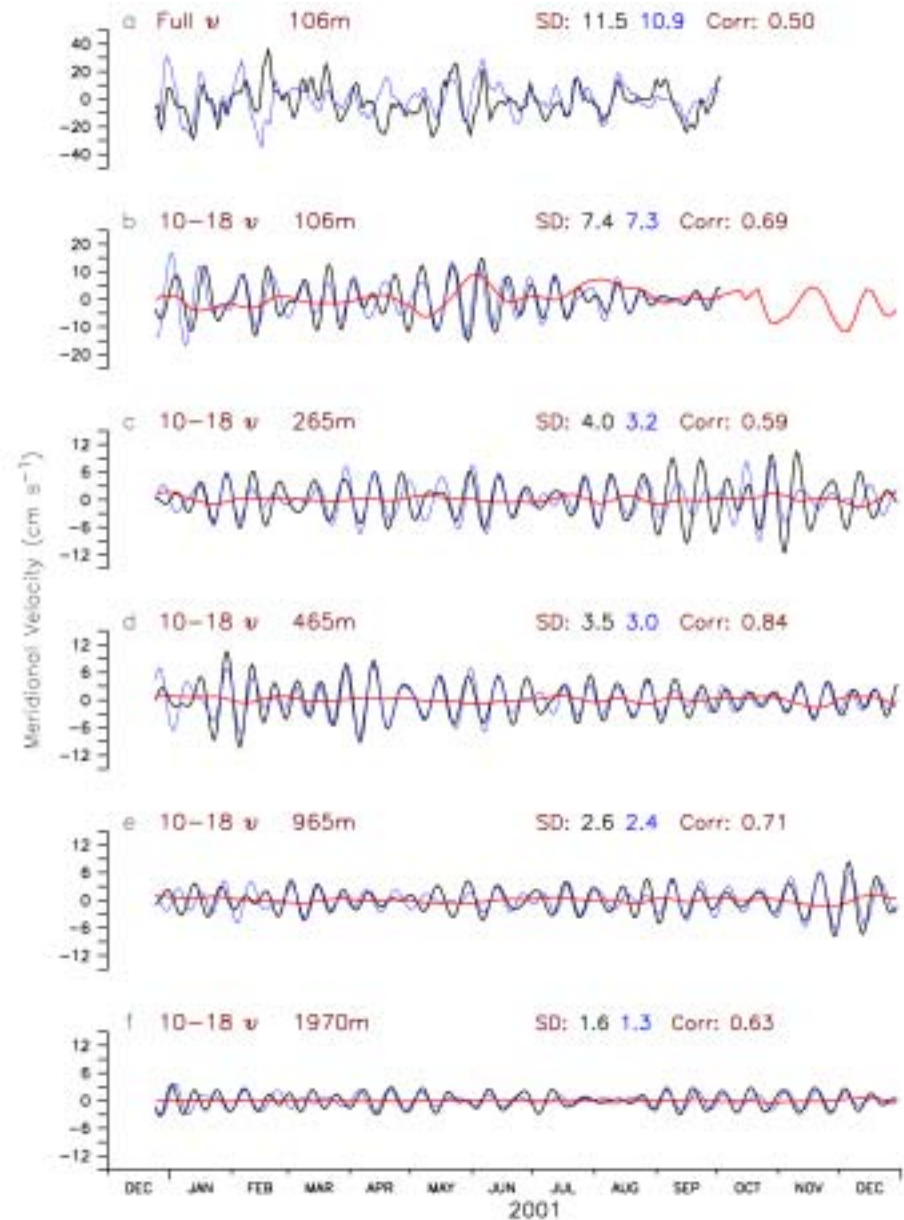
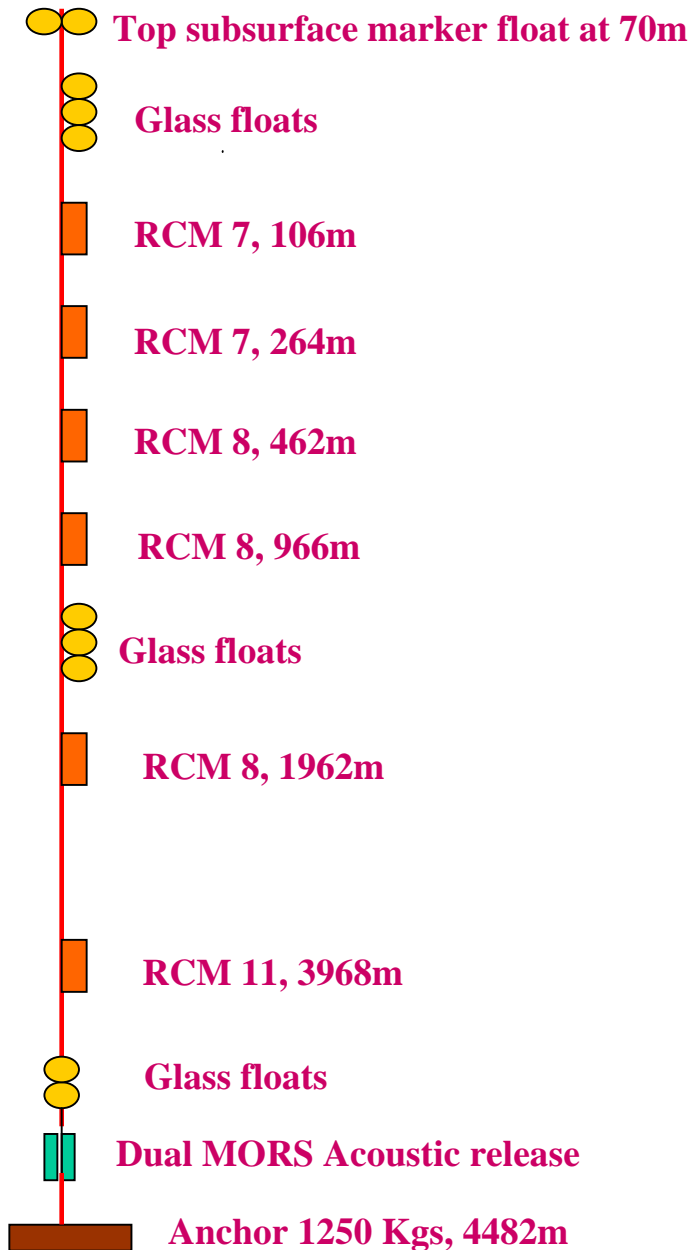


MODEL

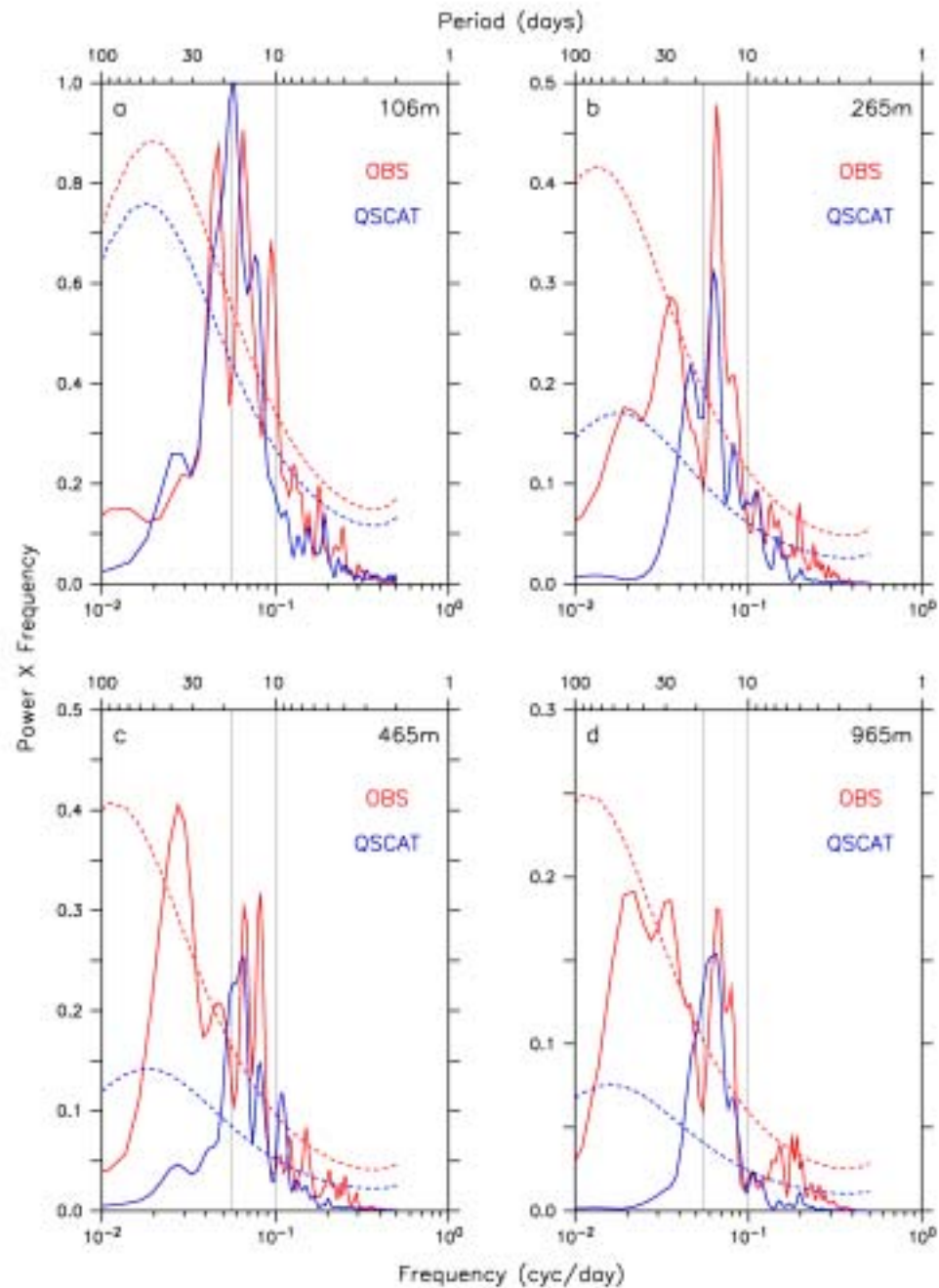


v variability: mainly 14-day Yanai waves at all depths + 30-60 day ?? below ~150m

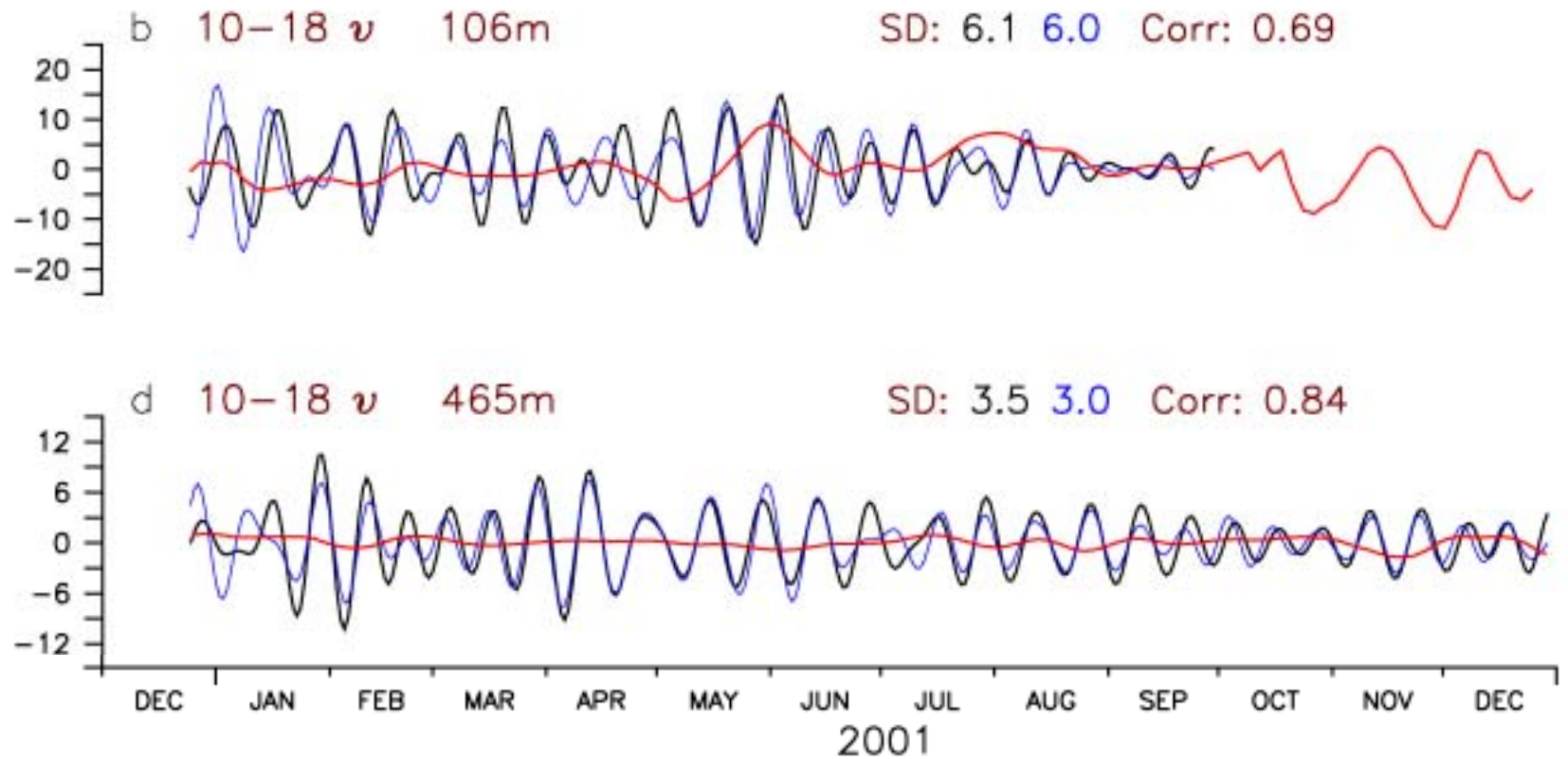
93°E NIO Obs and Model



POWER SPECTRUM ψ at observed depth 0° 93° E



MERIDIONAL VELOCITY (v) 0° 93°E Model vs Obs.

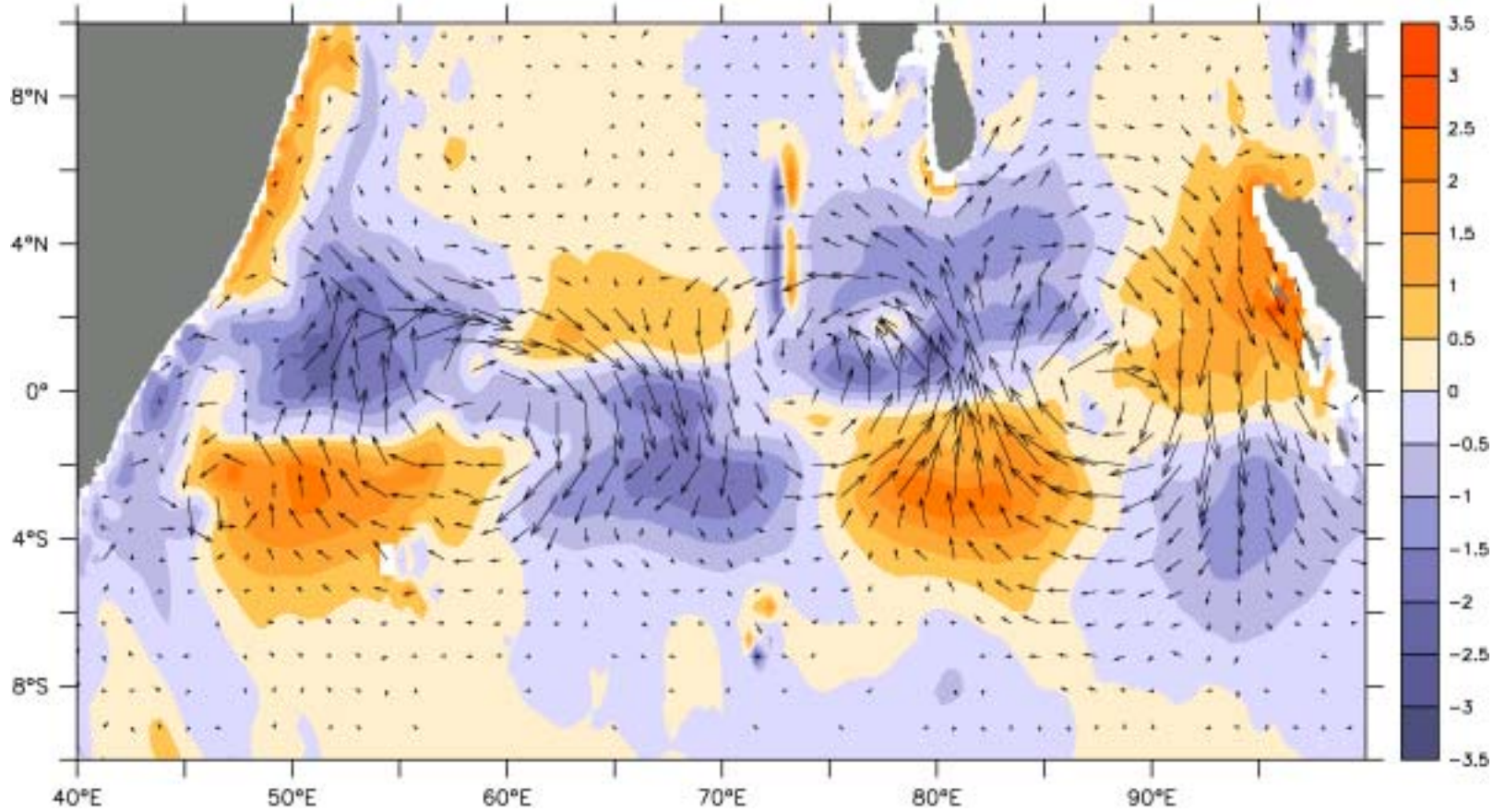


From NIO Observations

Period	Zonal wavelength (km)
10 Jan – 7 Feb 2001	3400
2 Mar – 22 Mar 2001	6100
1 Jun – 5 Jul 2001	2100
25 Jul – 30 Aug 2001	3100
5 Sep 2001 – 15 Oct 2001	3100

a. 93°E		b. 83°E	
Period	Vertical wavelength (m)	Period	Vertical wavelength (m)
30 Aug-27 Sep	4700	25 Feb-20 Mar	3200
2 Nov-27 Nov	1400	10 Oct-3 Nov	3200

VERTICAL VELOCITY (100m) AND CURRENTS (50m) 28 May 2001

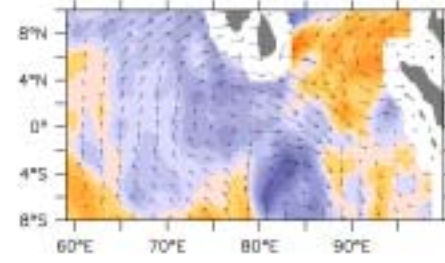
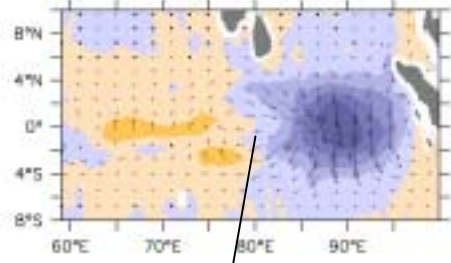


~3,300 km

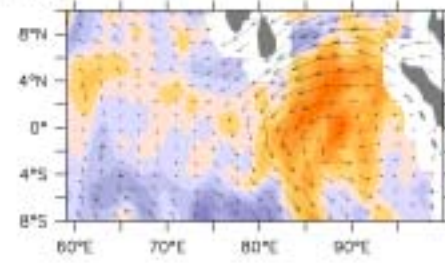
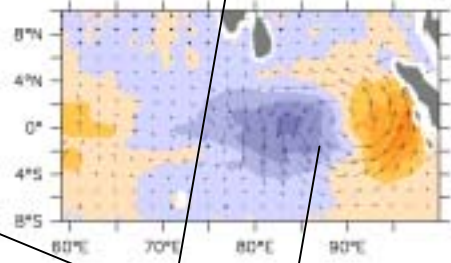
Meridional Velocity and Vectors at 50m

Windstress and its Curl

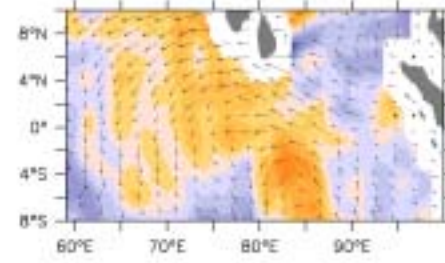
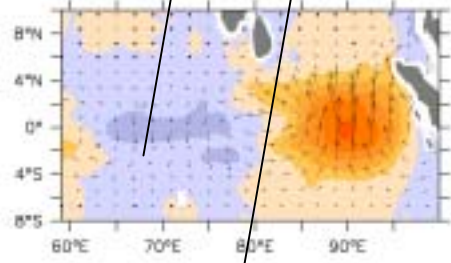
10 AUG 2000



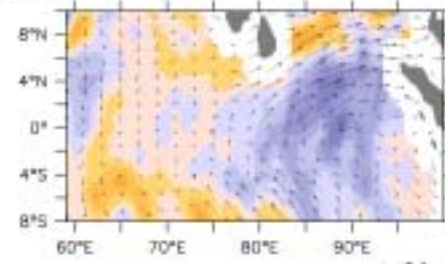
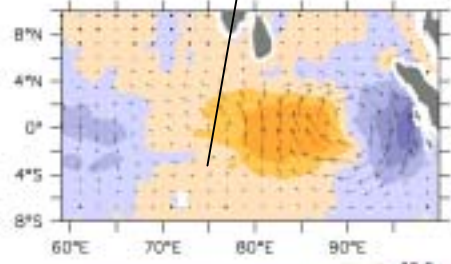
13 AUG 2000



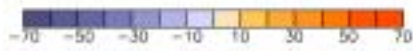
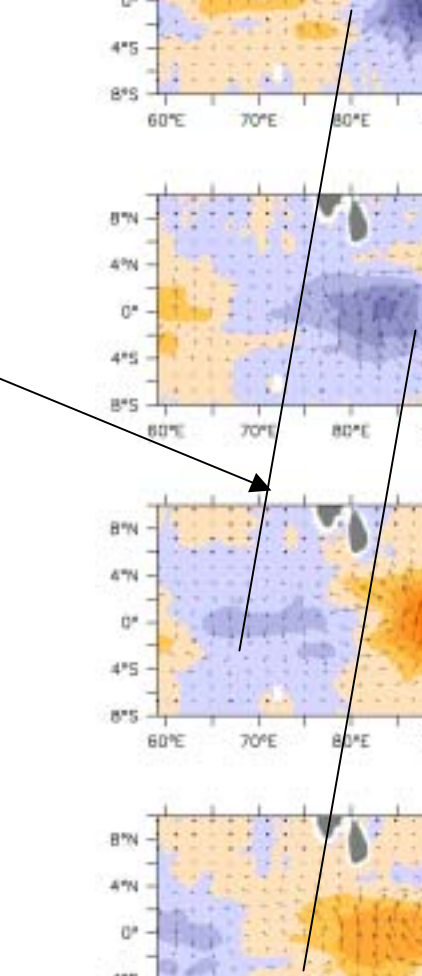
16 AUG 2000



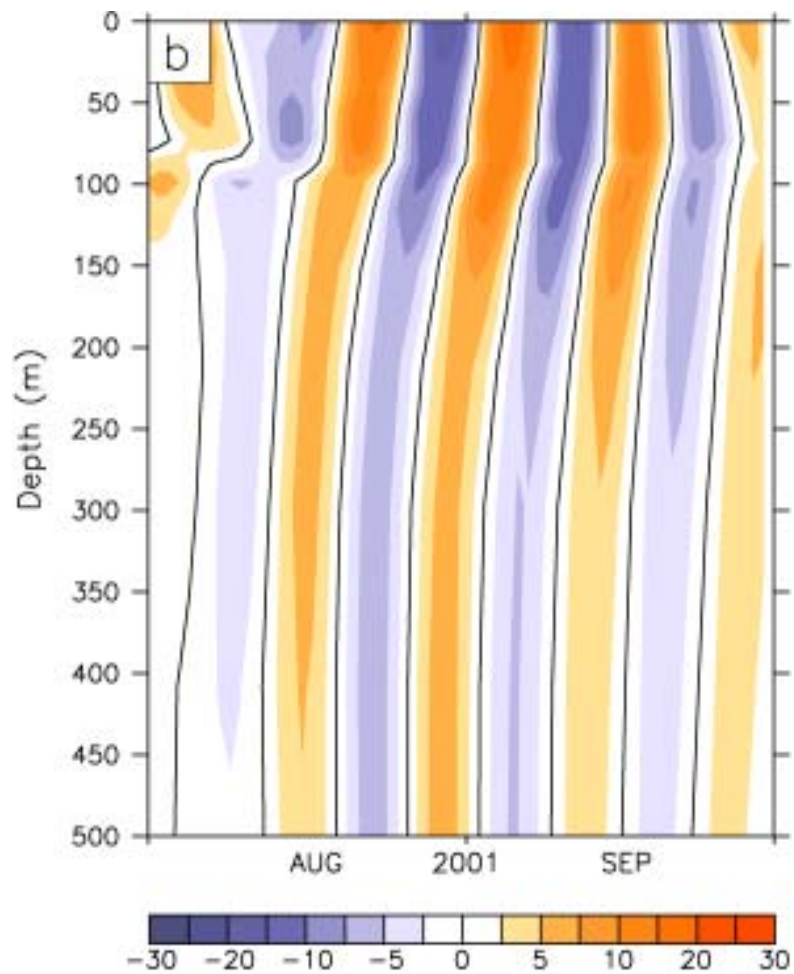
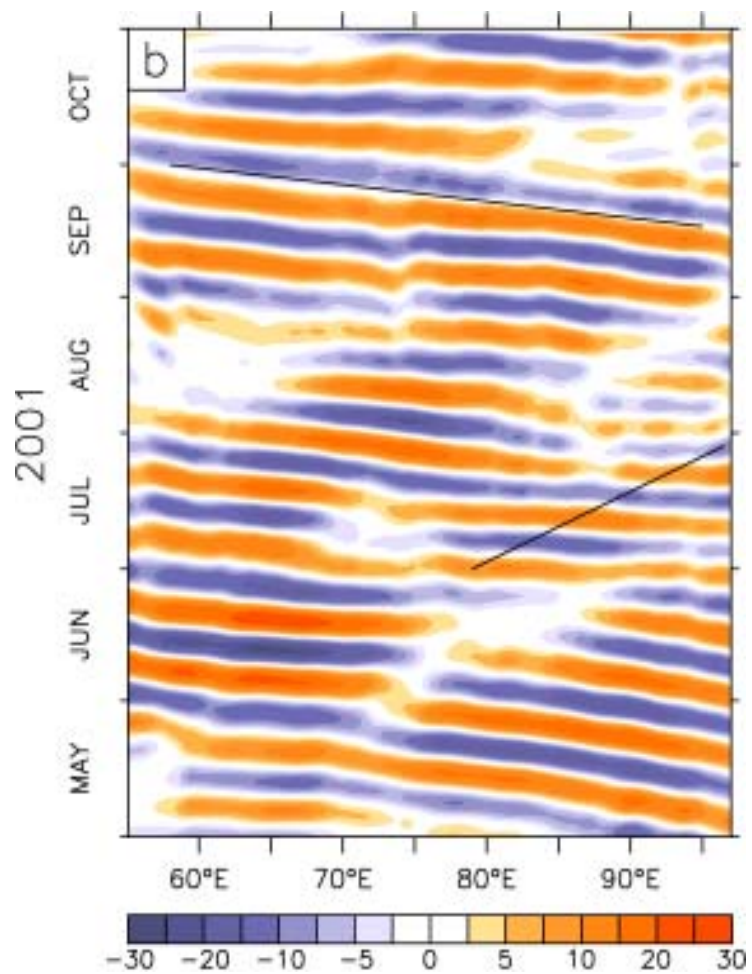
19 AUG 2000

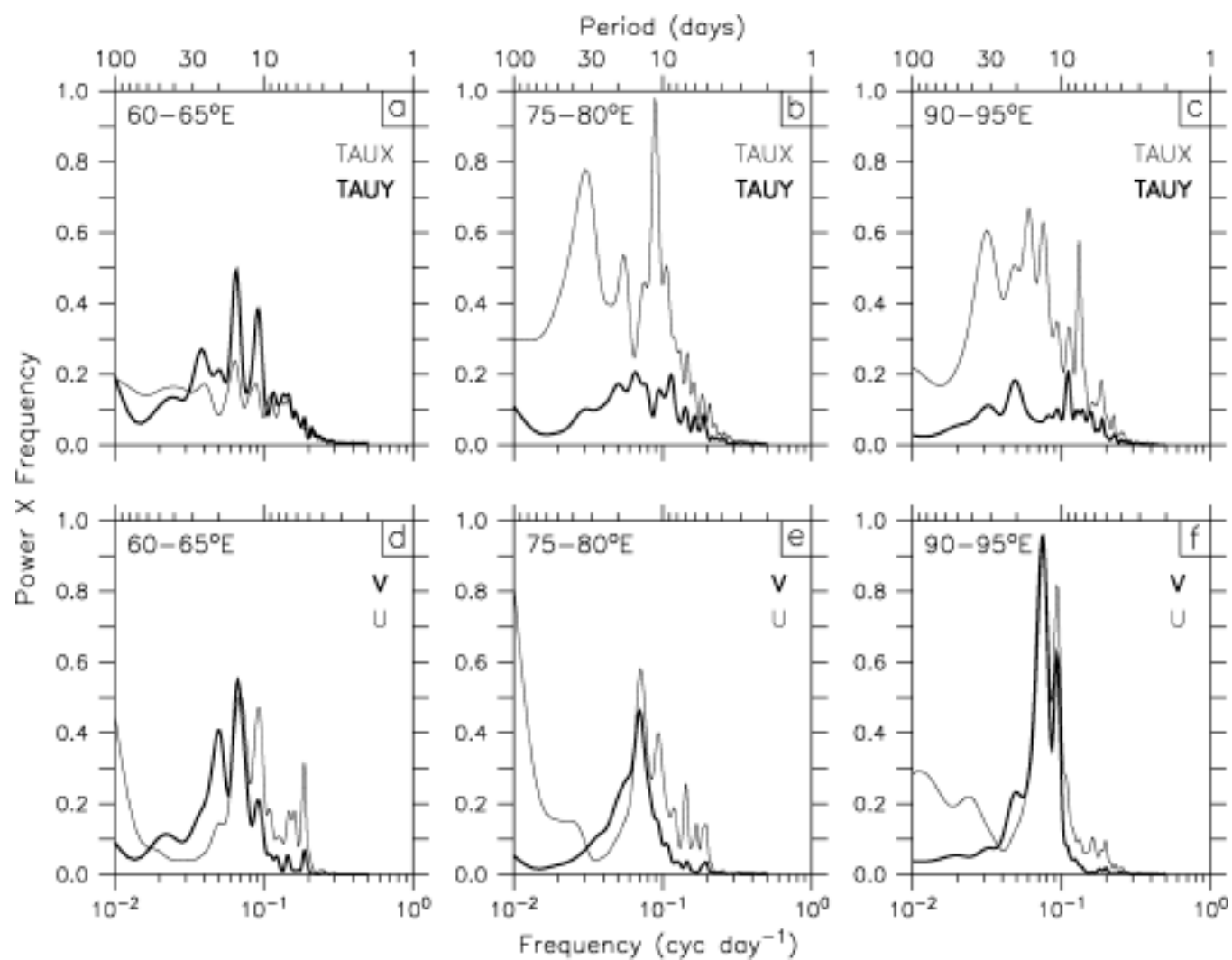


~4 m/s

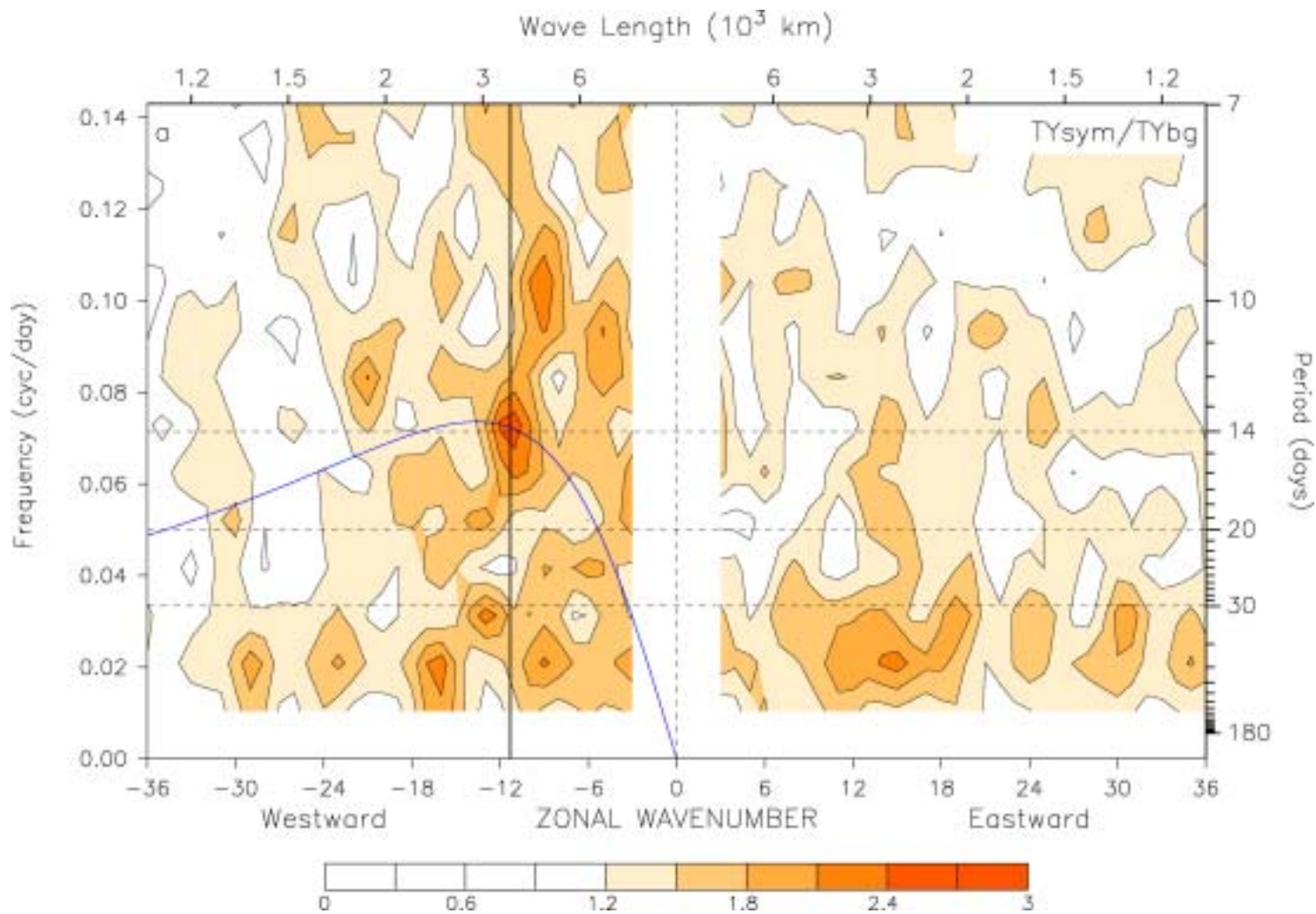


10-18 day Model v 1°S-1°N

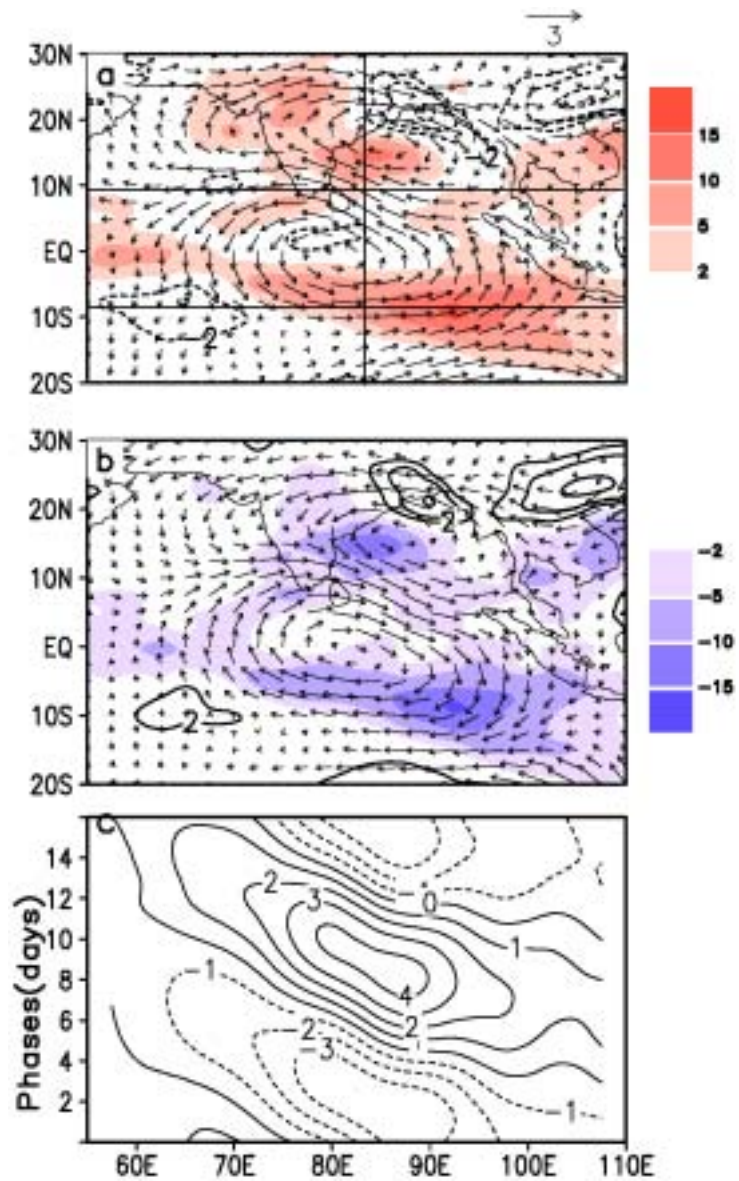




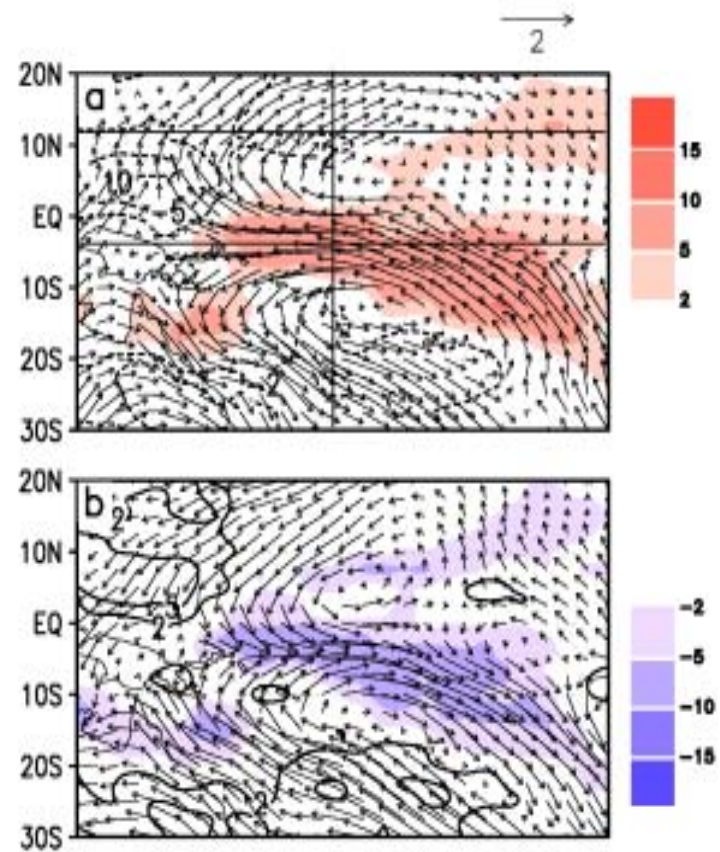
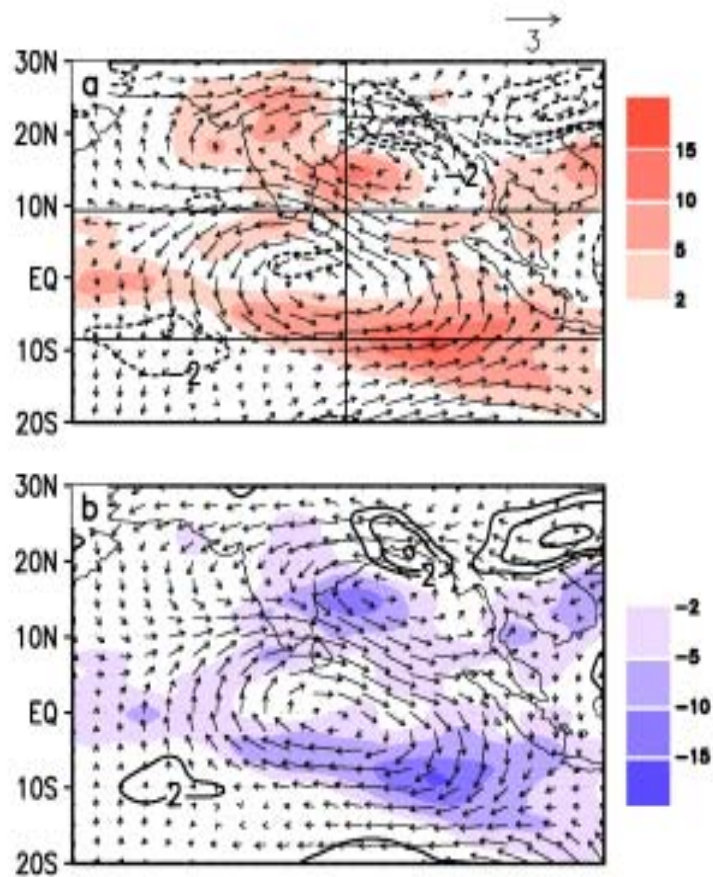
SPACE-TIME SPECTRUM τ_y

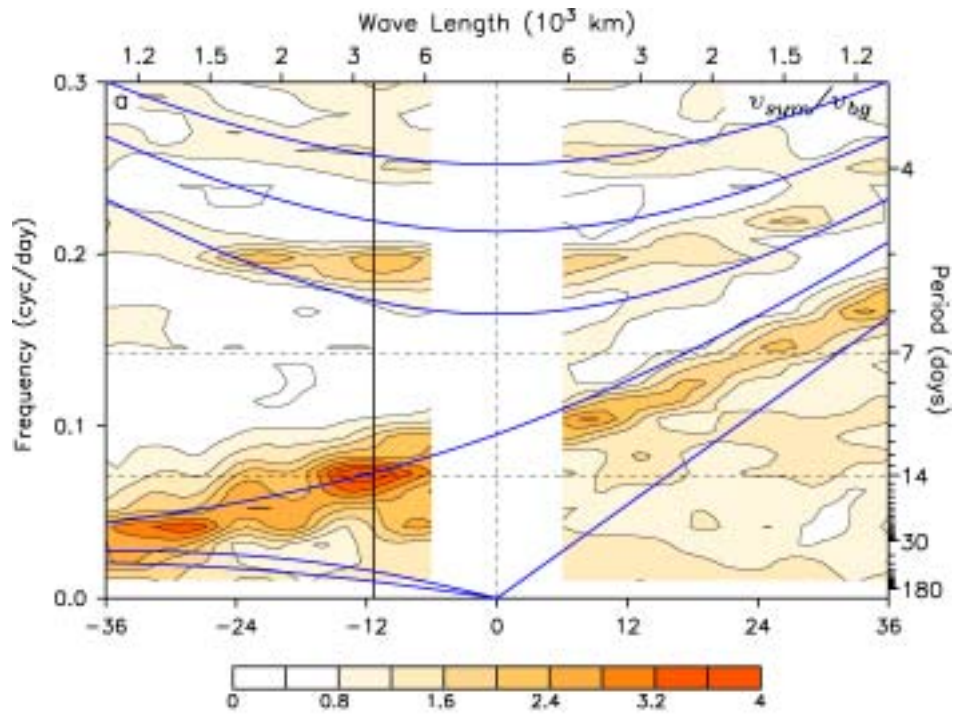


QBO: Chatterjee & Goswami,
2004 QJRMS



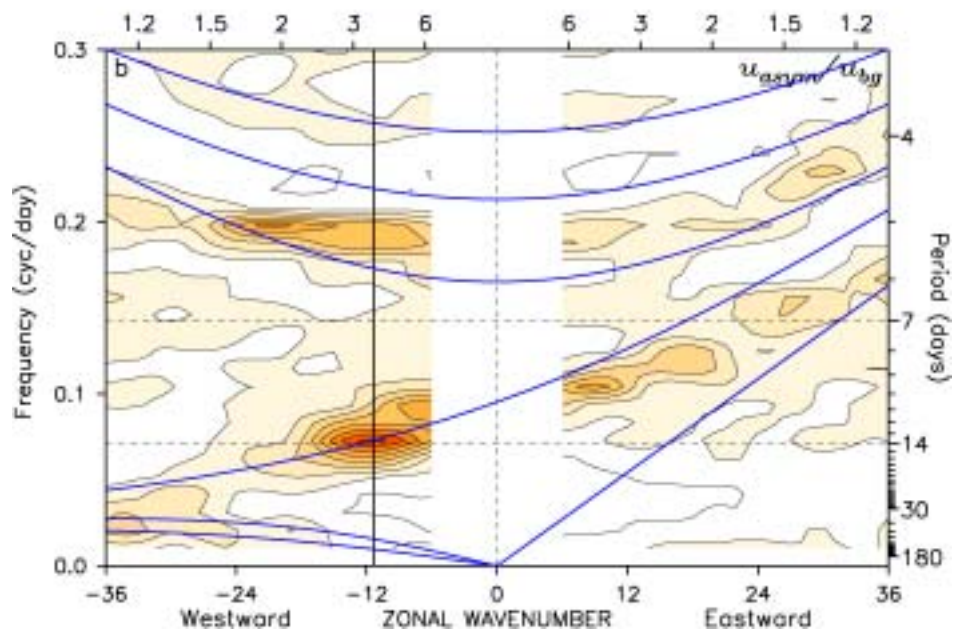
CHATTERJEE and GOSWAMI

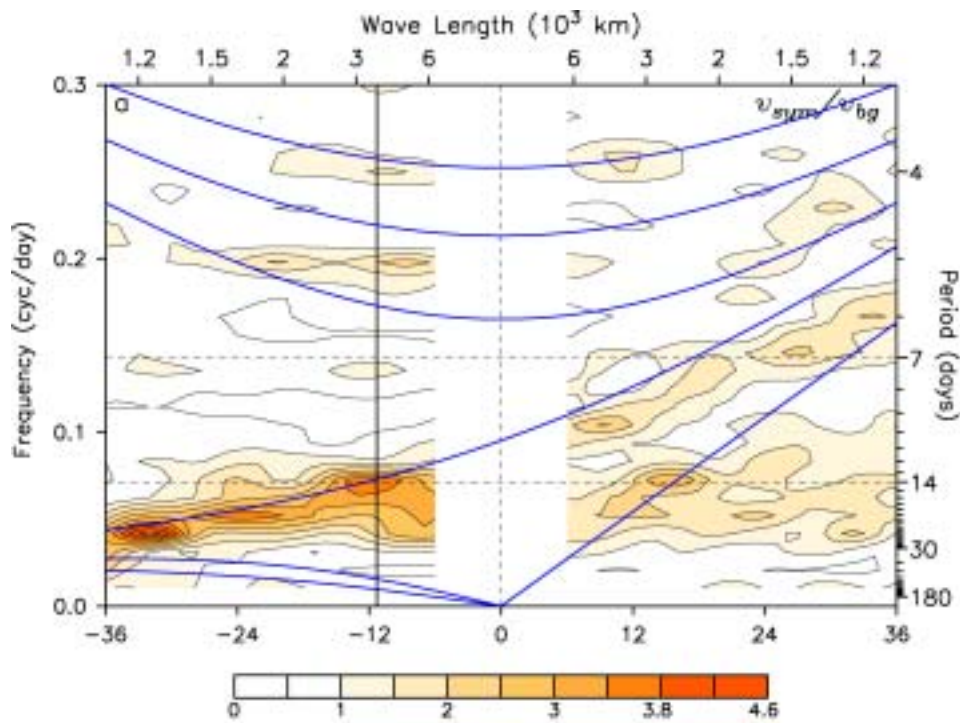




SPACE-TIME SPECTRUM

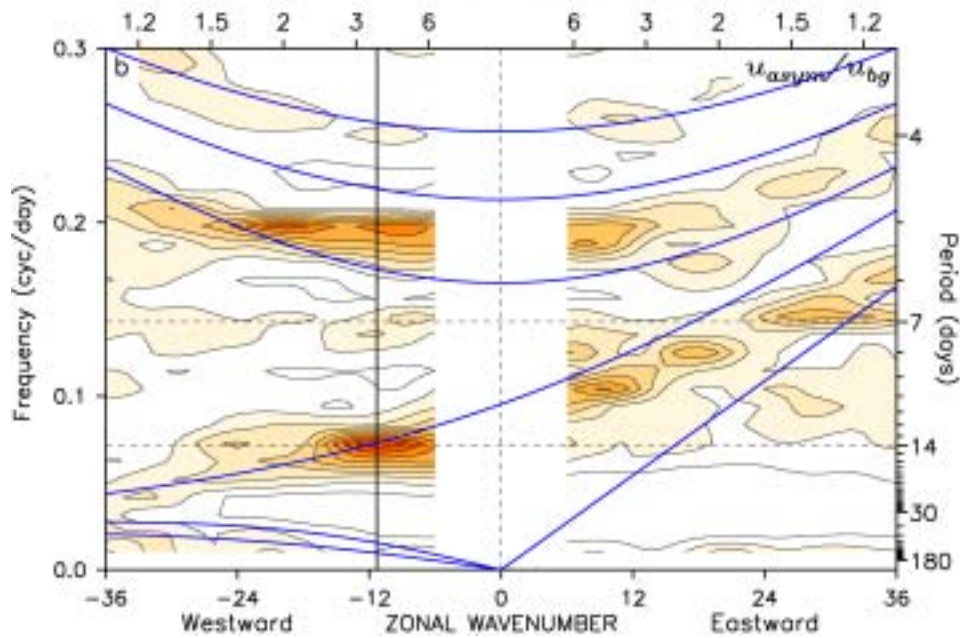
v 50m





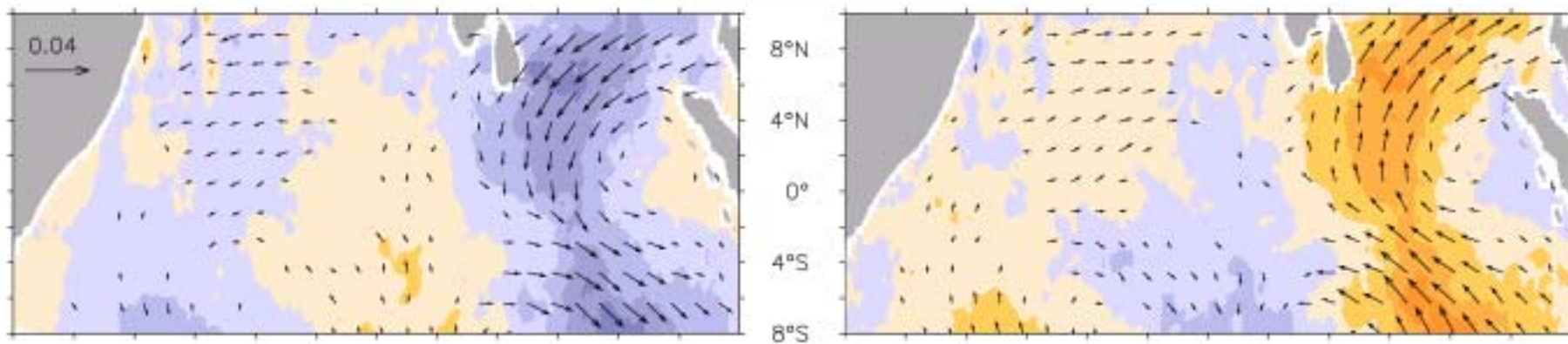
SPACE-TIME SPECTRUM

v 500m

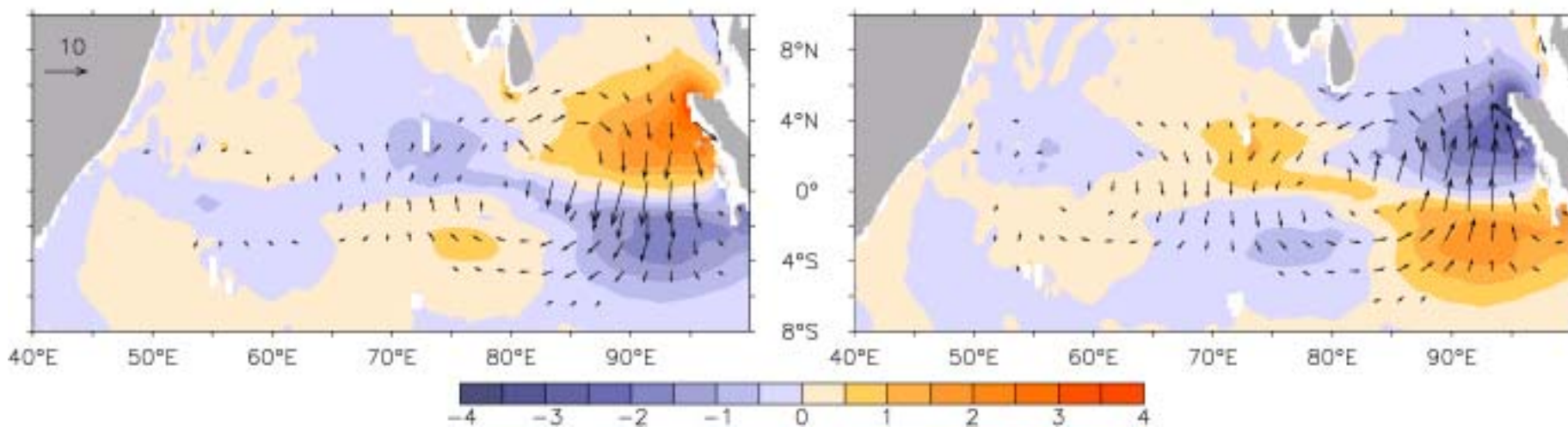


COMPOSITE HORIZONTAL STRUCTURE OF THE BIWEEKLY WAVE

Meridional wind stress and vectors (N m^{-2}) 85–90°E composite

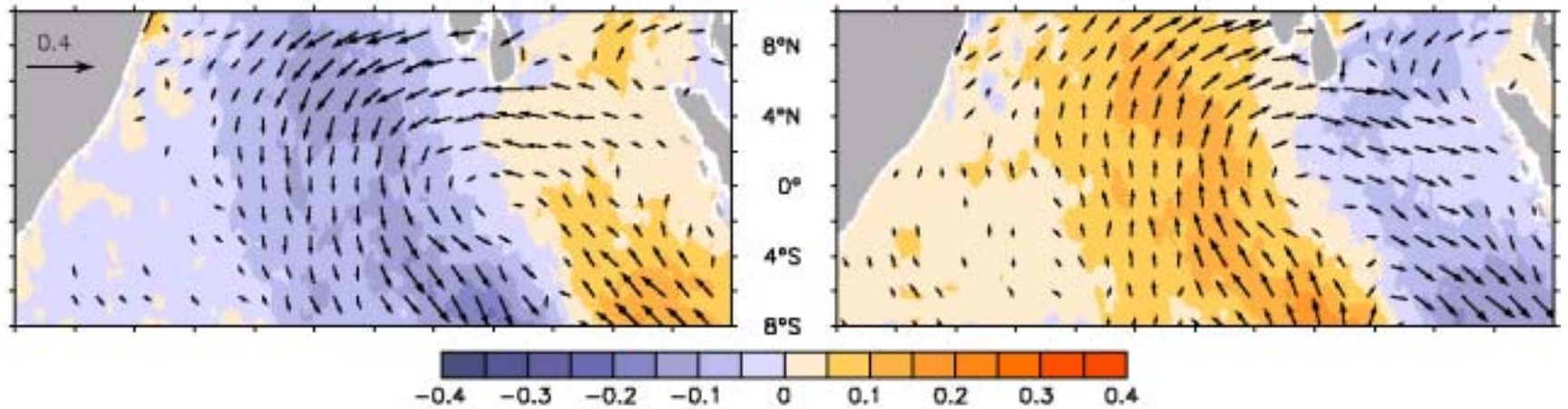


Vertical velocity (m day^{-1}) and current vectors (cm s^{-1}) at 100m 90–95°E composite

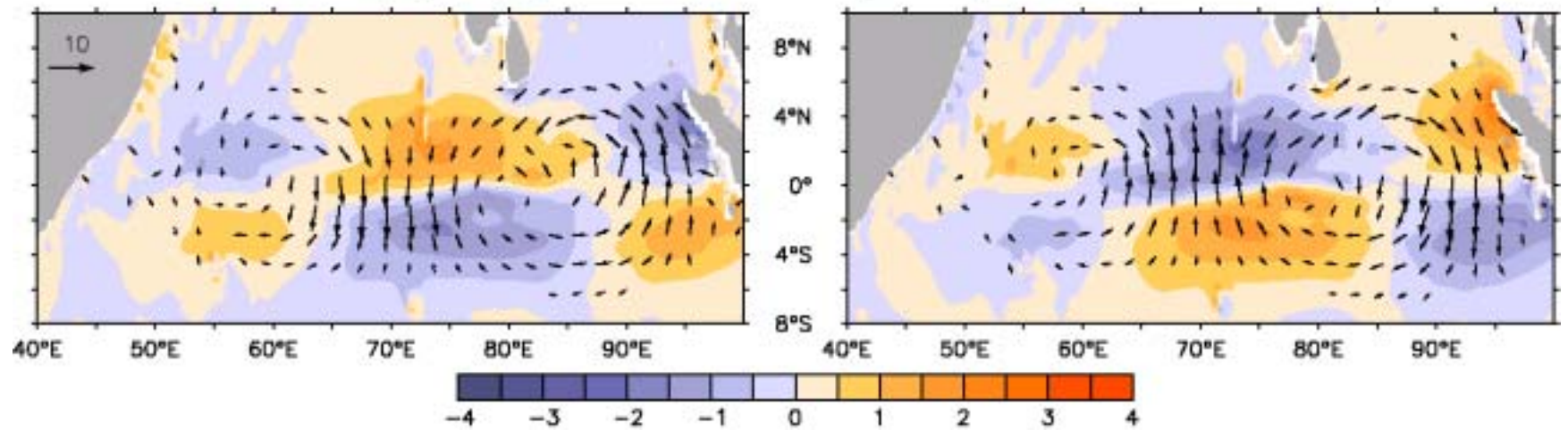


COMPOSITE HORIZONTAL STRUCTURE OF THE BIWEEKLY WAVE

Meridional wind stress and vectors (dyn cm^{-2}) 70–75°E composite

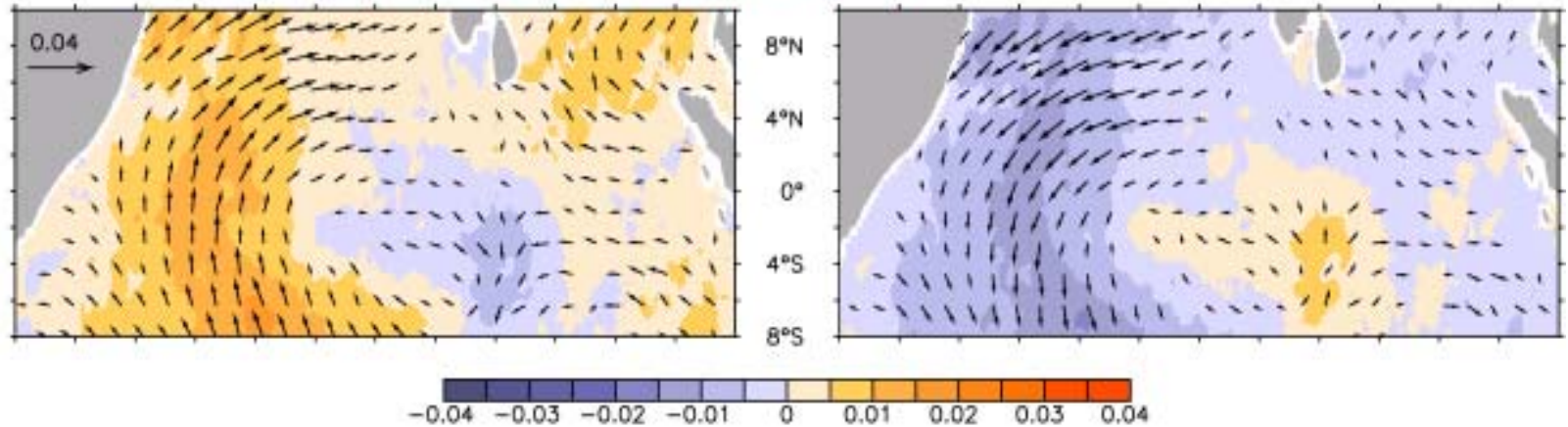


Vertical velocity (m day^{-1}) and current vectors (cm s^{-1}) at 100m 70–75°E composite

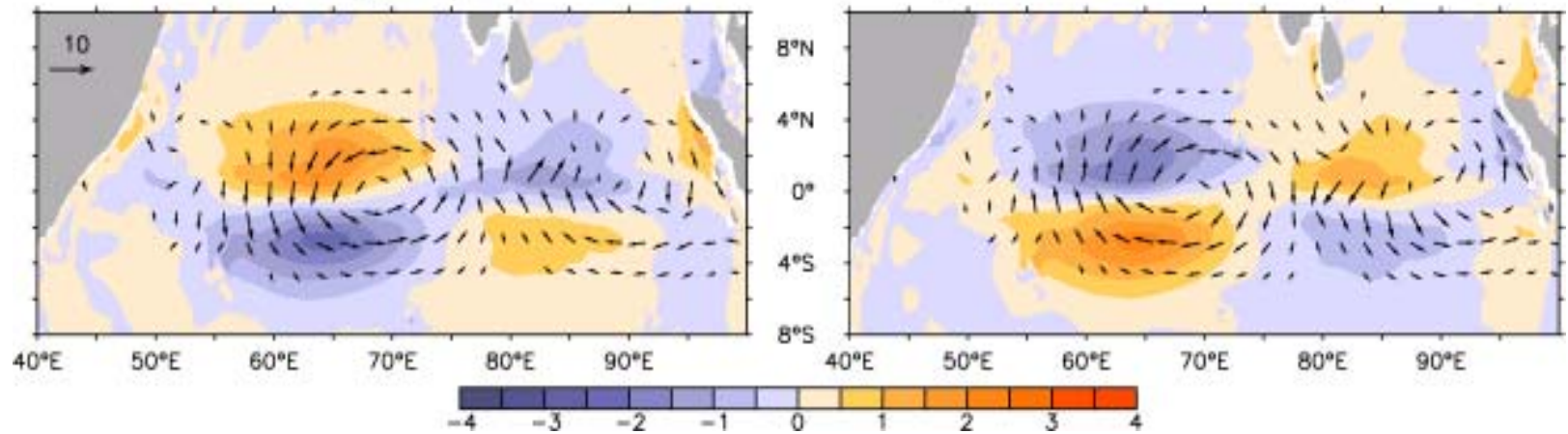


COMPOSITE HORIZONTAL STRUCTURE OF THE BIWEEKLY WAVE

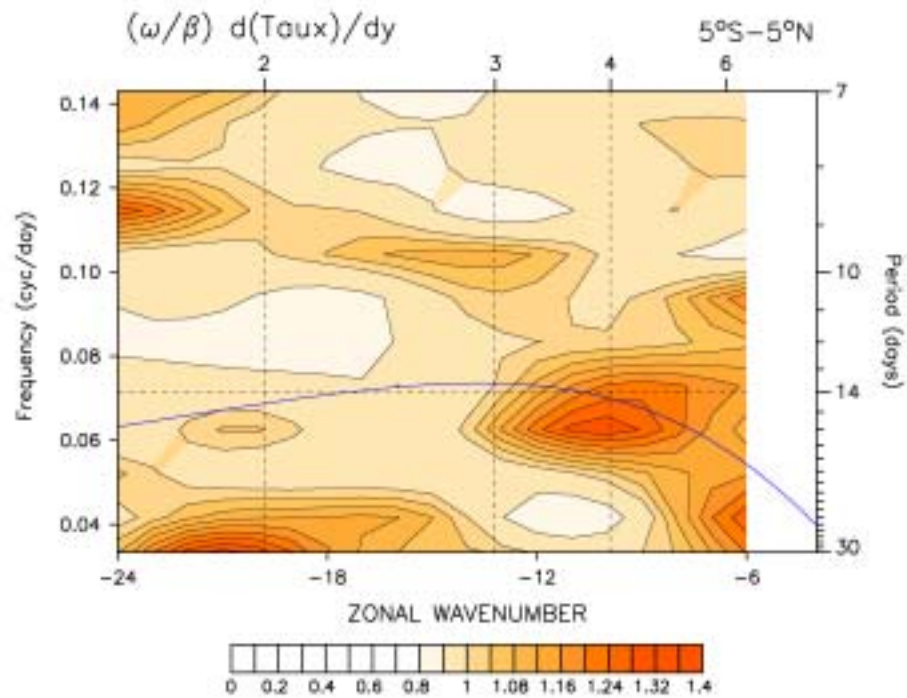
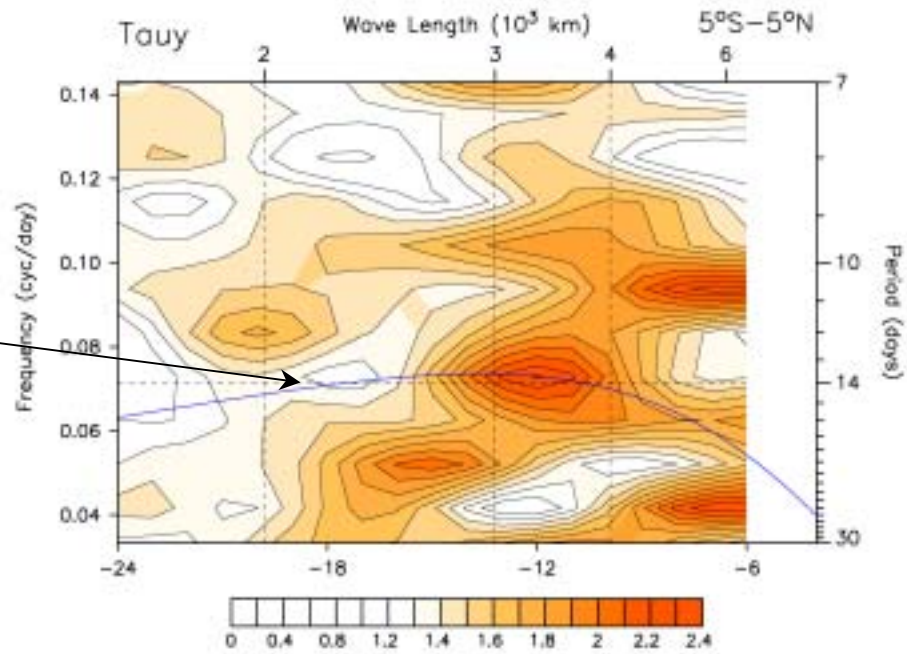
Meridional wind stress and vectors (N m^{-2}) 55–65°E composite



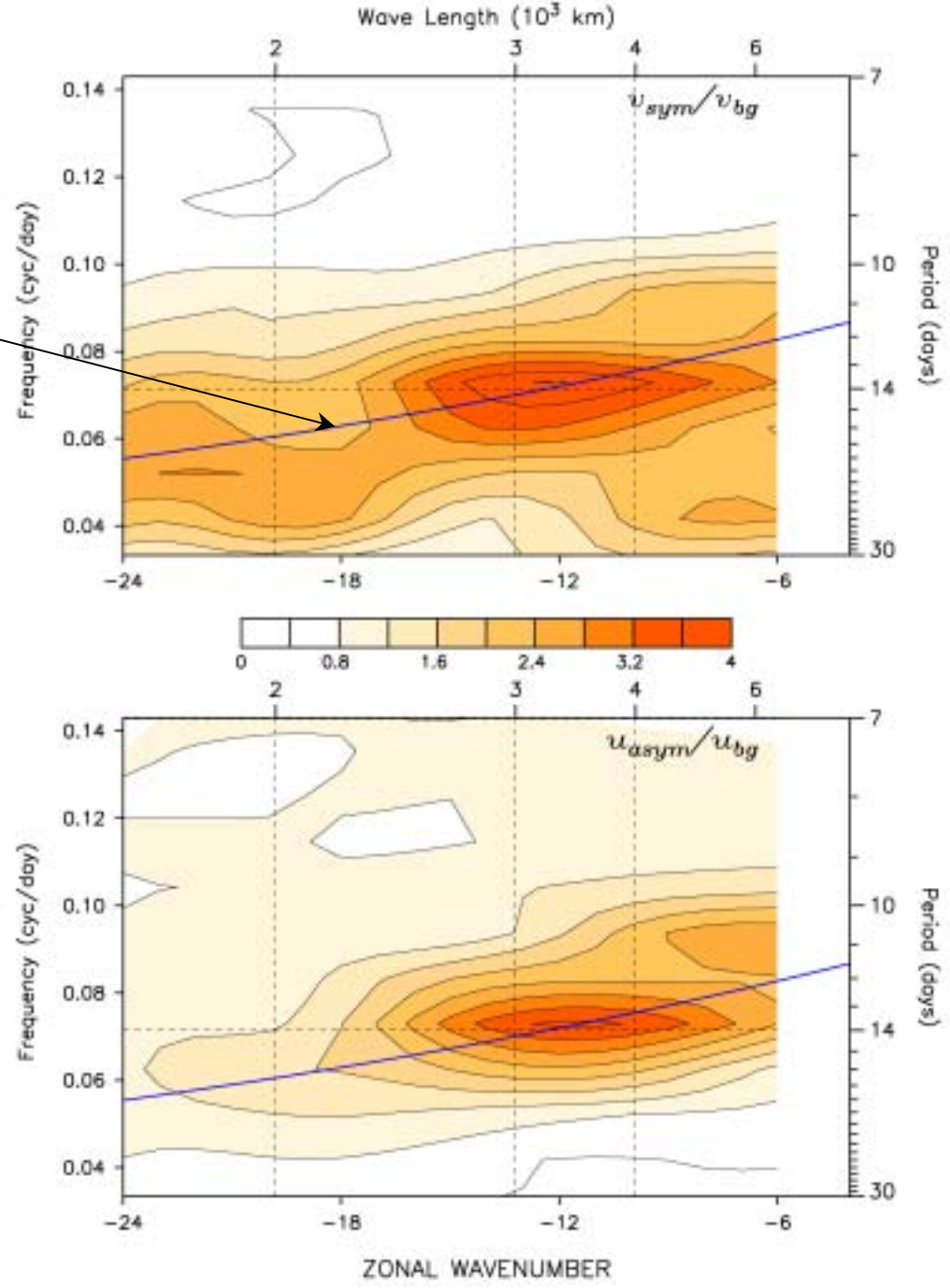
Vertical velocity (m day^{-1}) and current vectors (cm s^{-1}) at 100m 60–65°E composite



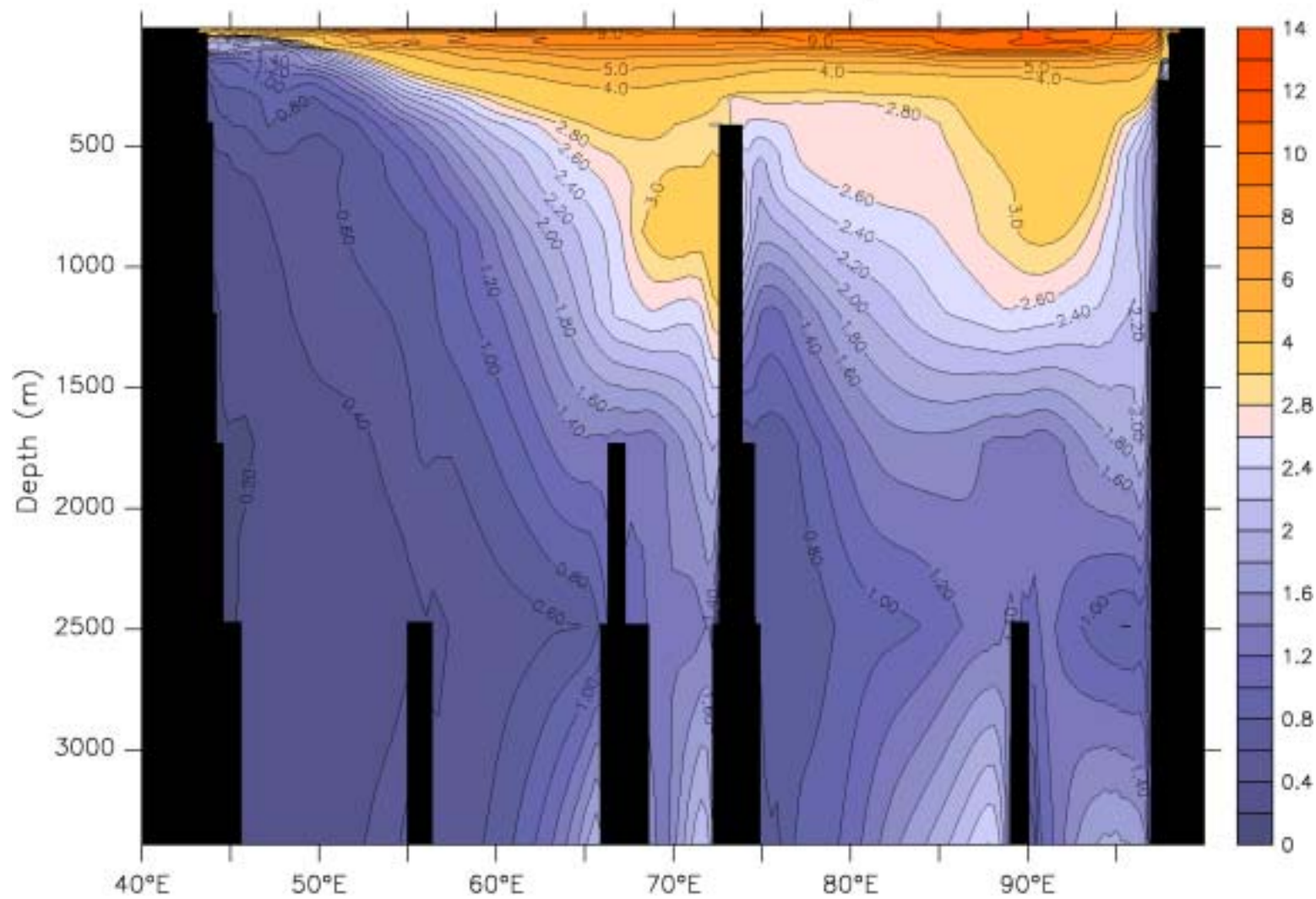
Rossby wave dispersion
curve $c = 15 \text{ ms}^{-1}$



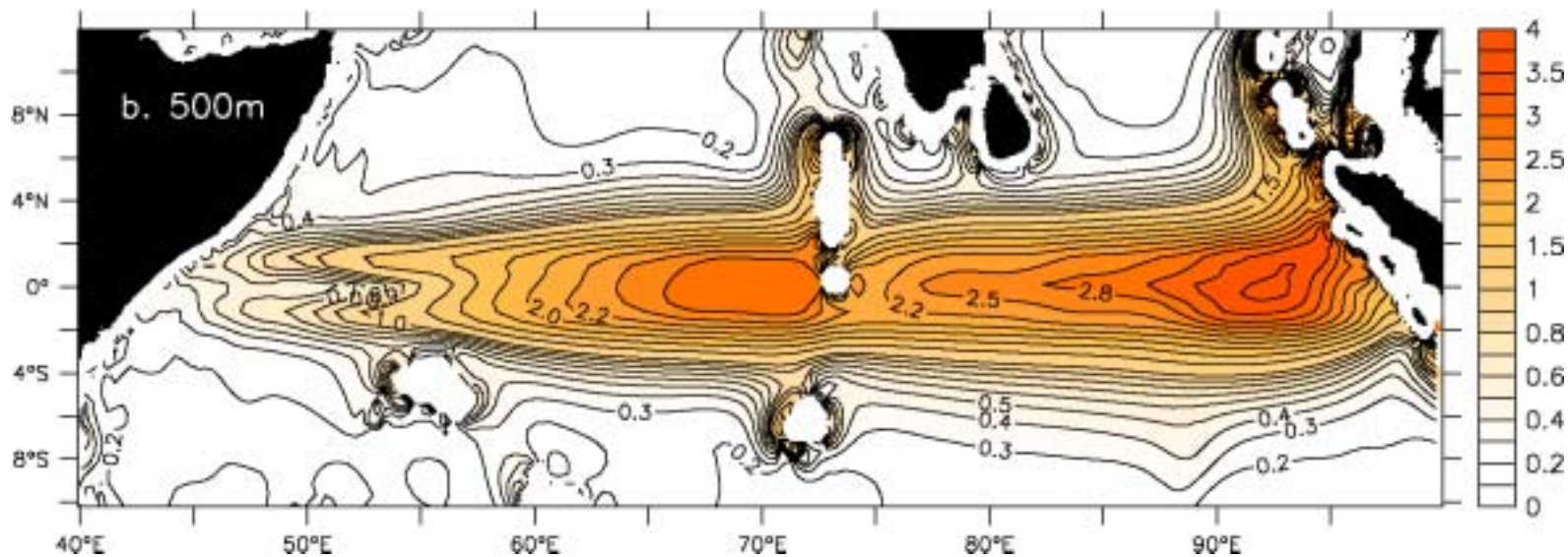
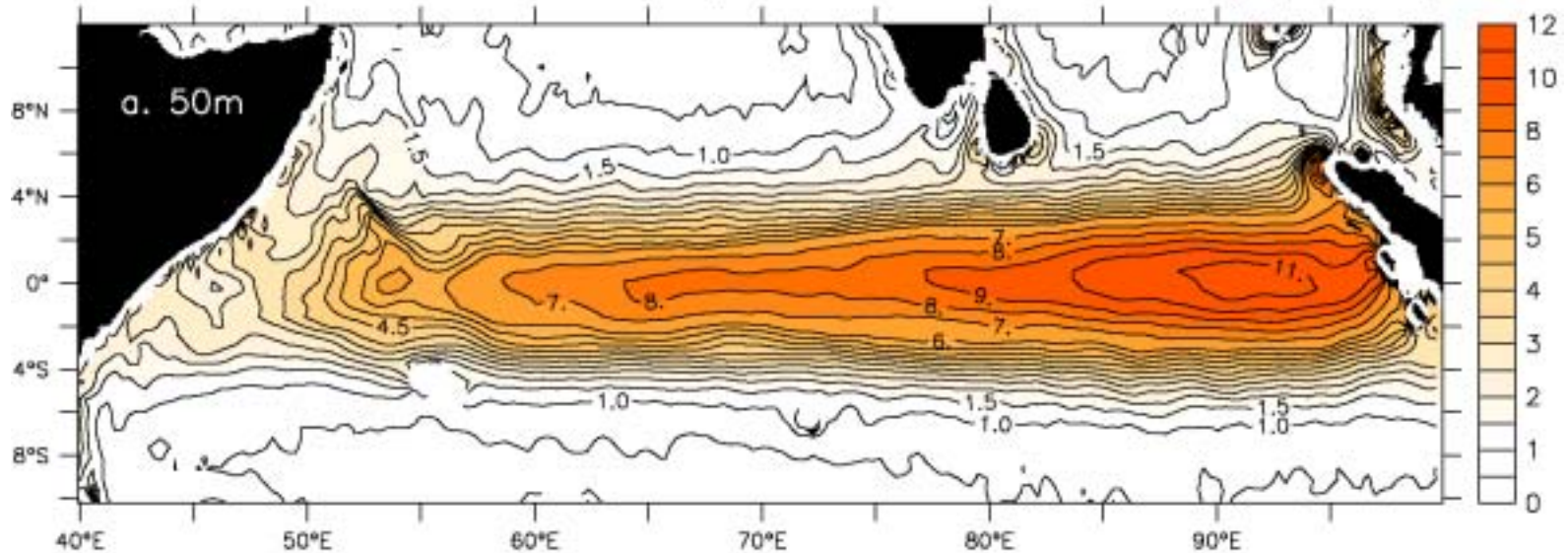
Yanai wave dispersion curve $c=2.1 \text{ ms}^{-1}$

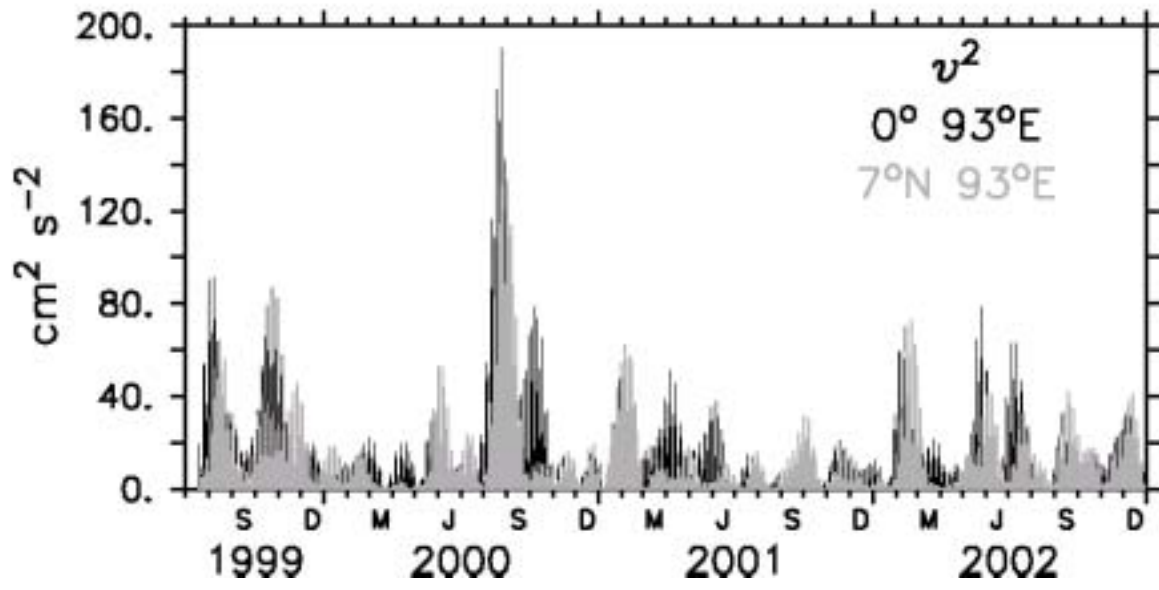
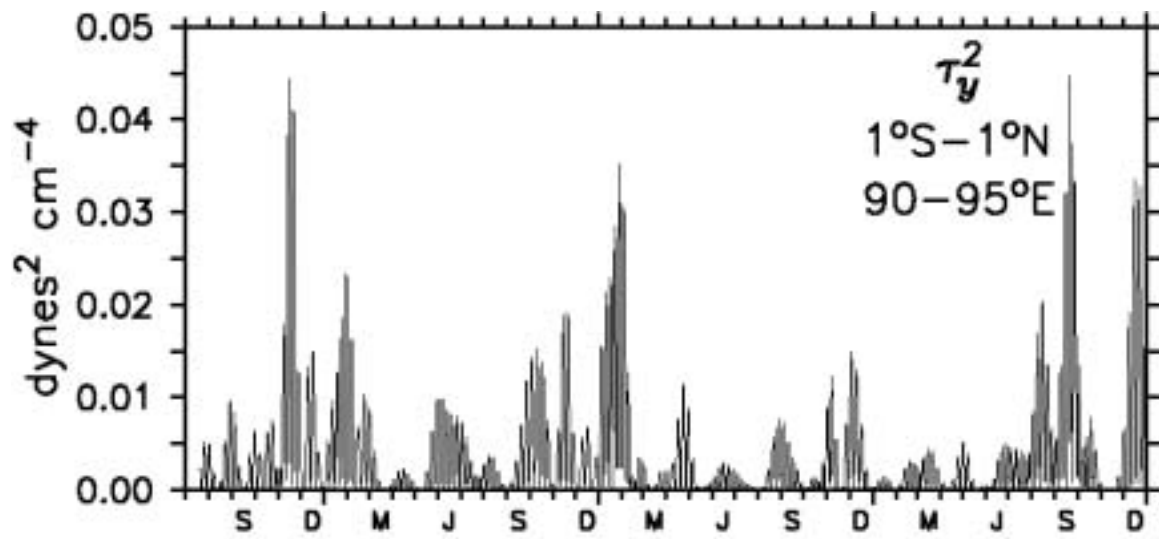


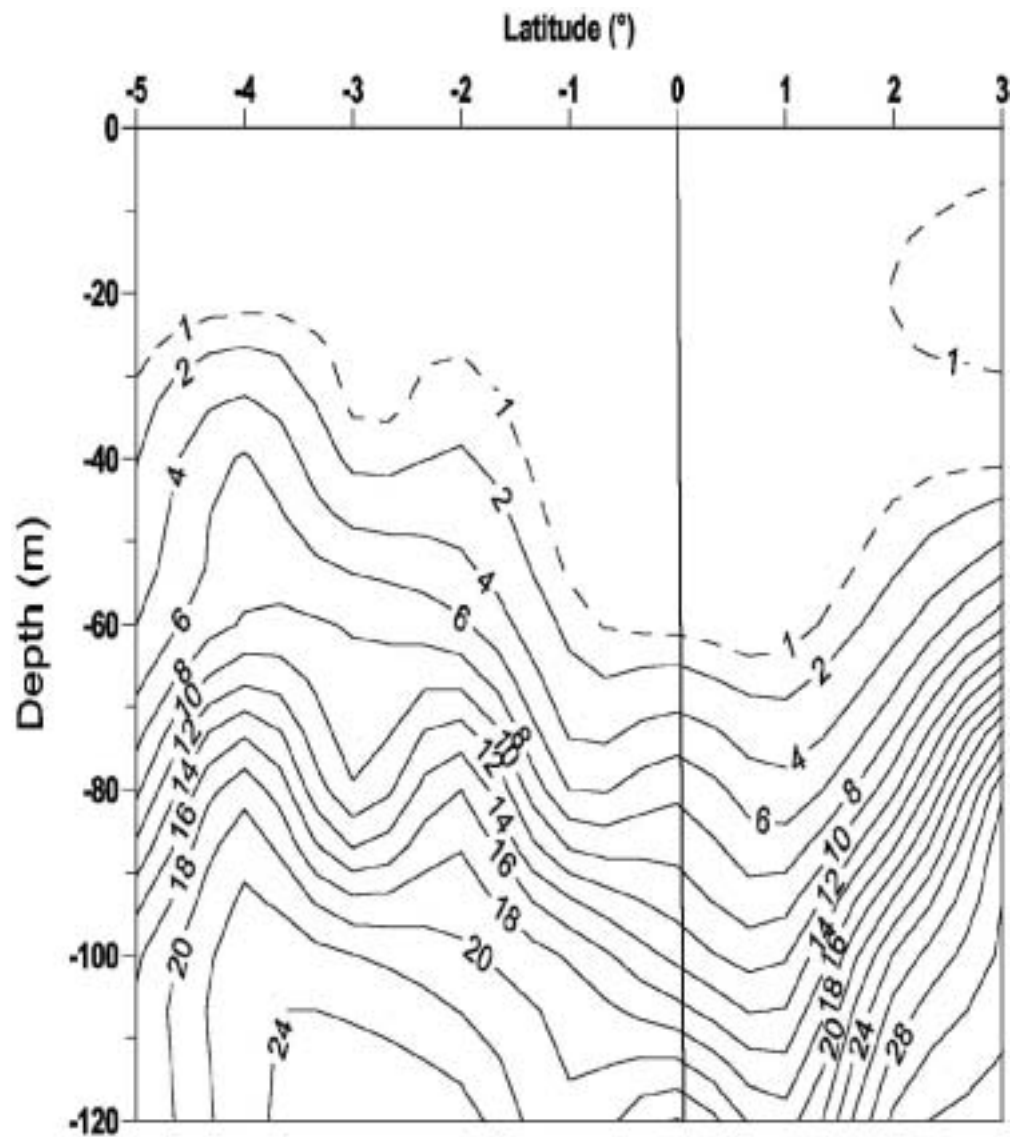
STANDARD DEVIATION 10-18 day filtered v 0°



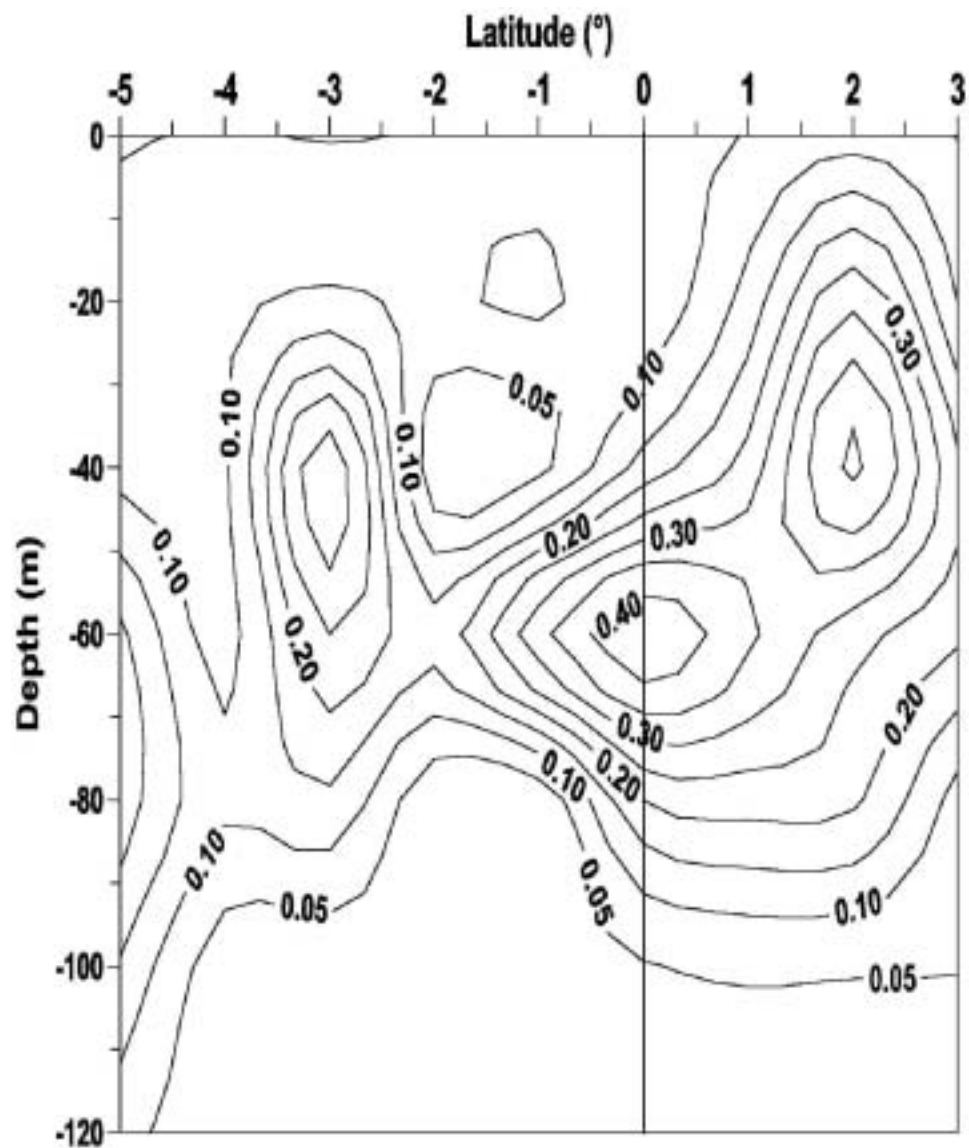
STANDARD DEVIATION 10–18 day filtered meridional velocity (cm s^{-1})







Distribution of Nitrate (micro mole) along 77°E section in the equatorial Indian Ocean during 19-25 Nov. 2002

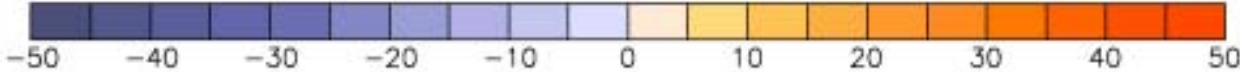
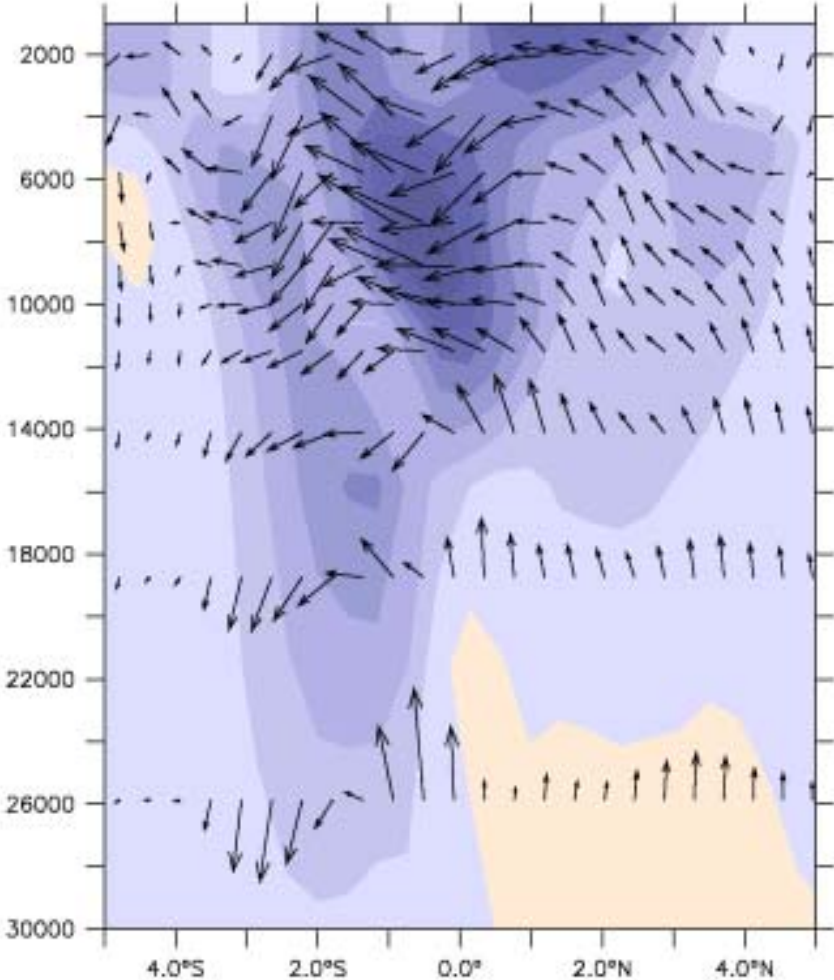
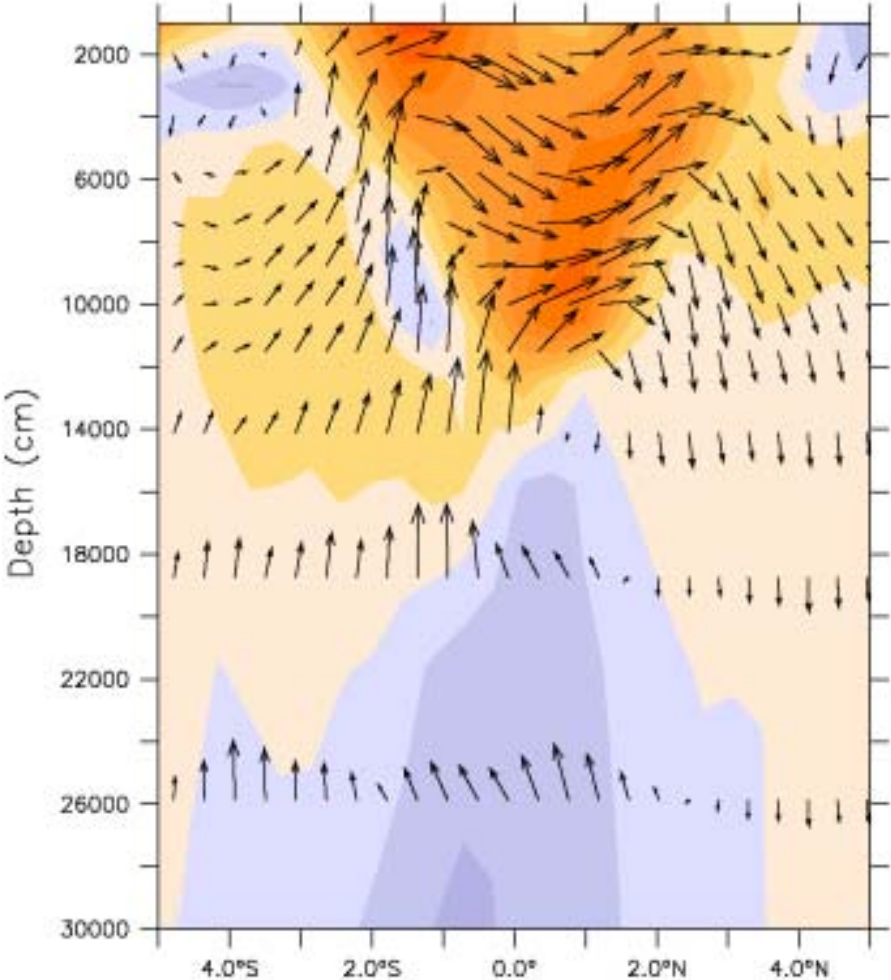


Distribution of chlorophyll a (micro gram/litre) along 77°E section in the equatorial Indian Ocean during 19-25 Nov. 2002

MODEL V,W 77°E

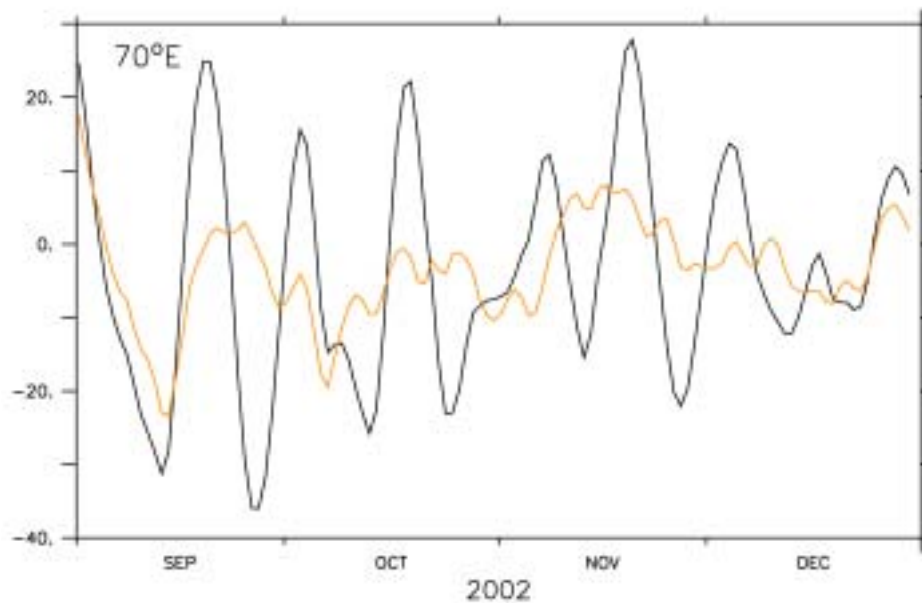
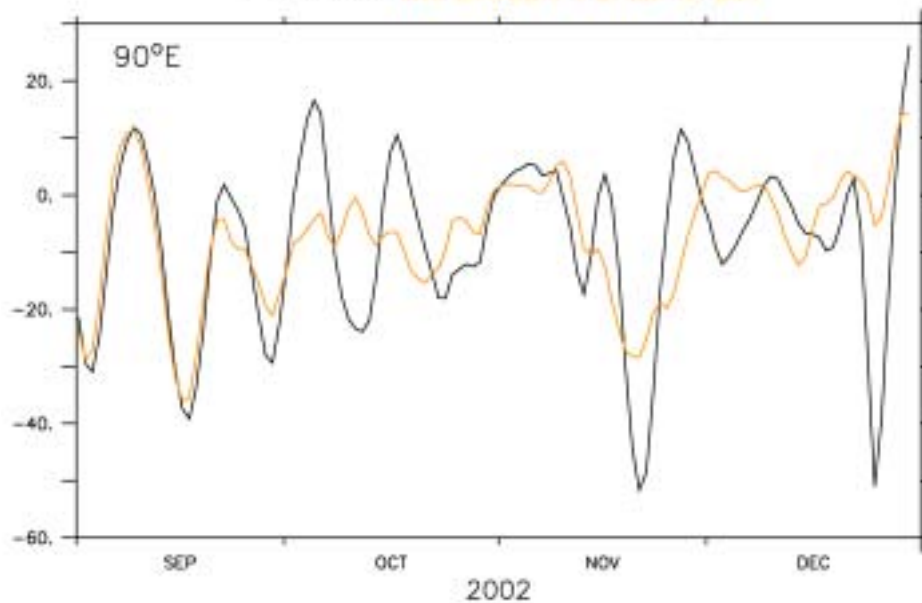
19-20 NOVEMBER 2002

24-25 NOVEMBER 2002

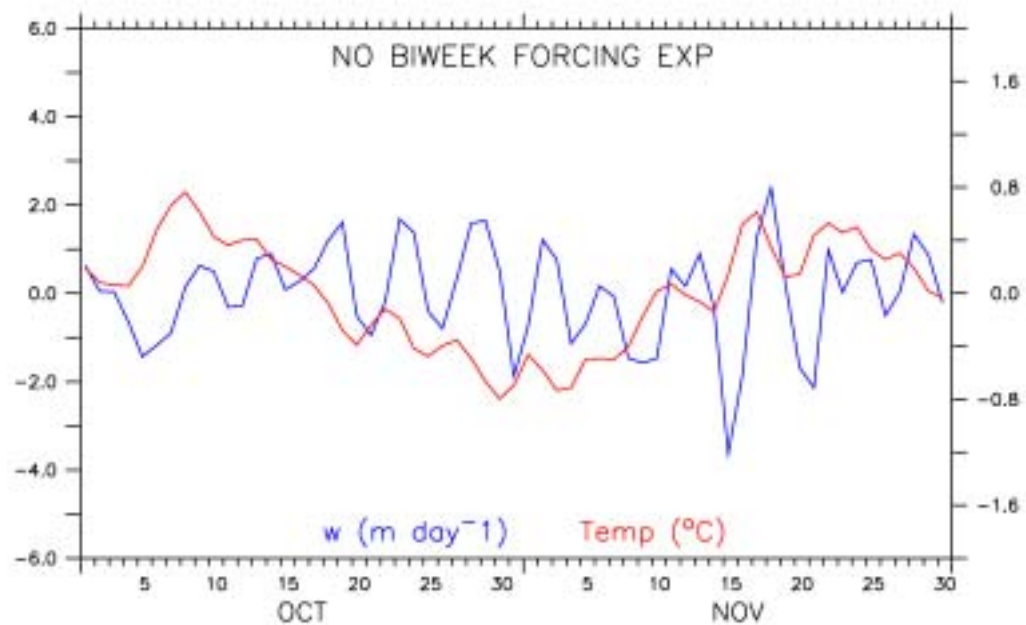
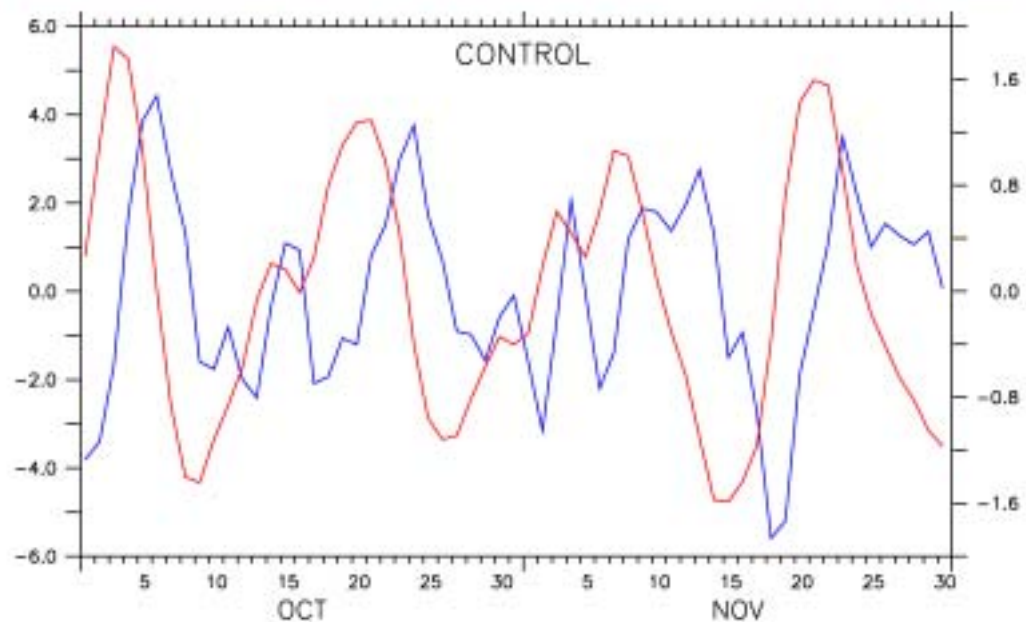


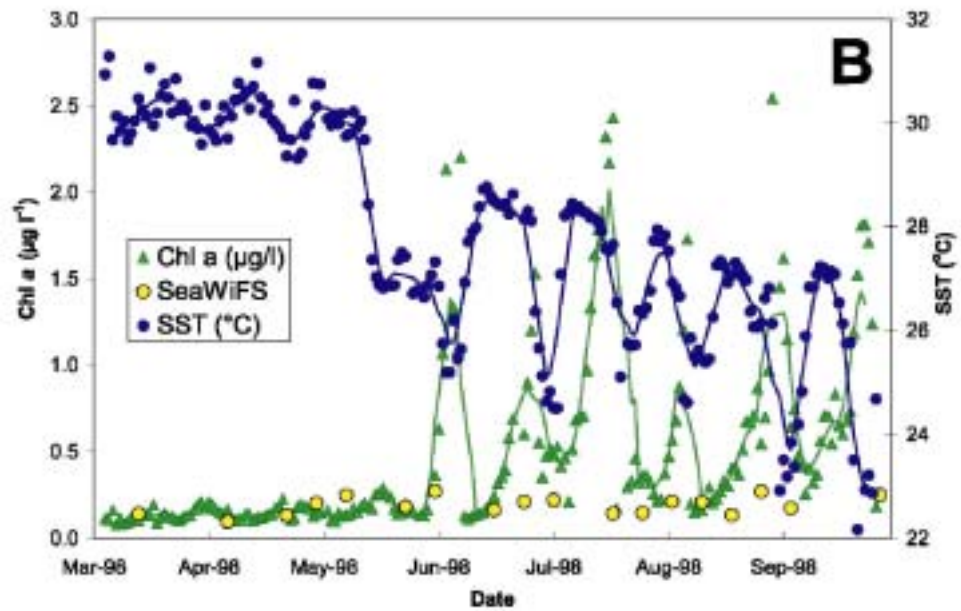
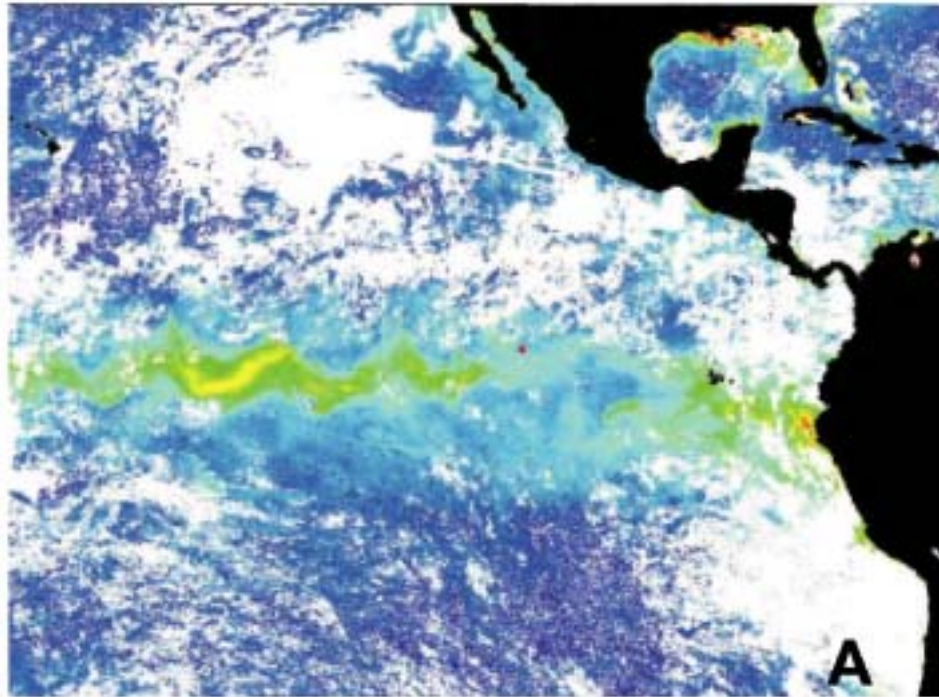
MERIDIONAL CURRENT 1°S-1°N 50m

CONTROL NO BIWEEK FORCING EXP



Effect of biweekly waves on w and temp 77°E 2-4°N 2002





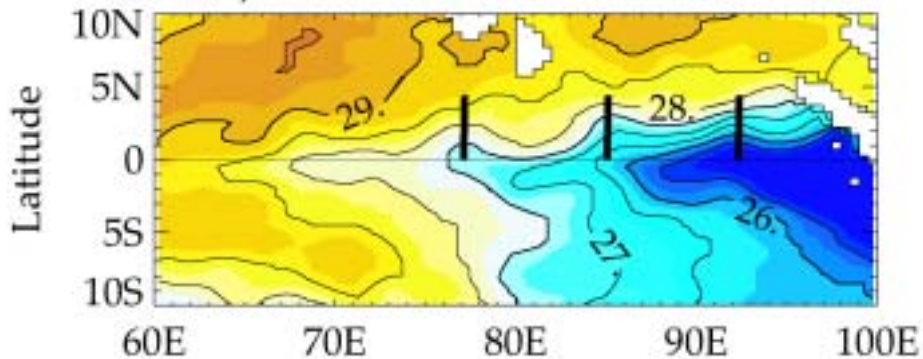
Chavez et al., 1999

CONCLUSIONS

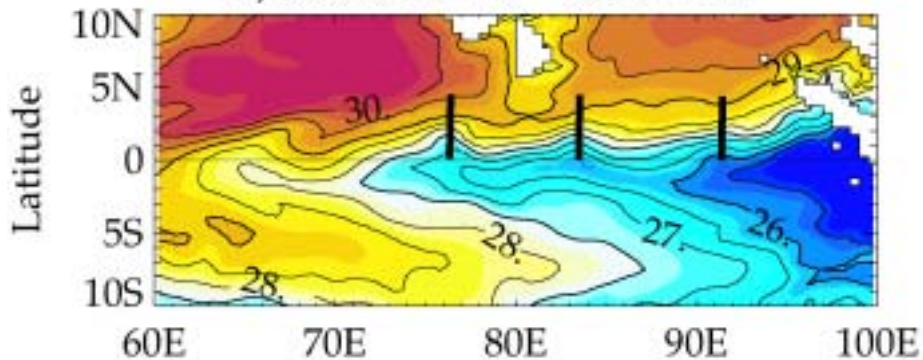
- Accurate winds give good model currents – currents are deterministic away from the western boundary.
- Observed currents have distinct biweekly variability. The model simulates this, but not the 30-60 day variability.
- The biweekly mode is a westward propagating Yanai wave with ~14 day period and 3000-4500 km wavelength, resonantly forced by the atmospheric quasi-biweekly mode.
- The biweekly wave is associated with intermittent, off-equator upwelling/downwelling (1-8 metres per day) throughout the year.
- Upwelling followed by mixing is an irreversible process. The biweekly mode might influence subsurface temperature and biology.

Subseasonal variability might influence seasonal and longer time scale changes in Indian Ocean currents, SST and Climate

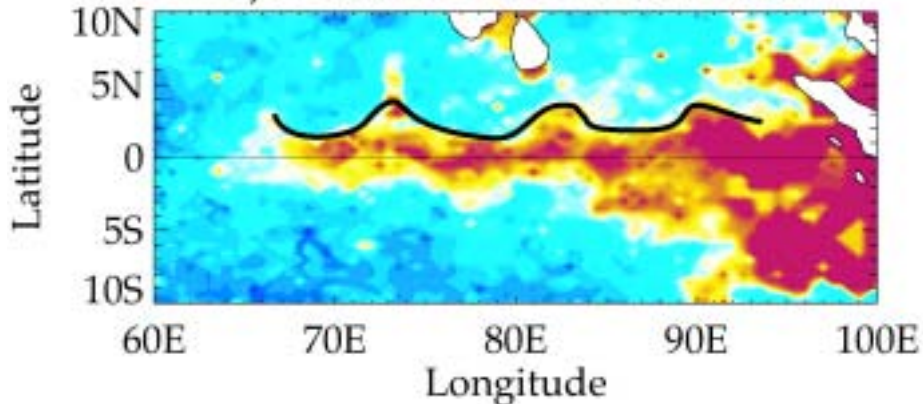
a) AVHRR SST 19971109



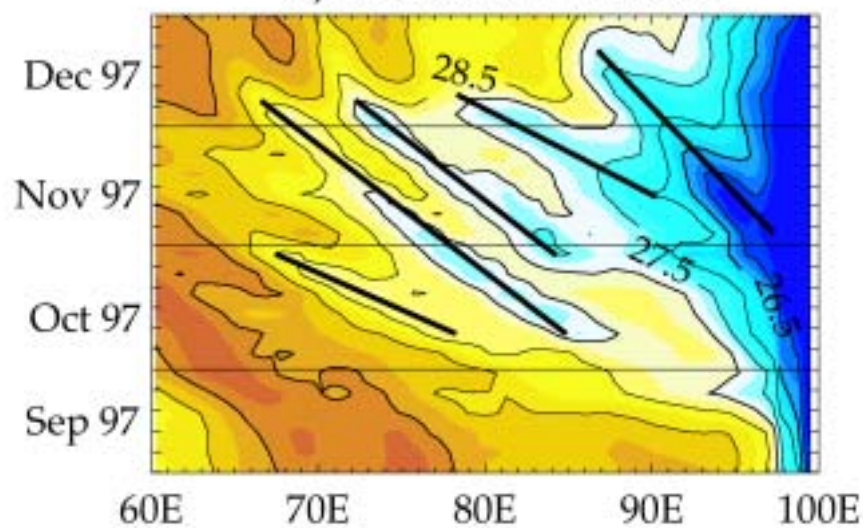
b) Model SST 19971109



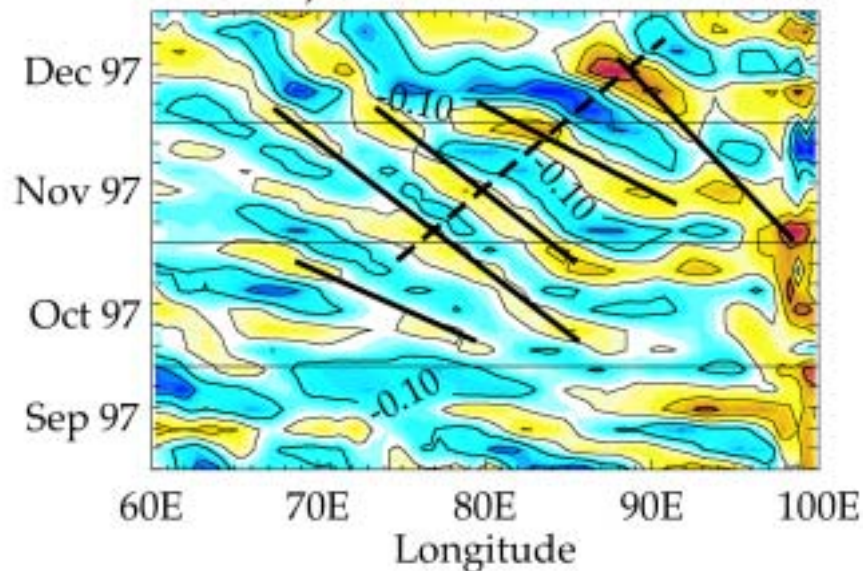
c) SeaWiFS Chl 19971117



d) Model 0-3°N SST



e) Model 2°S-2°N V



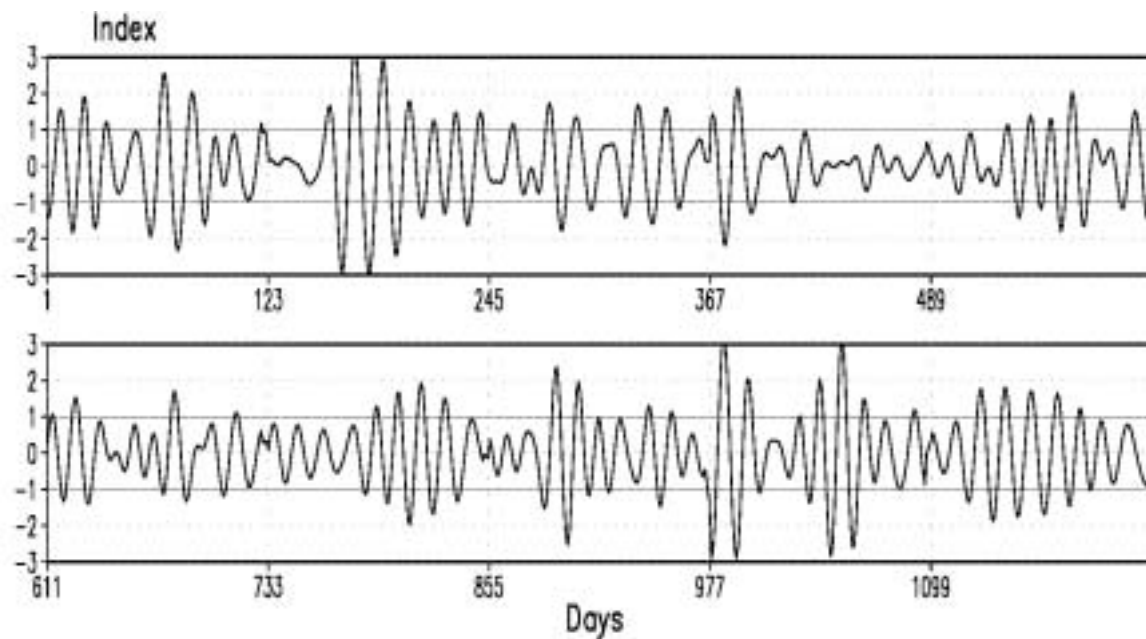
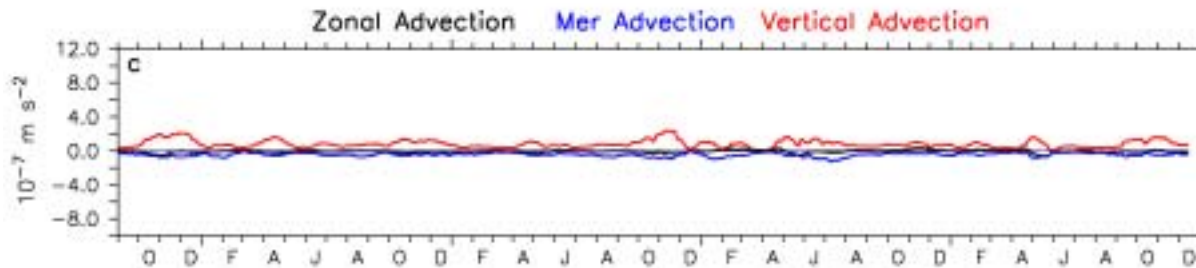
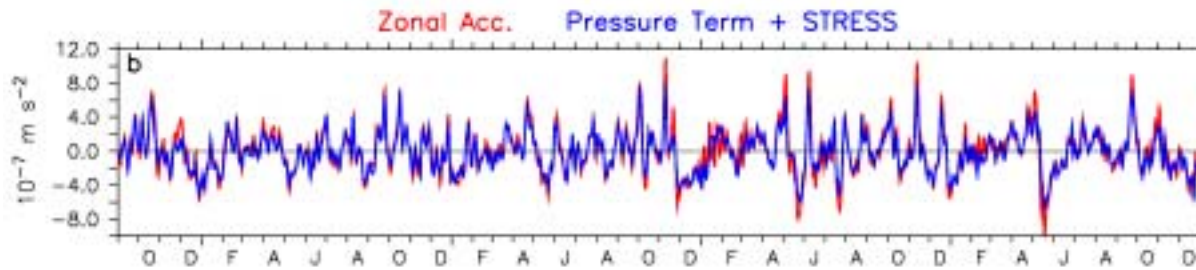
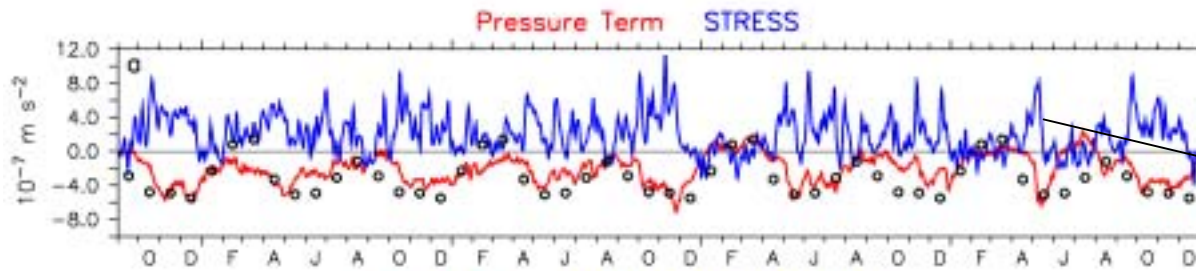
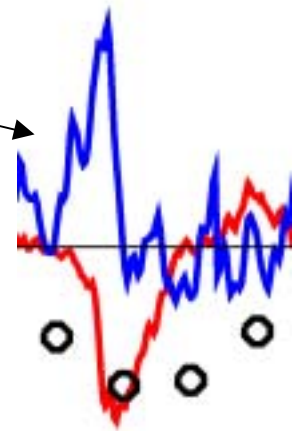


Figure 2: QBM index derived from the first two PC's of combined EOF of 10-20 day filtered zonal and meridional winds at 850 hPa and OLR for 10 years normalized by its own standard deviation.

UPPER OCEAN MOMENTUM BALANCE 60-95°E 1°S-1°N 0-120m



SUBSURFACE OCEAN MOMENTUM BALANCE 60-95°E 1°S-1°N 120-200m

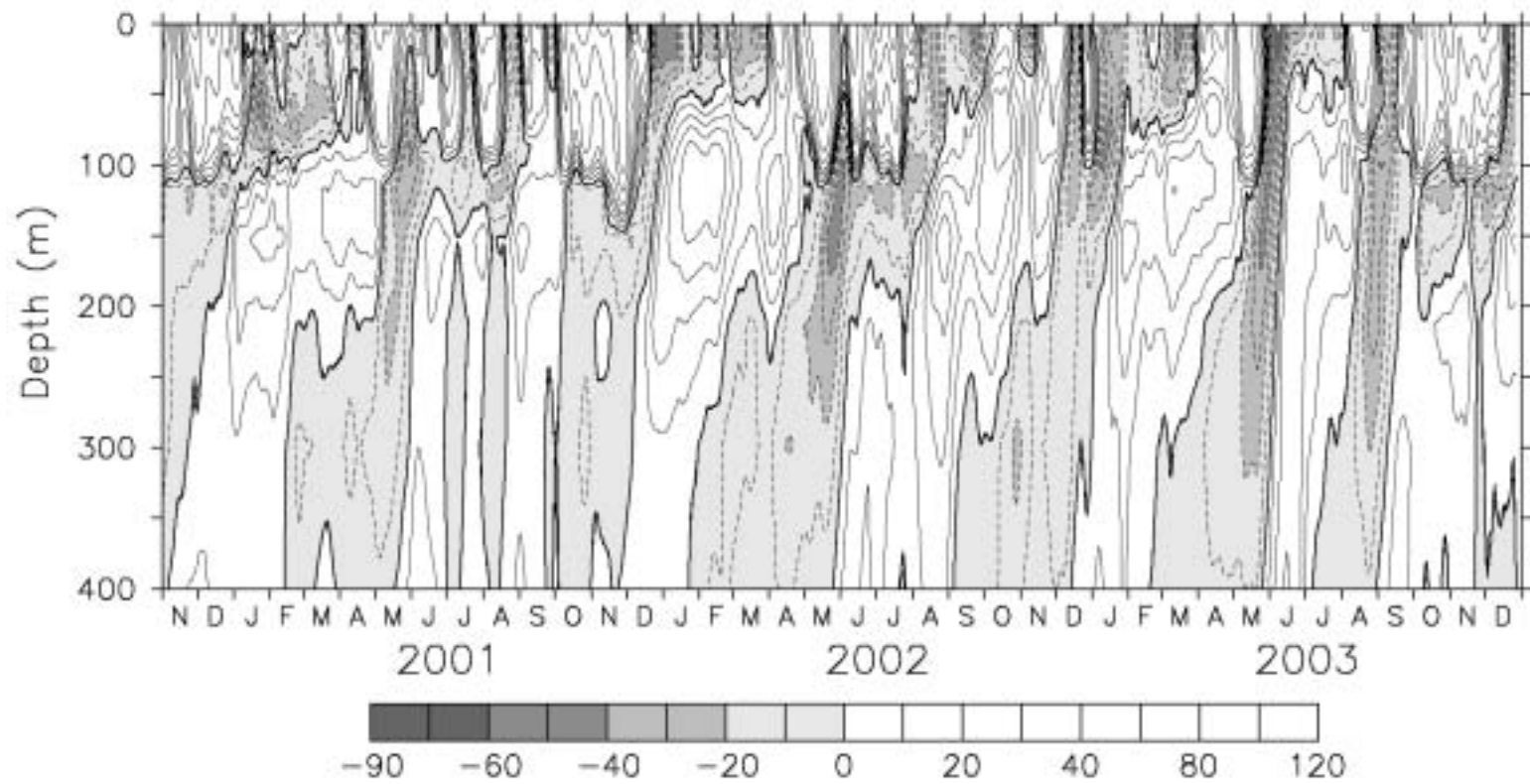


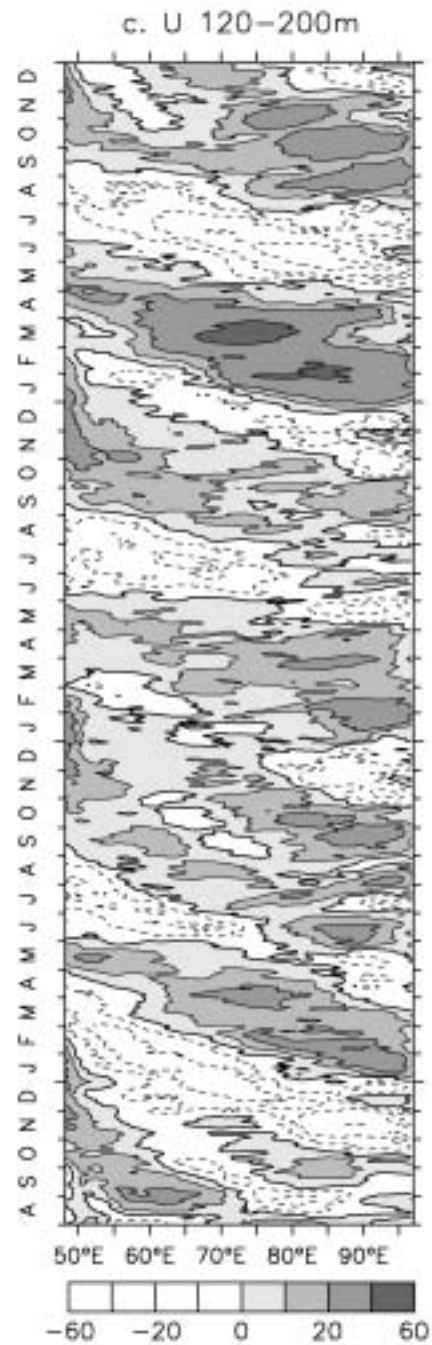
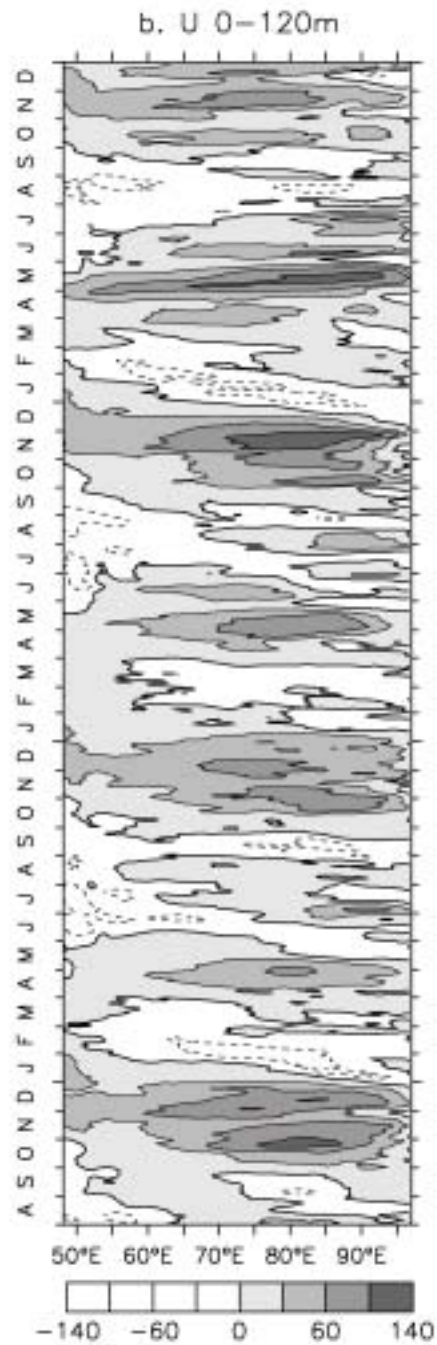
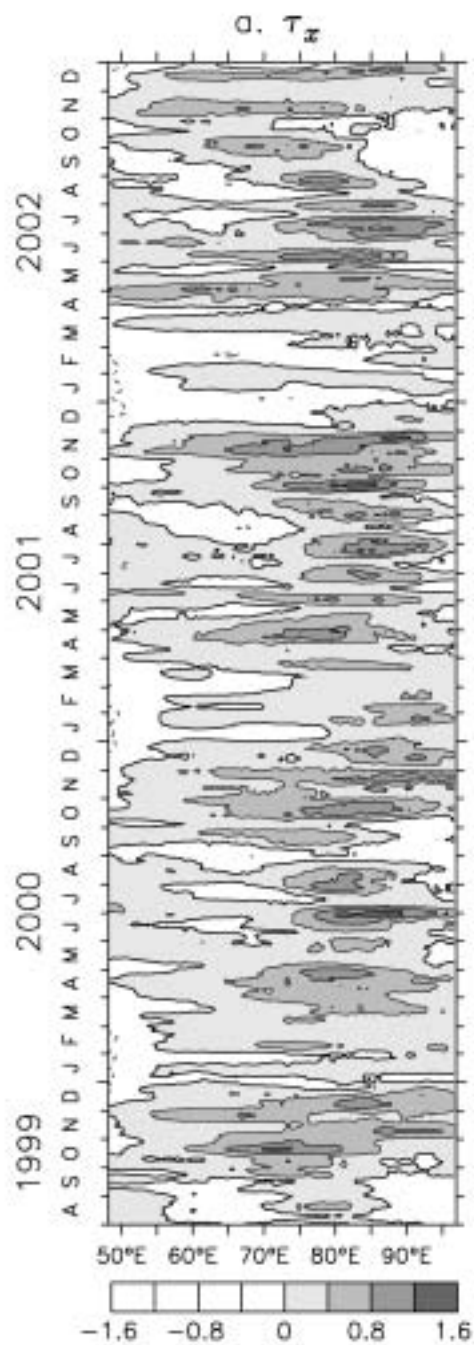
A J

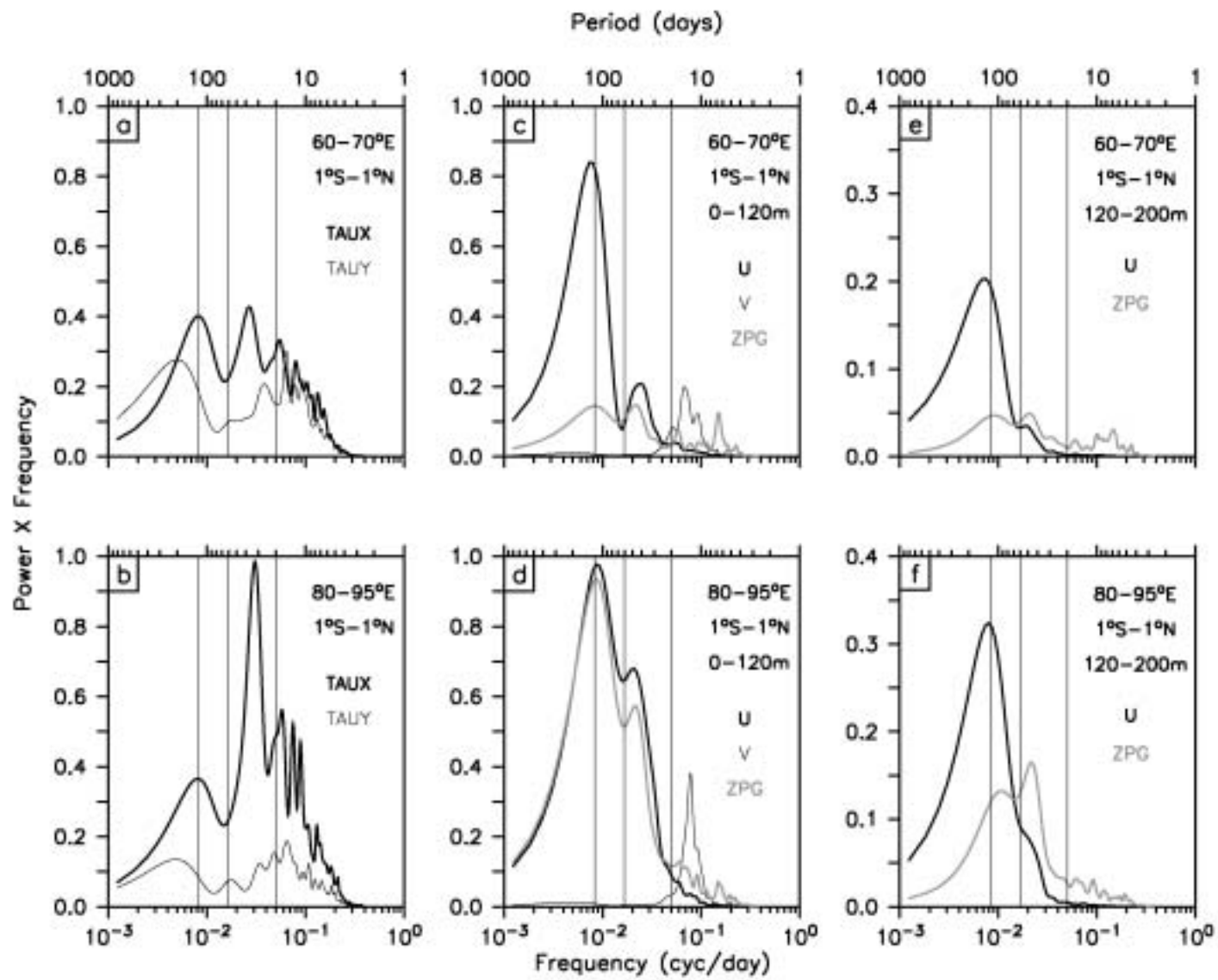
Accelerations $\sim 10^{-8}$ g

u variability: Eq. Jets + Rossby & Kelvin waves from boundaries

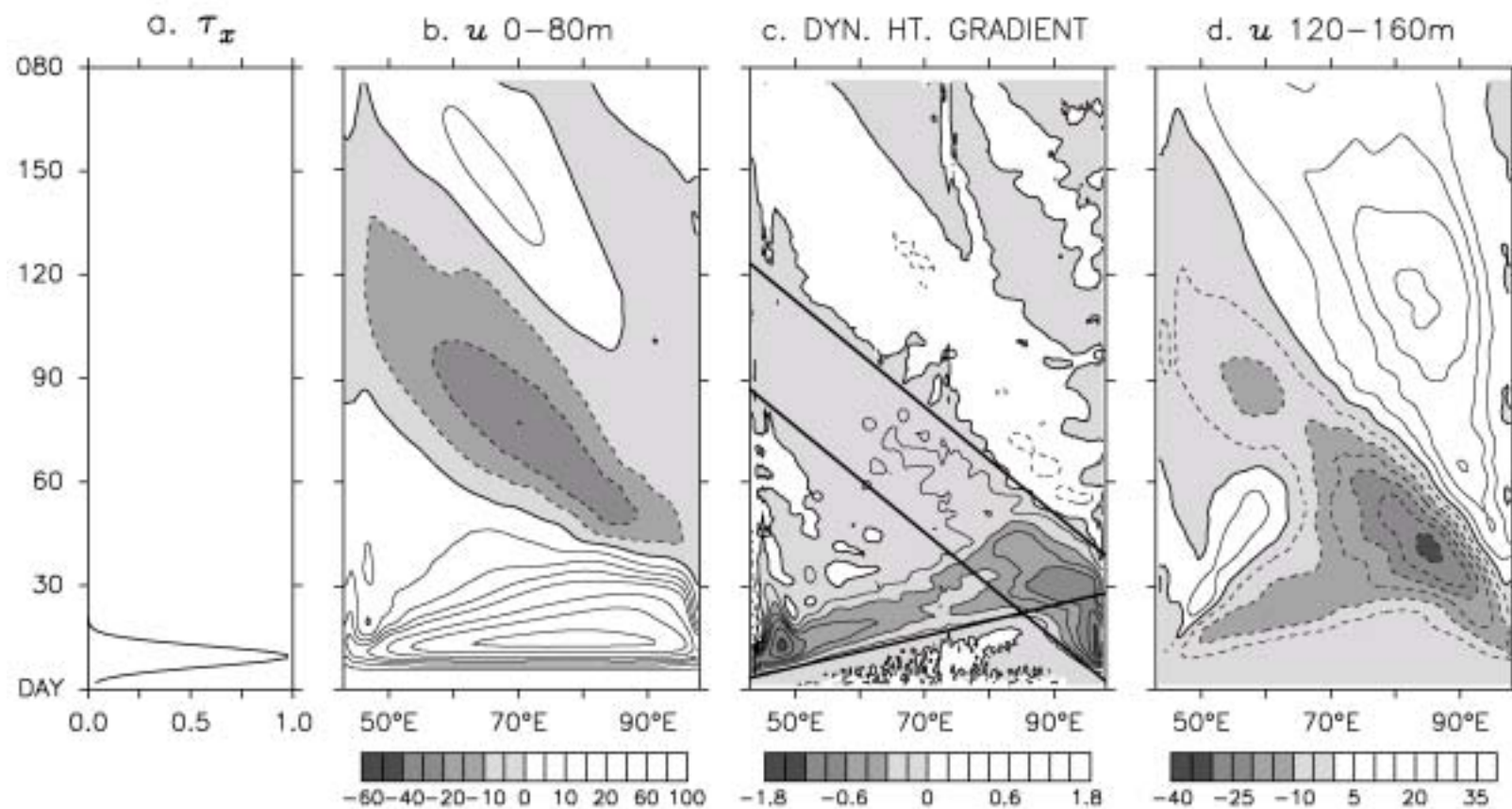
ZONAL VELOCITY 0° 90°E



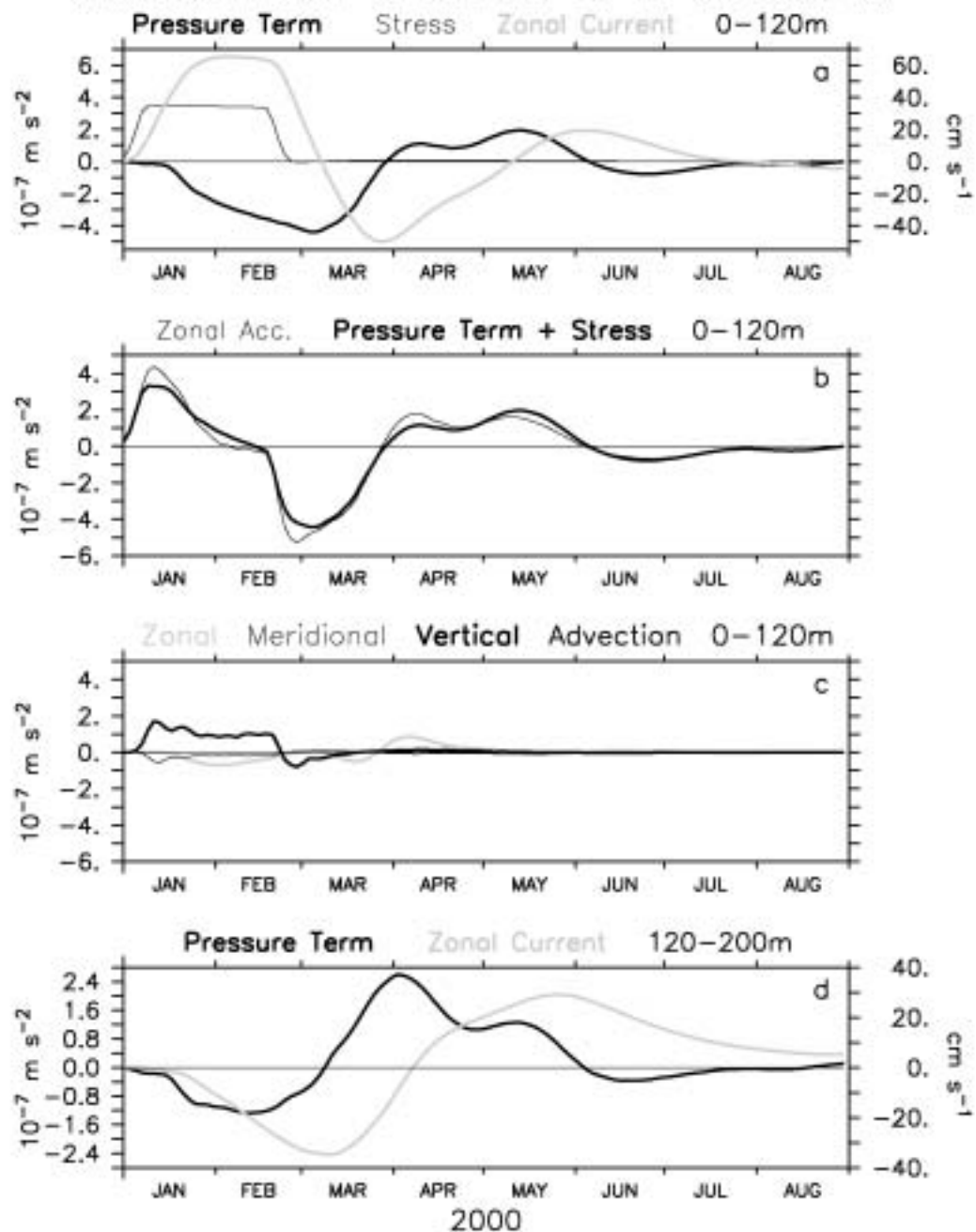




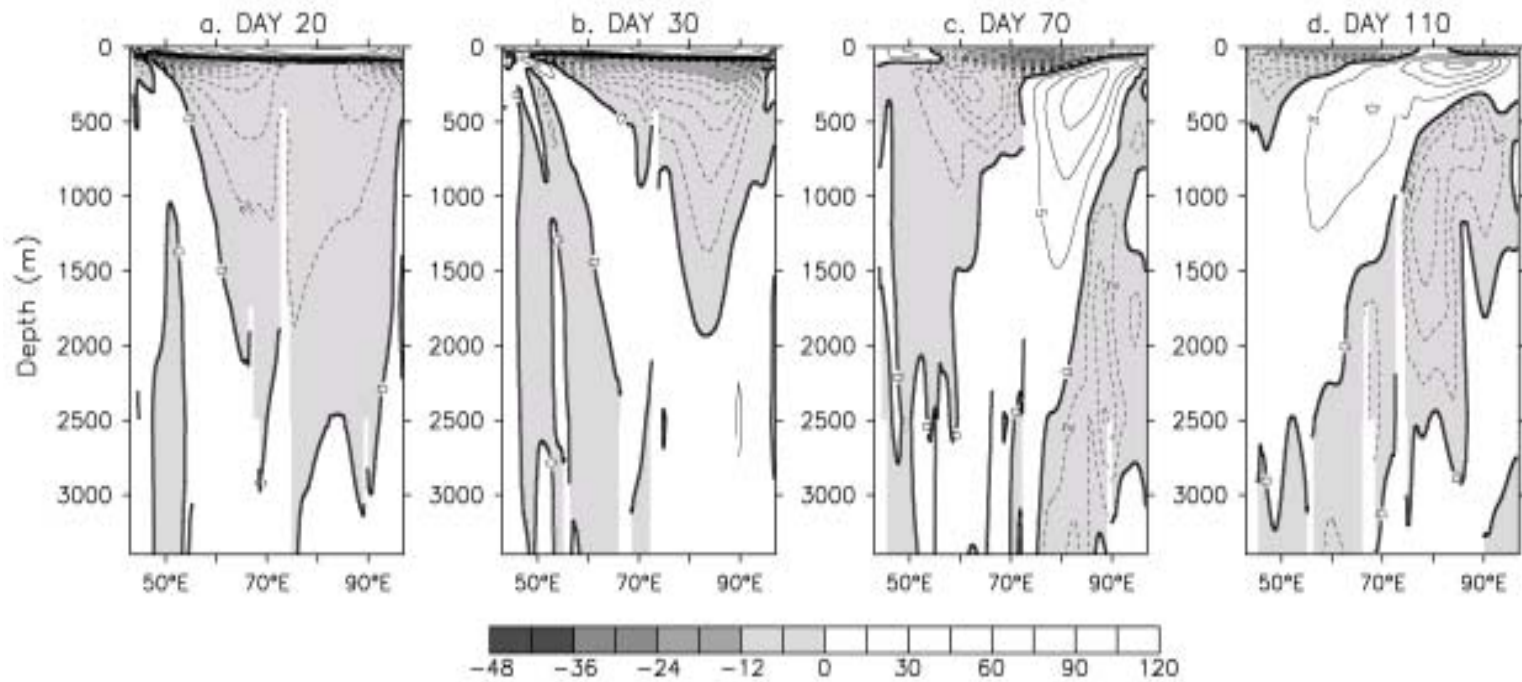
20-DAY BURST EXP

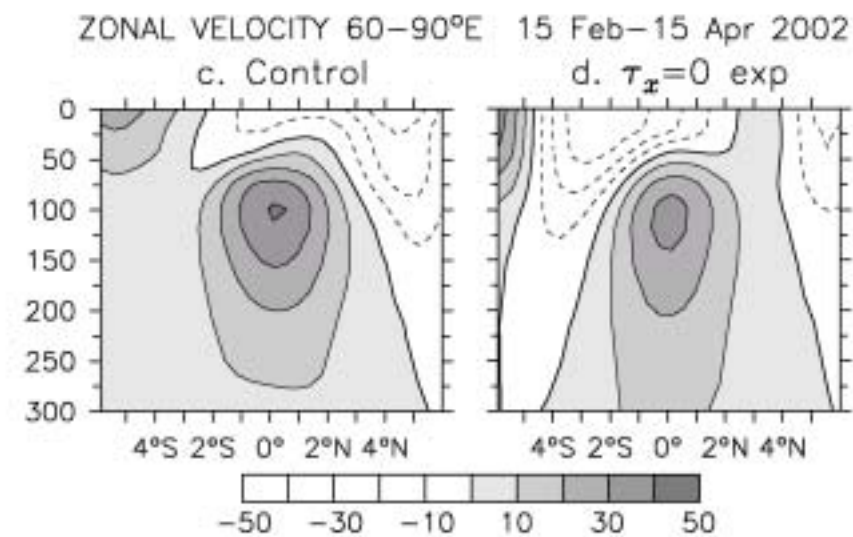
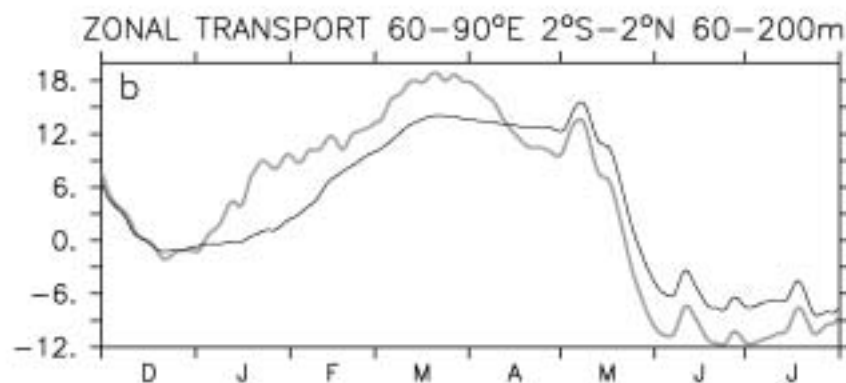
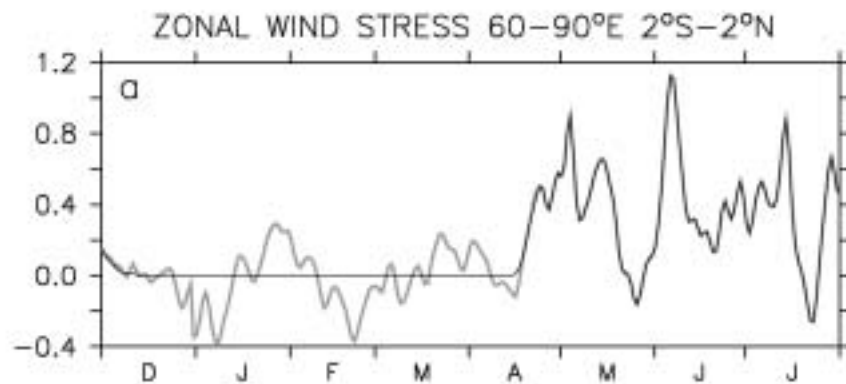


MOMENTUM BALANCE 70-80°E 1°S-1°N 60-DAY BURST EXP

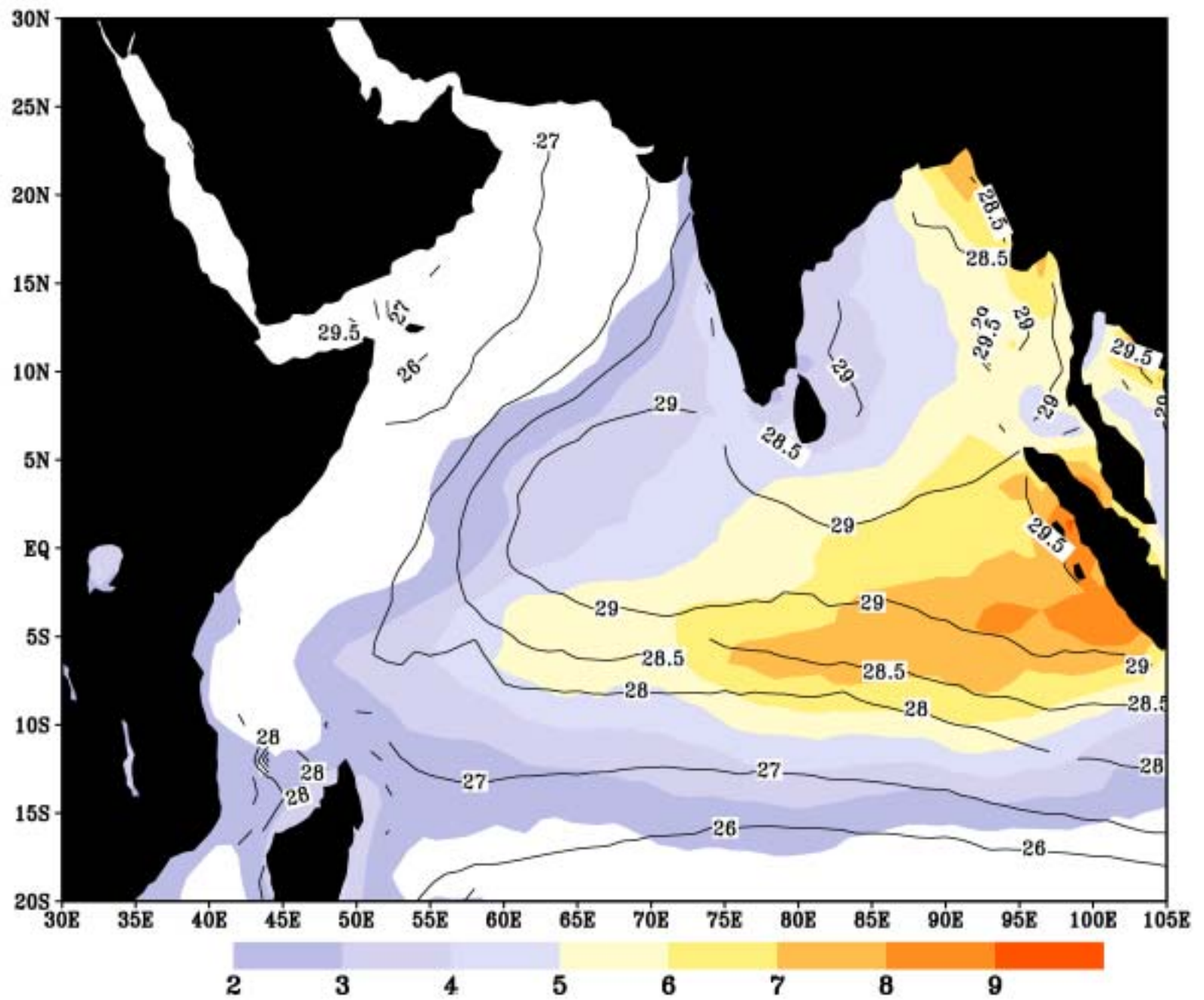


ZONAL VELOCITY 20-DAY BURST EXP

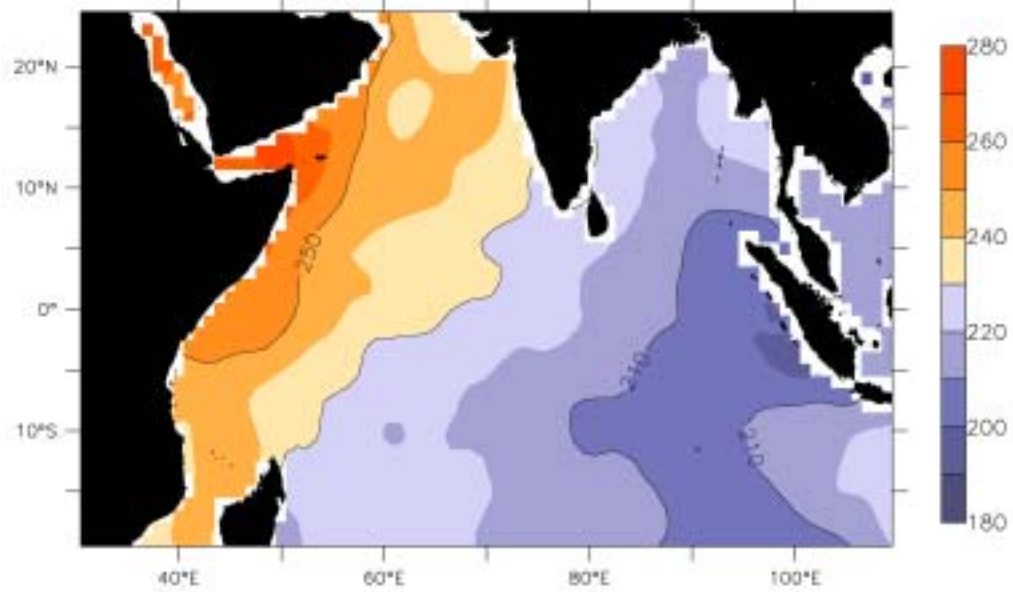




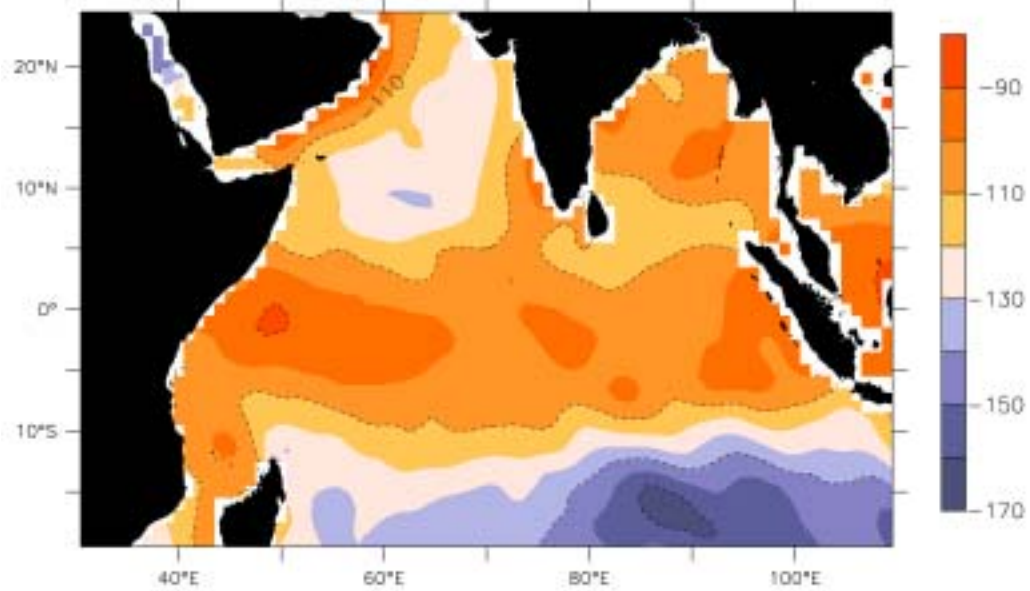
GPCP RAIN (mmday⁻¹), TMI SST (°C)



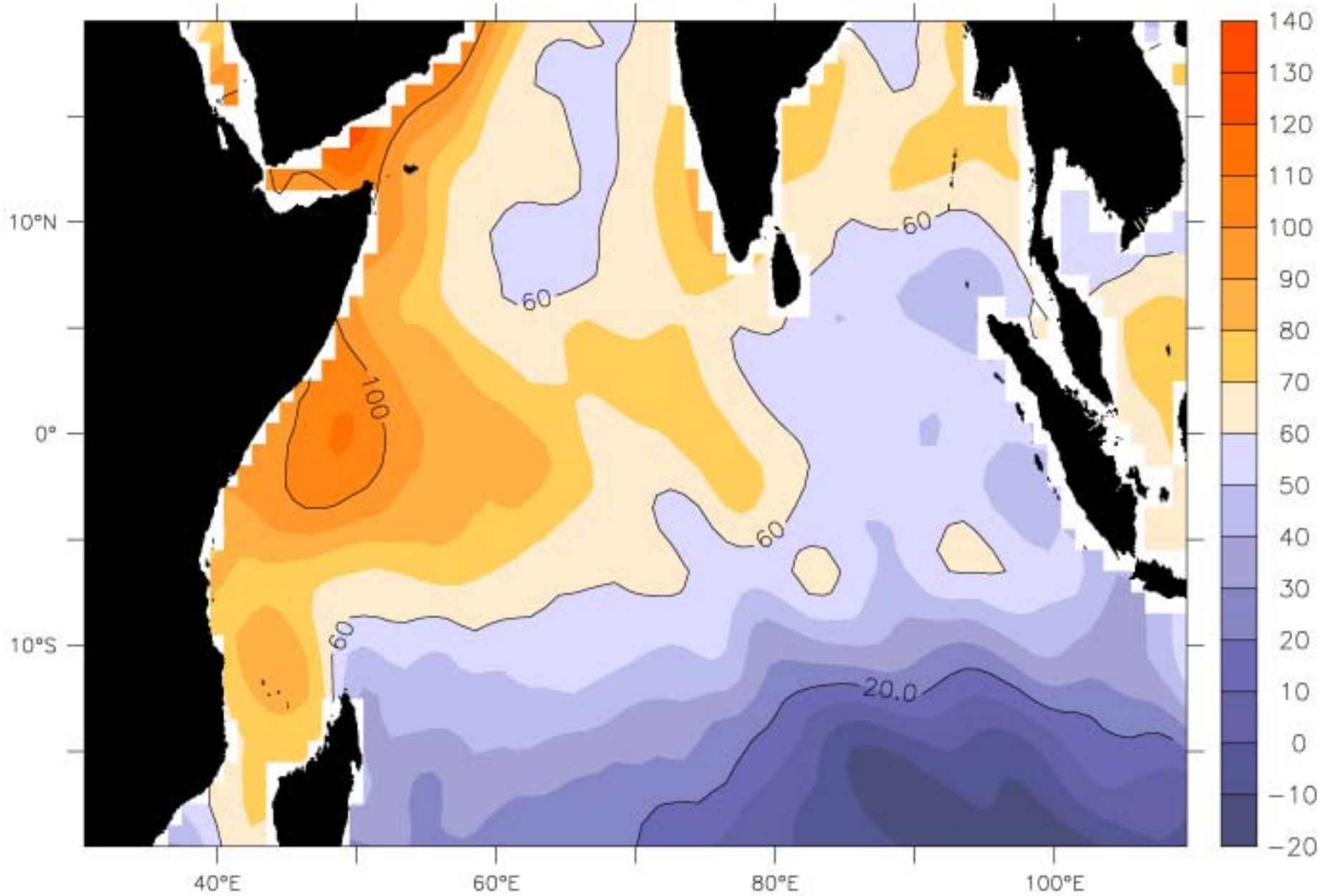
SOC FLUXES
SHORTWAVE RADIATION (Wm^{-2})



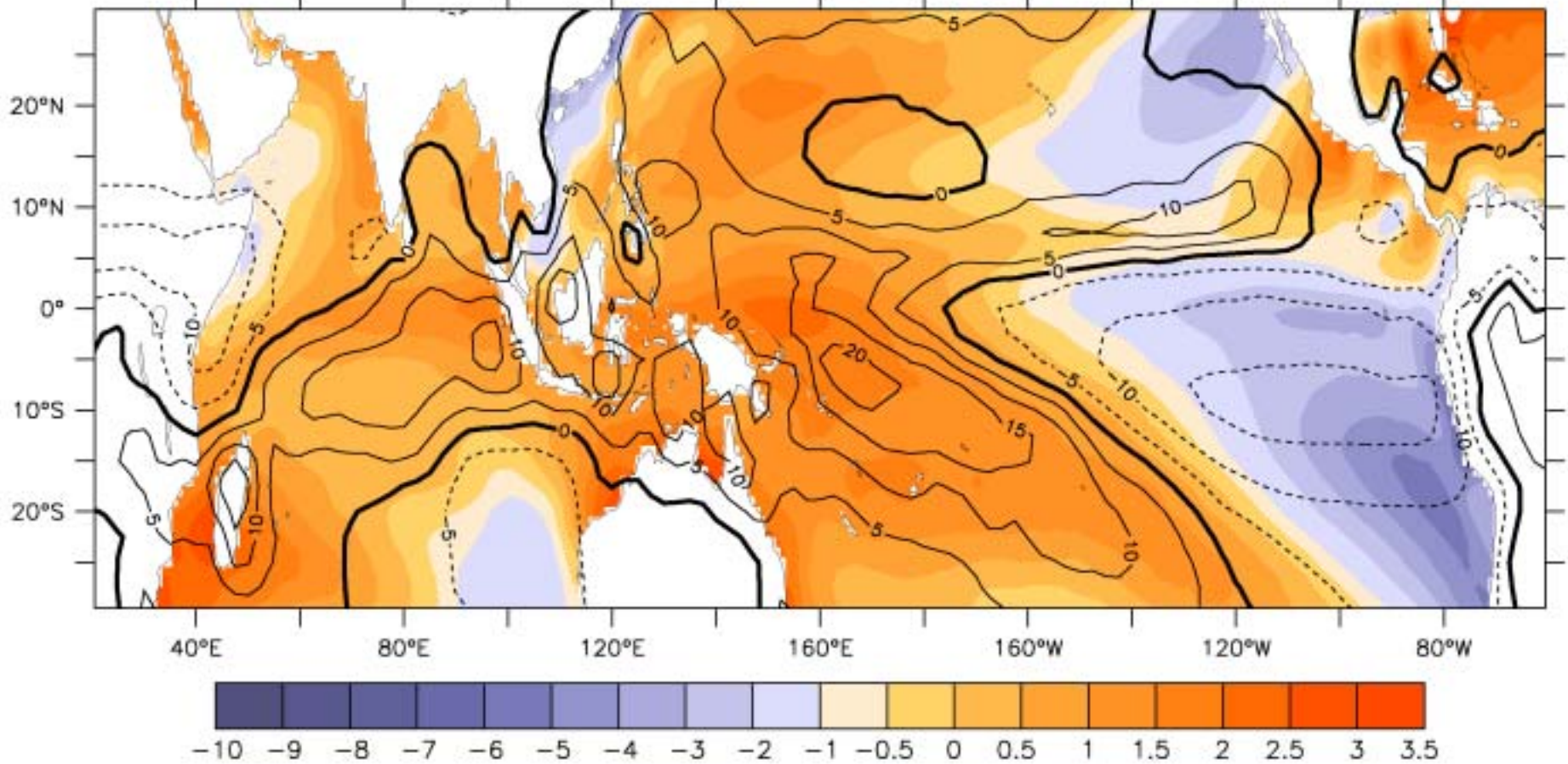
LATENT HEAT FLUX (Wm^{-2})



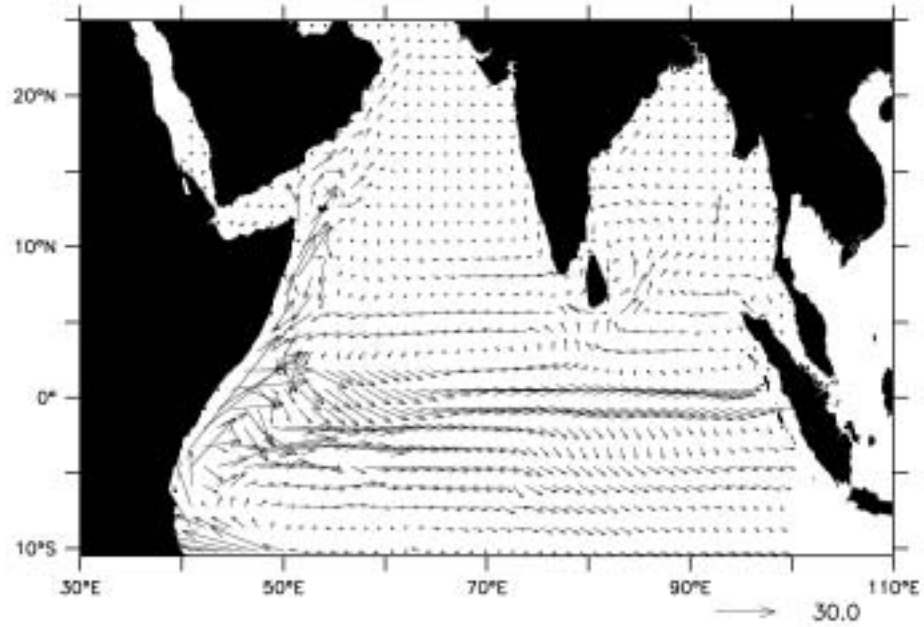
NET HEAT FLUX (Wm^{-2})



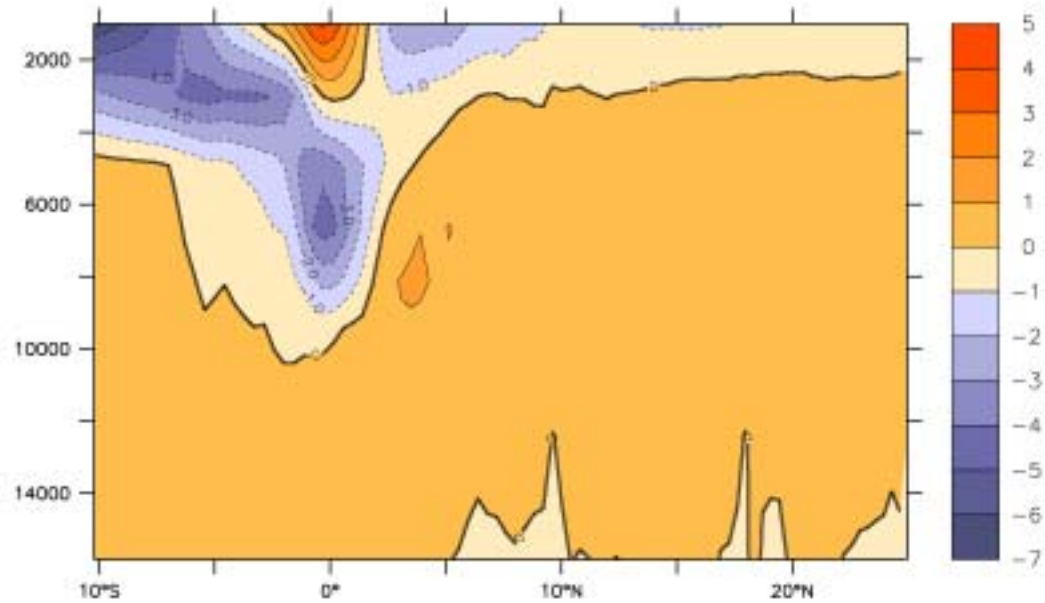
EAST-WEST ASYMMETRY SST ($^{\circ}\text{C}$), RAIN (cm month^{-1}) WINTER



MODEL CURRENTS (cm s^{-1}) 50m



Meridional Current (cm/s)



JAMSTEC

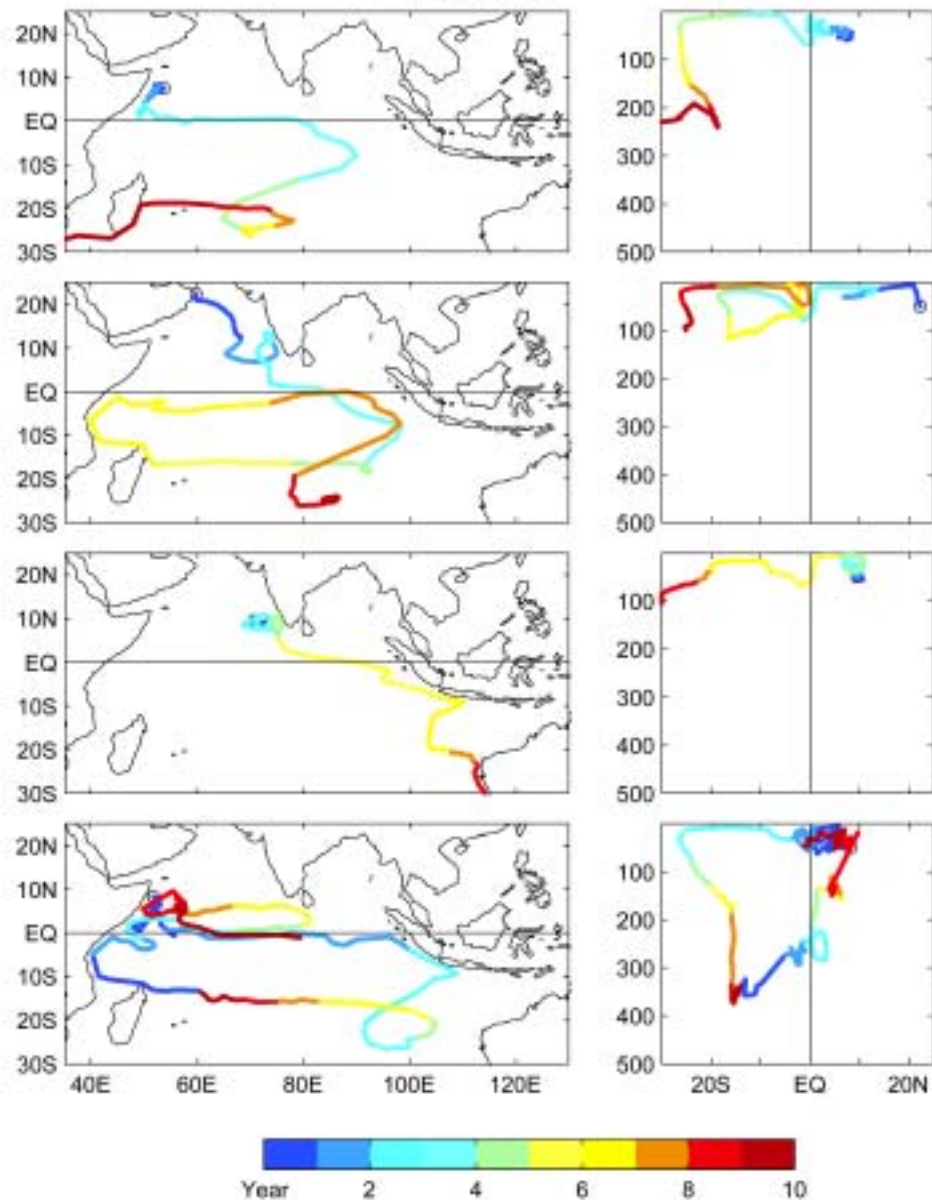
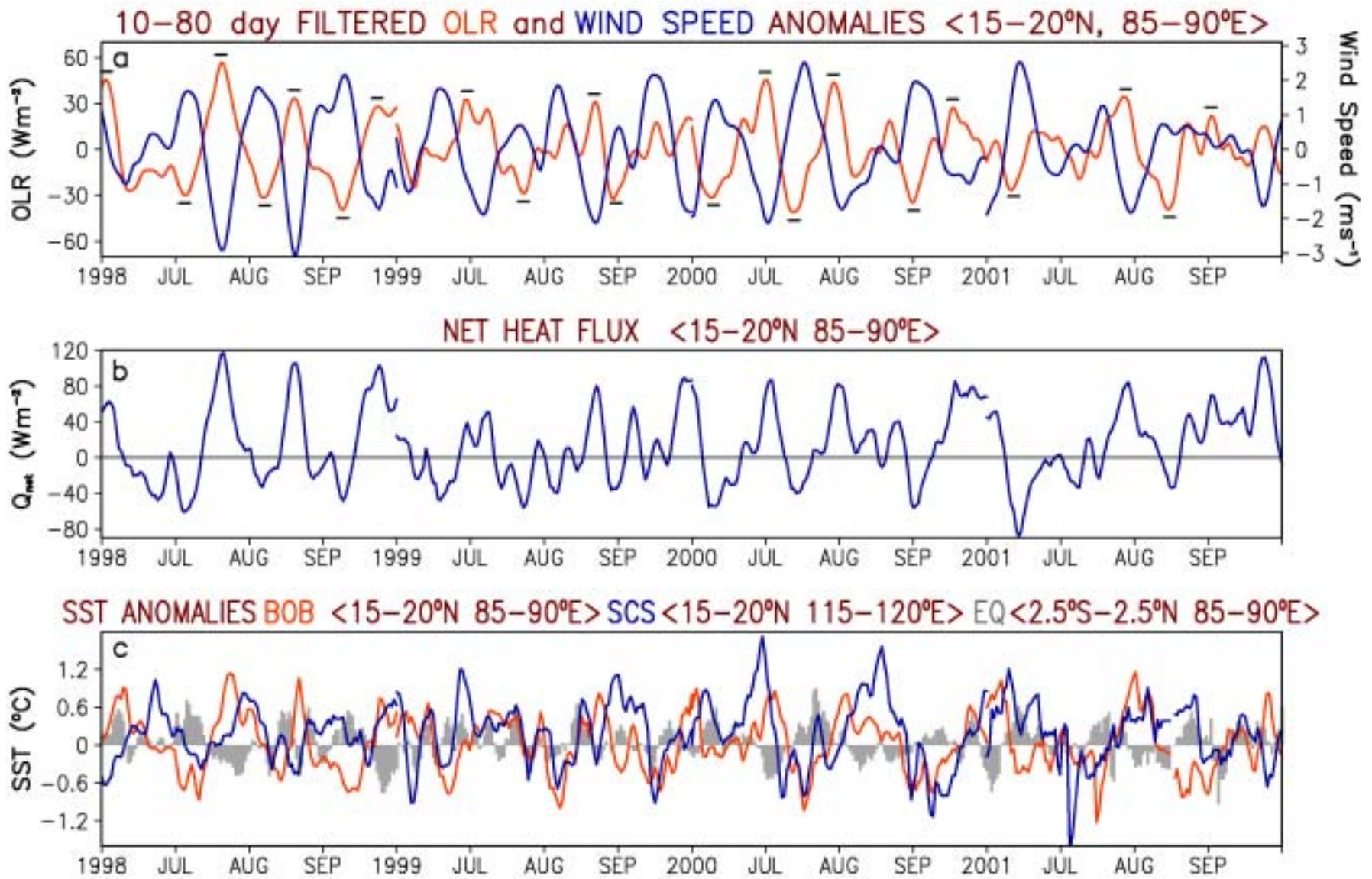
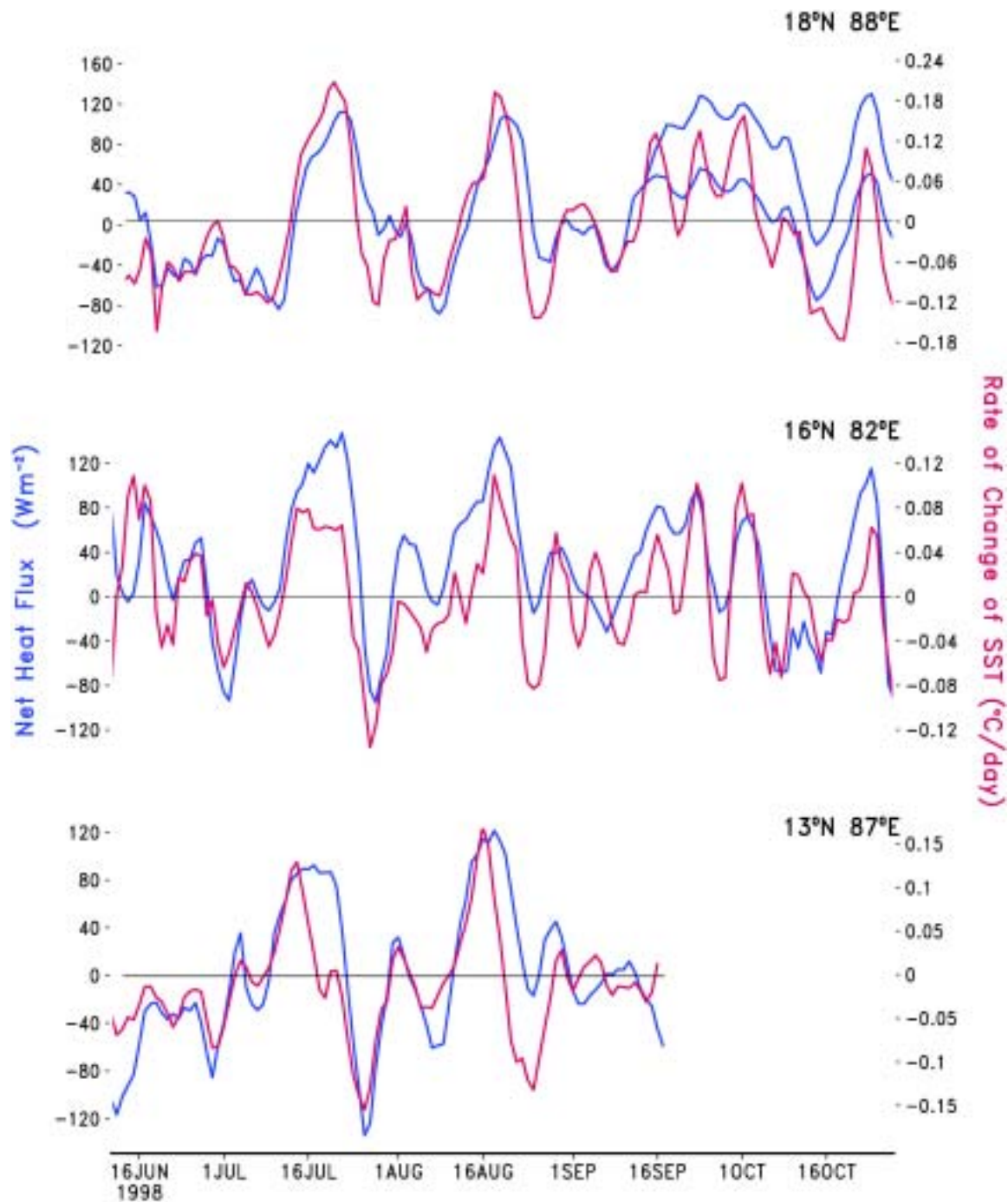


Figure 7: Four drifter trajectories tracked forwards in time using the annual-mean velocity field of the JAMSTEC solution, showing x - y and y - z views in corresponding left and right panels. The trajectories illustrate types of commonly occurring pathways. Color indicates the time in years since the release of the drifter and colors repeat after 10 years.





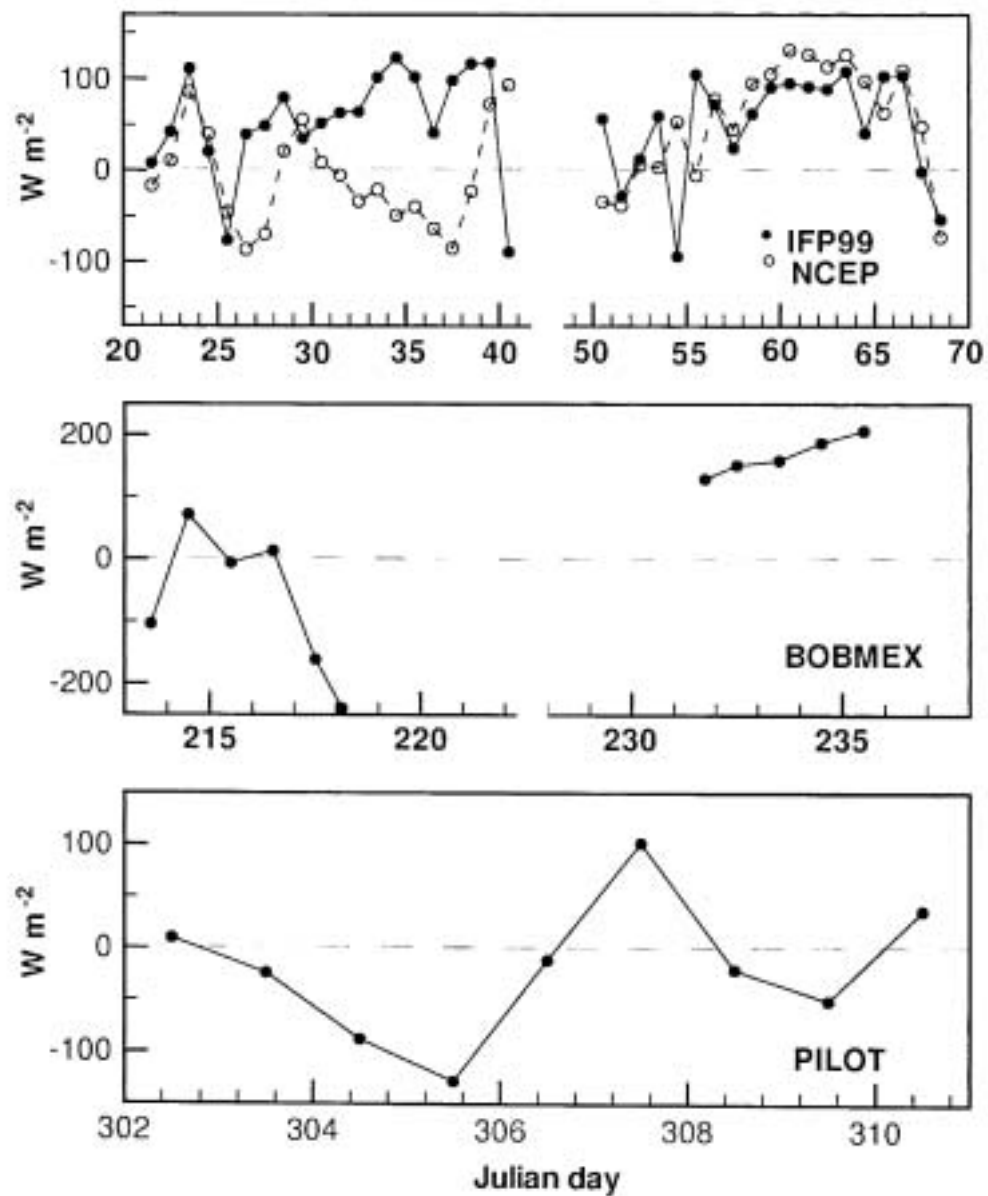
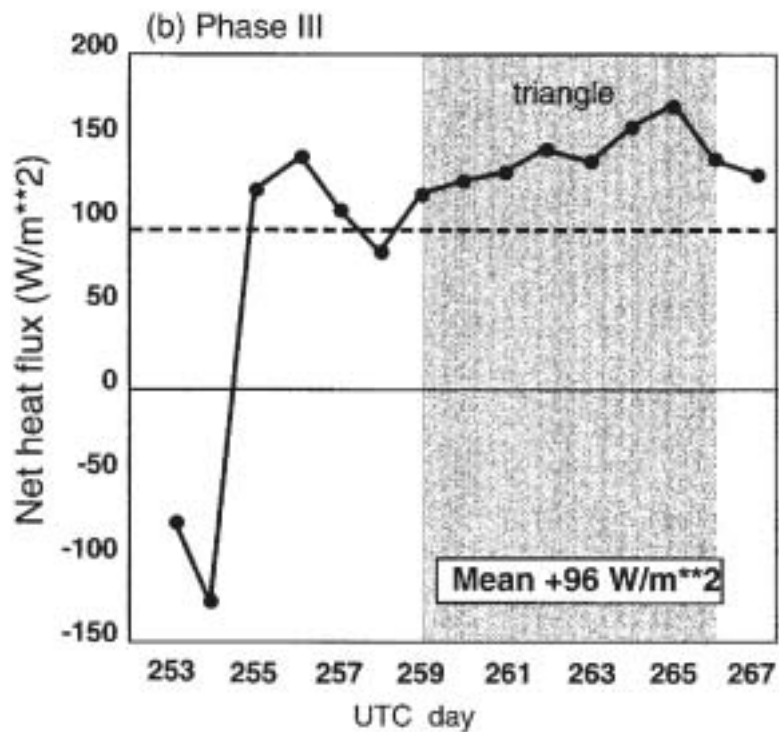
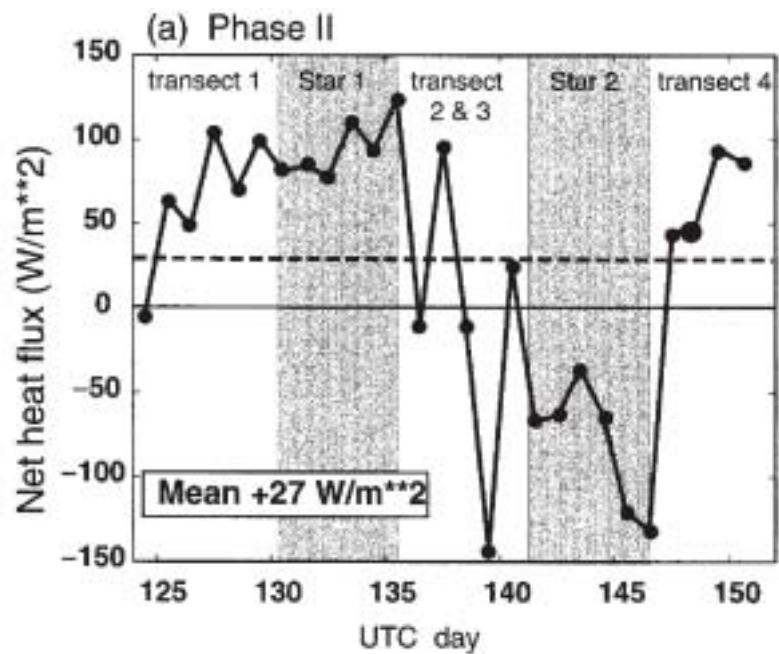
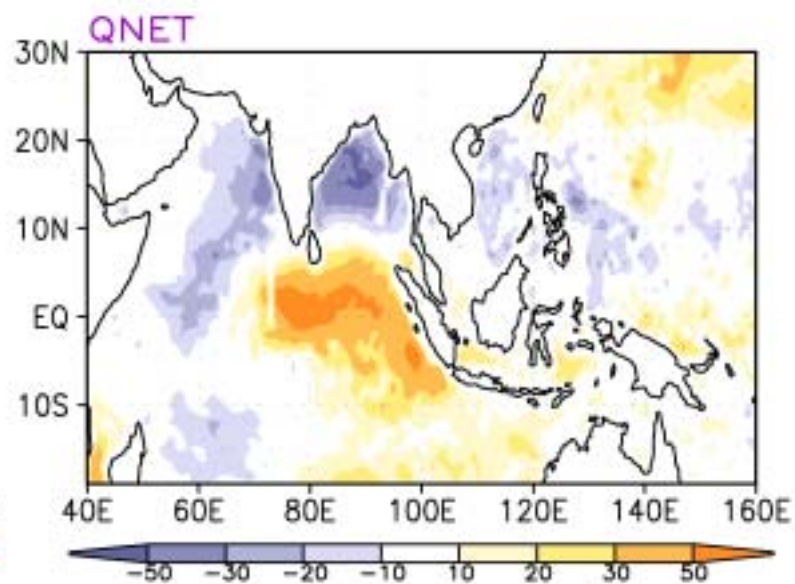
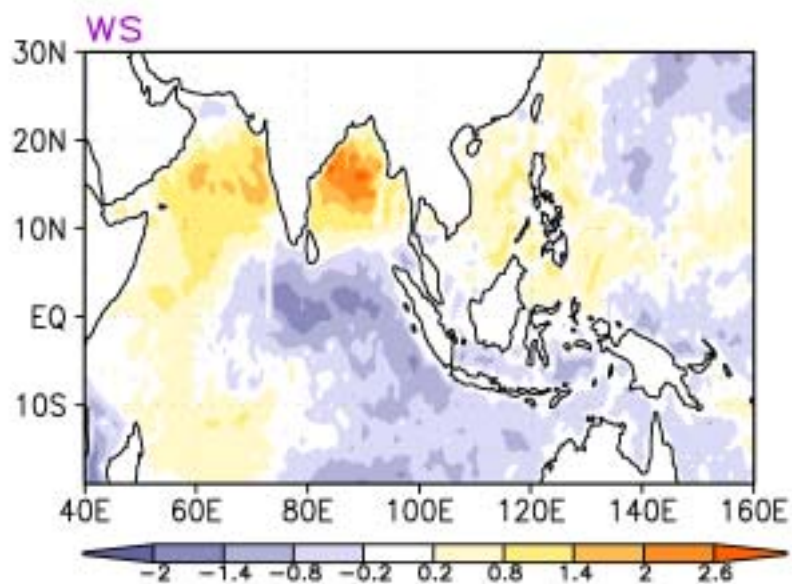
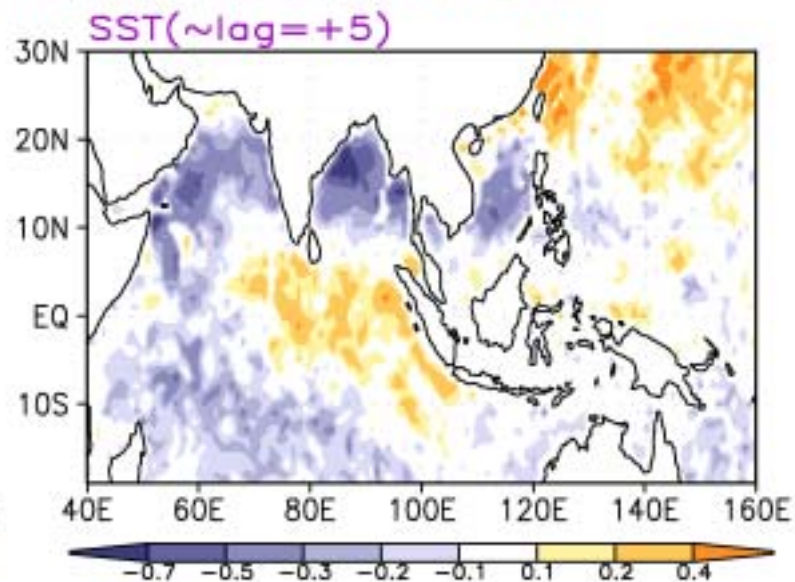
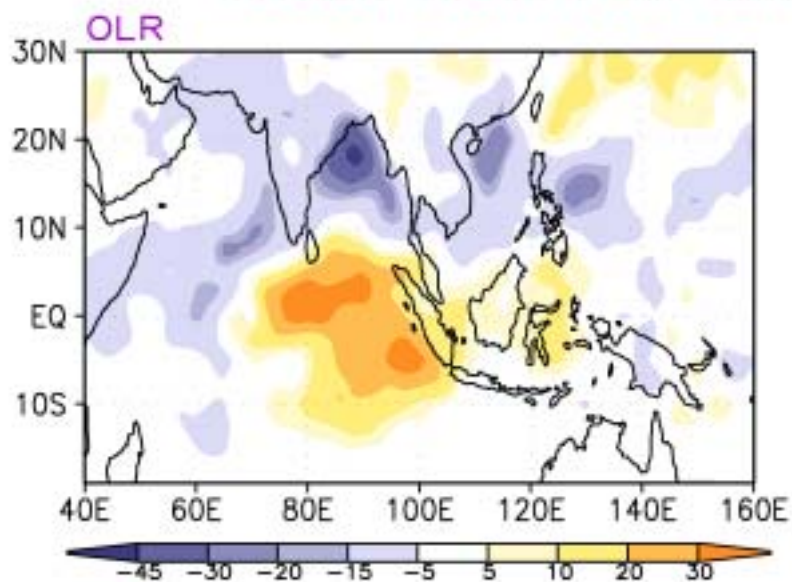


FIG. 3. Variation of daily net heat flux for (top) IFP99, (middle) BOBMEX, and (bottom) PILOT. Also shown in (top) is NCEP re-analysis net heat flux.

JASMINE



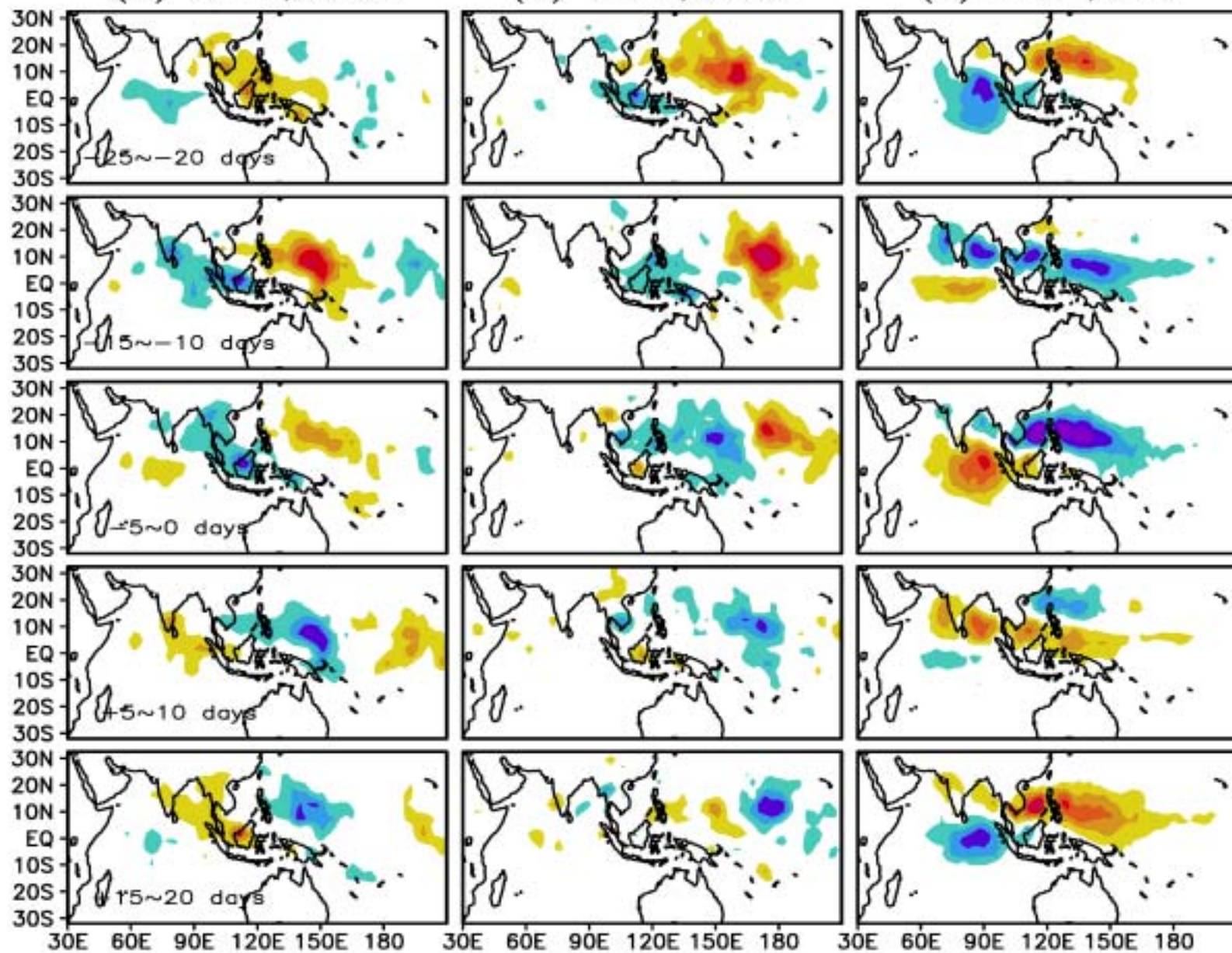
CLOUDY NORTH BAY COMPOSITE JJAS 1998-2001



(a) Sum,CGCM

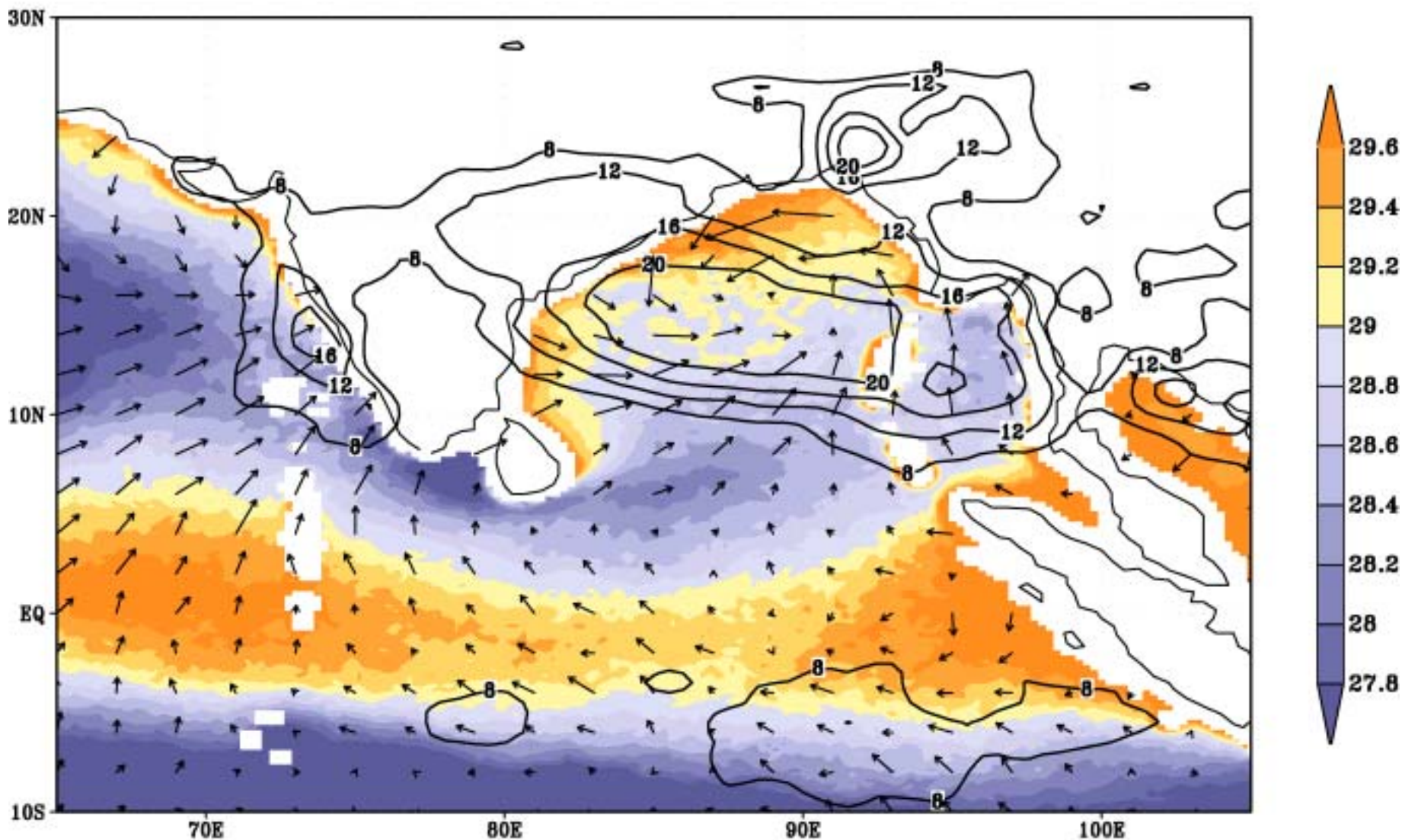
(b) Sum,AGCM

(c) Sum,OBS

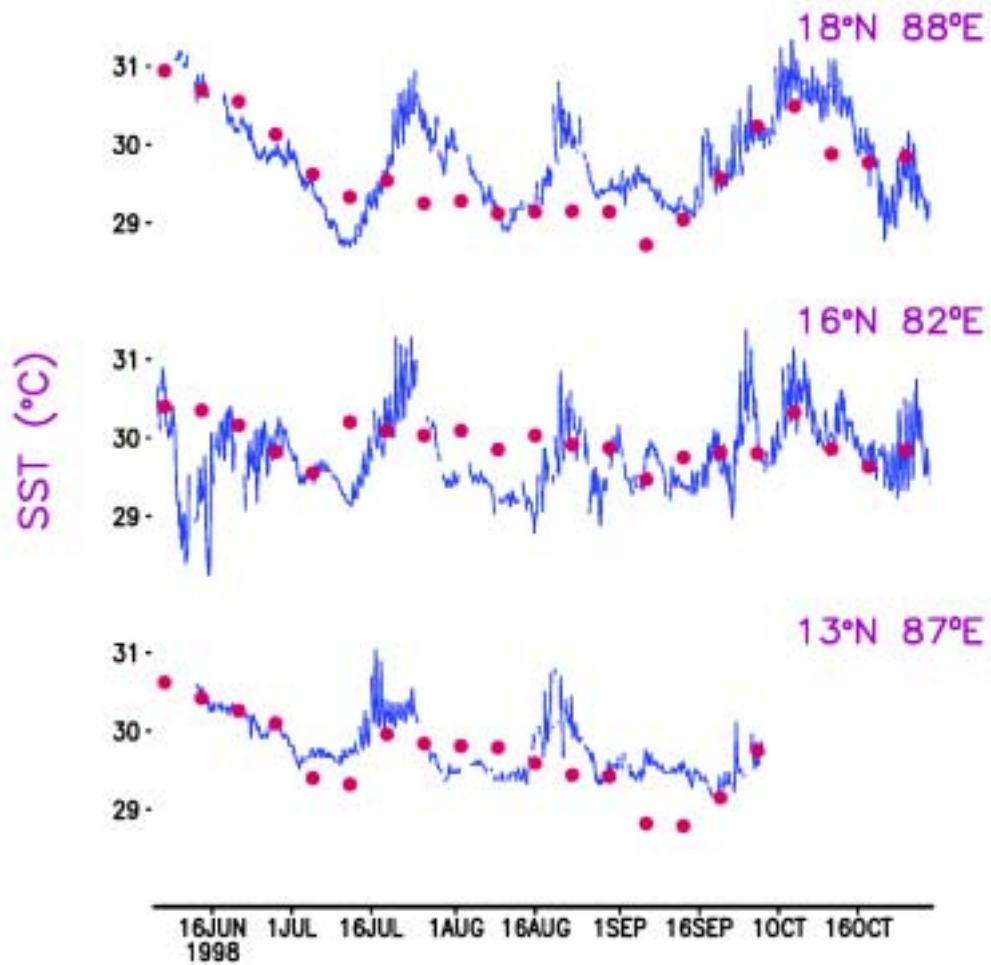
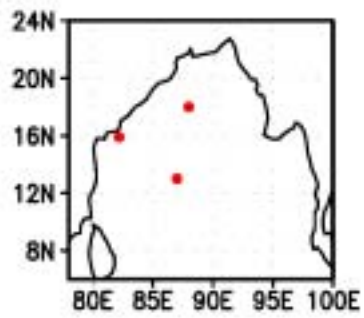


COMPOSITE <12-16°N>

GPCP RAIN (mmday⁻¹), QSCAT WIND ANOMALIES (ms⁻¹) & TMI SST (°C)

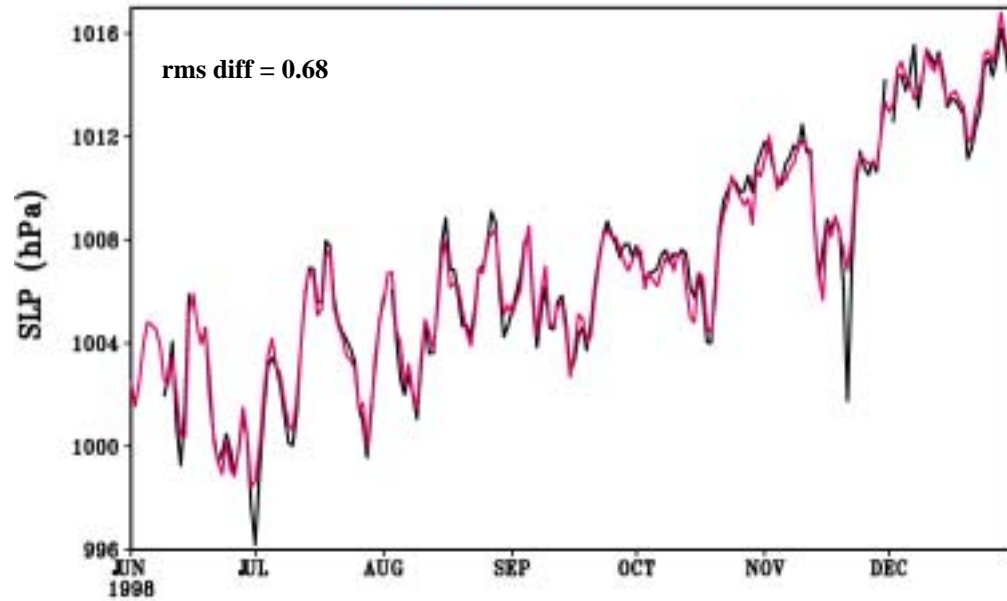


3

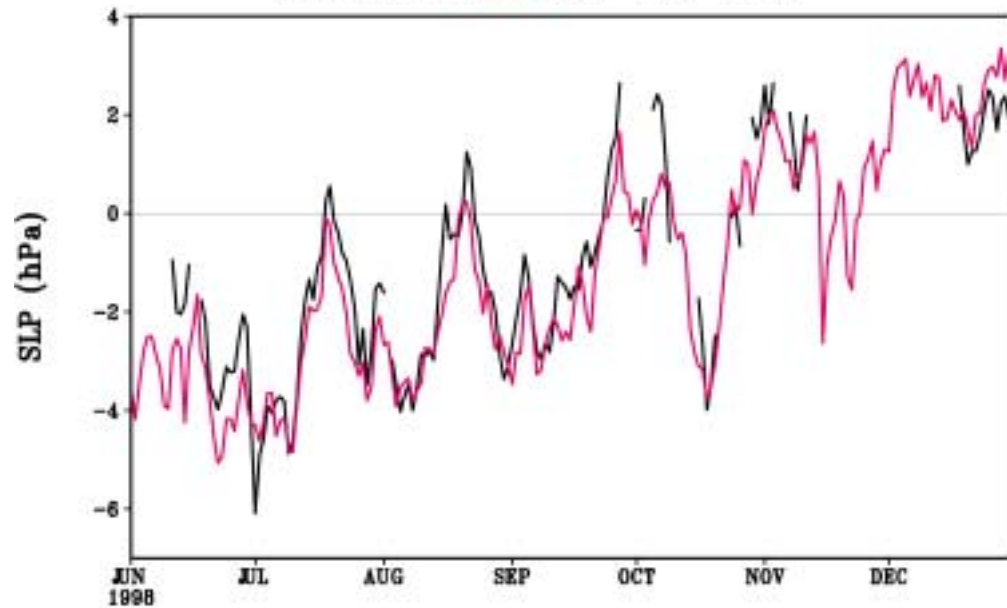


SEA LEVEL PRESSURE (hPa)

BUOY and NCEP at DS4(18°N, 88°E) 1998



BUOY and NCEP DS4-DS3 1998



MODEL BASIC EQUATIONS

$$u_t = -\nabla \cdot (u \mathbf{u}) + v \left(f + \frac{u \tan \phi}{a} \right) - \left(\frac{1}{a \rho_o \cdot \cos \phi} \right) p_\lambda + (\kappa_m u_z)_z + F^u$$

$$v_t = -\nabla \cdot (v \mathbf{u}) - u \left(f + \frac{u \tan \phi}{a} \right) - \left(\frac{1}{a \rho_o} \right) p_\phi + (\kappa_m v_z)_z + F^v$$

$$w_z = -\nabla_h \cdot \mathbf{u}_h$$

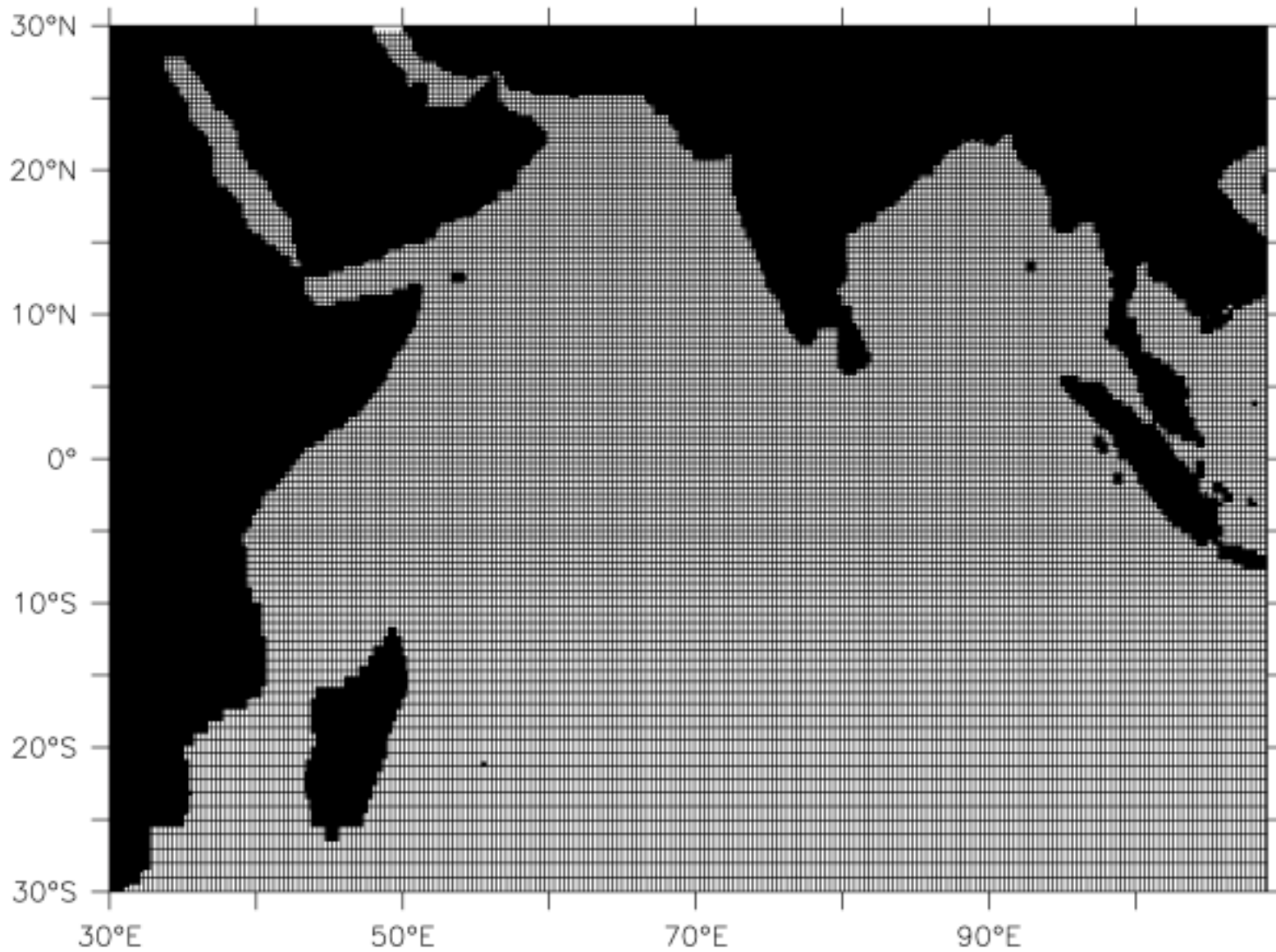
$$p_z = -\rho g$$

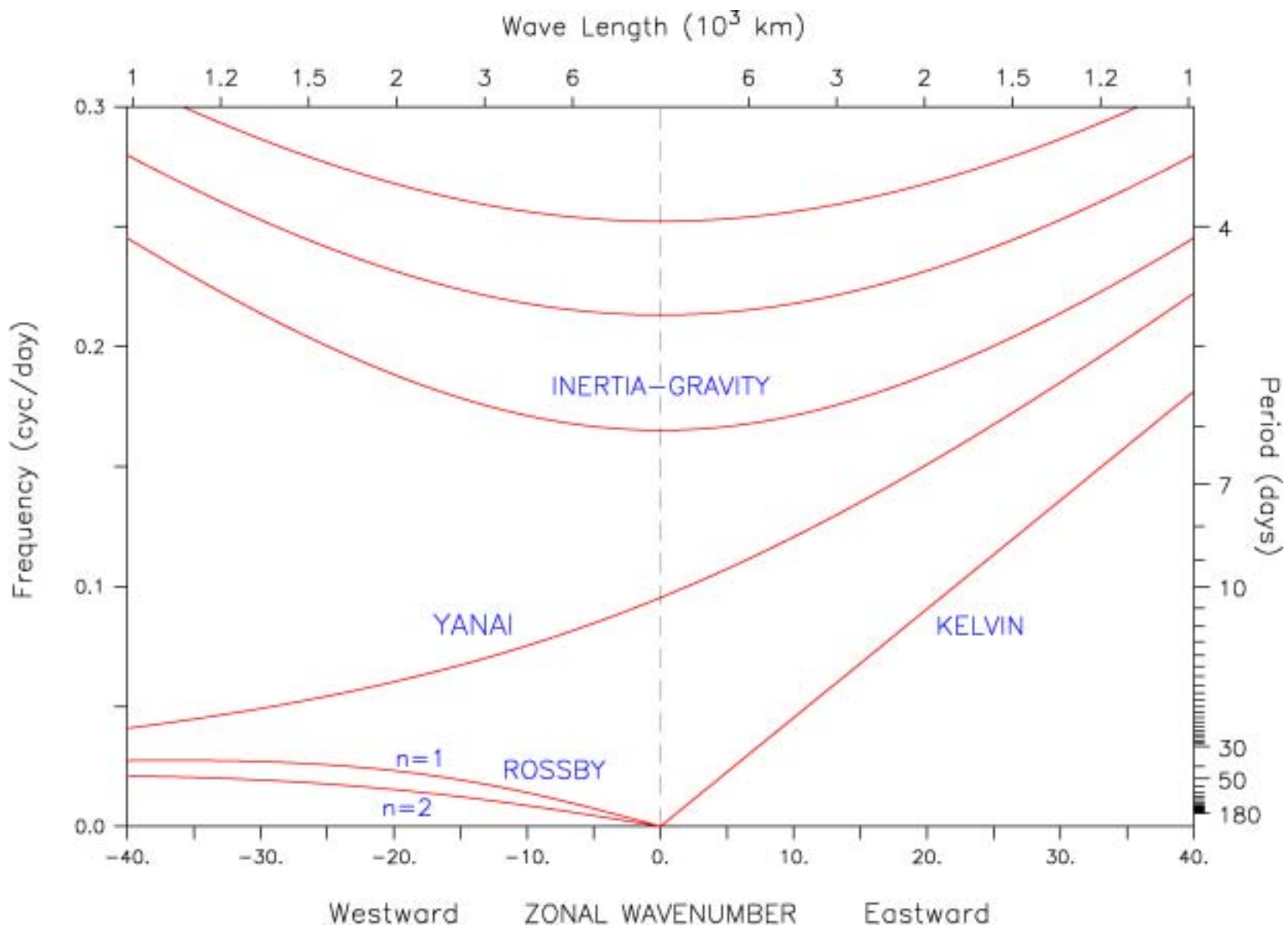
$$\theta_t = -\nabla \cdot [\mathbf{u} \theta + \mathbf{F}(\theta)]$$

$$s_t = -\nabla \cdot [\mathbf{u} s + \mathbf{F}(s)]$$

$$\rho = \rho(\theta, s, z).$$

MODEL DOMAIN AND GRID





CONCLUSIONS

- **Climate in our region is made of 10-60 day intraseasonal events**
- **These climate events probably involve air-sea-land interaction**
- **Intraseasonal events are likely to be predictable 15-25 days ahead (*Waliser, Goswami, Webster, Hendon, Wheeler ...*)**
- **Understanding of intraseasonal air-sea-land interaction will improve in the next few years**